

Turning the Page: Advancing Paper-Based Microfluidics for Broad Diagnostic Application

Max M. Gong and David Sinton

Version Post-print/accepted manuscript

Citation (published version) Gong, Max M., and David Sinton. "Turning the page: advancing paper-based microfluidics for broad diagnostic application." *Chemical reviews* 117, no. 12 (2017): 8447-8480 DOI:10.1021/acs.chemrev.7b00024.

Publisher's Statement This document is the Accepted Manuscript version of a Published Work that appeared in final form in *Chemical Reviews*, copyright © American Chemical Society after peer review and technical editing by the publisher. To access the final edited and published work see 10.1021/acs.chemrev.7b00024

How to cite TSpace items

Always cite the **published version**, so the author(s) will receive recognition through services that track citation counts, e.g. Scopus. If you need to cite the page number of the **author manuscript from TSpace** because you cannot access the published version, then cite the TSpace version **in addition to** the published version using the permanent URI (handle) found on the record page.

This article was made openly accessible by U of T Faculty.
Please [tell us](#) how this access benefits you. Your story matters.

Turning the Page: Advancing Paper-Based Microfluidics for Broad Diagnostic Application

Max M. Gong^{1,2} and David Sinton^{1*}

¹Department of Mechanical and Industrial Engineering, University of Toronto, 5 King's College Rd., Toronto, Ontario, Canada M5S 3G8.

²Department of Biomedical Engineering, Wisconsin Institutes for Medical Research, University of Wisconsin-Madison, 1111 Highland Ave., Madison, Wisconsin, USA 53705

*Correspondence should be addressed to: sinton@mie.utoronto.ca

Infectious diseases are a major global health issue. Diagnosis is a critical first step in effectively managing their spread. Paper-based microfluidic diagnostics first emerged in 2007 as a low-cost alternative to conventional laboratory testing, with the goal of improving accessibility to medical diagnostics in developing countries. This review examines the advances in paper-based microfluidic diagnostics for medical diagnosis in the context of global health from 2007 to 2016. Theory of fluid transport in paper is first presented. The next section examines the strategies that have been employed to control fluid and analyte transport in paper-based assays. Tasks such as mixing, timing, and sequential fluid delivery have been achieved in paper and have enabled analytical capabilities comparable to conventional laboratory methods. The following section examines paper-based sample processing and analysis. The most impactful advancement here has been the translation of nucleic acid analysis to a paper-based format. Smartphone-based analysis is another exciting development with potential for wide dissemination. The last core section of the review highlights emerging health applications, such as male fertility testing and wearable diagnostics. We conclude the review with future outlook, remaining challenges, and emerging opportunities.

CONTENTS

1	INTRODUCTION	3
2	FLUID TRANSPORT IN PAPER.....	6
3	2.1. Classical Models.....	7
4	2.2. Alternative Models	10
5	BASIC OPERATIONS FOR DIAGNOSTICS	15
6	3.1. Two-dimensional Flow.....	15
7	3.2. Three-dimensional Flow.....	19
8	3.2.1. Stacked 3D μ PADs	19
9	3.2.2. Origami-based 3D μ PADs	21
10	3.2.3. Single-sheet 3D μ PADs	24
11	3.3. Open Channel Flow	27
12	3.4. Time Delays.....	29
13	3.4.1. Chemical-based Delays.....	30
14	3.4.2. Physical Delays	35
15	3.5. Hydrogel-based Transport and Storage	37
16	3.6. Externally Actuated Structures.....	41
17	3.7. Analyte Concentration during Wetting.....	43
18	3.8. Post-wetting Analyte Concentration.....	45
19	SAMPLE PROCESSING AND ANALYSIS.....	51
20	4.1. Sample Collection	52
21	4.2. Complex Sample Preparation and Analysis	53
22	4.2.1. Whole Blood Processing.....	54
23	4.2.2. Nucleic Acid Analysis.....	58
24	4.3. Integrated Analysis.....	63
25	4.4. Quantitative Electrochemical Analysis	64
26	4.5. Quantitative Analysis with Consumer Technology.....	67
27	EMERGING APPLICATIONS.....	69
28	5.1. Male Infertility.....	69
29	5.2. Wearable Diagnostics.....	72
30	CONCLUSIONS AND OUTLOOK.....	75
31	6.1. Path to Translation and Commercialization	76
32	6.2. Final Comments.....	79
33	AUTHOR INFORMATION	81
34	Corresponding Author	81
35	Notes.....	81
36	Biographies.....	81
37	ACKNOWLEDGEMENTS	81
38	REFERENCES.....	82

1 INTRODUCTION

Global health is the practice of providing equitable healthcare to all people worldwide. Many factors underpin global health, stretching from environmental safety, through food and water quality, to disease control – all of which present opportunities for informative, low-cost diagnostics. Each of these factors are intimately coupled. For example, environmental pollution can lead to unsafe and unsanitary water sources (e.g., arsenic in drinking water), which in turn can increase the exposure of domesticated animals and humans to water-borne diseases. While environmental, food, and water safety and quality issues can be mitigated, in part, at the regional and local levels with relevant infrastructure, infectious diseases transcend national borders and present a health challenge that is truly global in scope.

Since 2000 alone, there have been several major pandemics including the severe acute respiratory syndrome (SARS) outbreak of 2003 in Asia, the H1N1 influenza epidemic of 2009 in North America, the Ebola virus outbreak of 2014 in West Africa, and the ongoing global Zika virus crisis. Our ability to contain these diseases largely depends on our ability to identify their root cause and diagnose those affected. Diagnostics is the first step to effectively manage the spread of disease. Unfortunately, the demand for effective diagnostics is often not met by an adequate supply of resources. Drawing on lessons from the recent Ebola virus epidemic, Bill Gates and others identified a number of factors that resulted in the slow response to the epidemic and the key challenges of point-of-care diagnostics in general, namely, the lack of relevant laboratory equipment and shortage of trained personnel.^{1–4} Much of the required equipment for diagnosing Ebola patients was not readily field-deployable (e.g., thermocyclers for quantitative polymerase chain reaction), and the skilled technicians needed to maintain these equipment were even scarcer in the heavily affected regions.¹ The key takeaway points from Gates' passionate argument are (1)

conventional laboratory testing is not ideal for rapid response to outbreaks, (2) testing needs to be decentralized and more accessible at the point-of-need, and (3) testing needs to be affordable.

Microfluidic diagnostic technologies show promise for accessible and affordable testing of infectious diseases.^{5–8} These fluidic systems with micron scaled features offer exceptional capability in sample processing and analysis at lower cost and material requirements than their laboratory counterparts. Many of these systems have been employed for immunosensing^{6,9} and nucleic acid testing^{10,11} of highly prevalent diseases such as the human immunodeficiency virus (HIV), hepatitis, tuberculosis, and malaria. Traditional microfluidic devices are typically made from silicon and glass,^{12–14} which provide geometrical precision and inertness for reuse but are expensive to scale. Contemporary polymer substrates, such as thermoplastics and poly(dimethylsiloxane),^{15–17} are moderate in cost and enable mid-to-high throughput fabrication. Recent trends in microfluidic point-of-care diagnostics, however, have moved towards inexpensive disposable materials, such as paper and thread,^{18,19} to further improve scalability and ease-of-use.

Paper (we use this term to refer to thin bulk-manufactured fibrous porous materials of all types) as a modern analytical substrate dates back to the 1940s and 1950s, when it was used for chromatography²⁰ and electrophoresis.²¹ In the 1980s, nitrocellulose membrane emerged as the platform for the home pregnancy test,²² and has remained a gold standard for lateral flow assays and commercial diagnostics more generally. Paper was conceived as a two-dimensional microfluidic diagnostic platform by George Whitesides' group in 2007, with the introduction of the microfluidic paper-based analytical device (μ PAD).²³ Since their pioneering work, there has been an exponential increase in paper-based diagnostics research. Several factors motivate this surge: (1) paper is inexpensive and ubiquitous; (2) paper is biocompatible; (3) paper wicks fluids via capillary action and does not require external pumping sources; (4) paper can be easily modified (i.e., chemically

treated, cut, folded, stacked); (5) paper can be safely disposed of by incineration; and (6) paper is scalable (i.e., amenable to printing and roll-to-roll manufacturing).²⁴

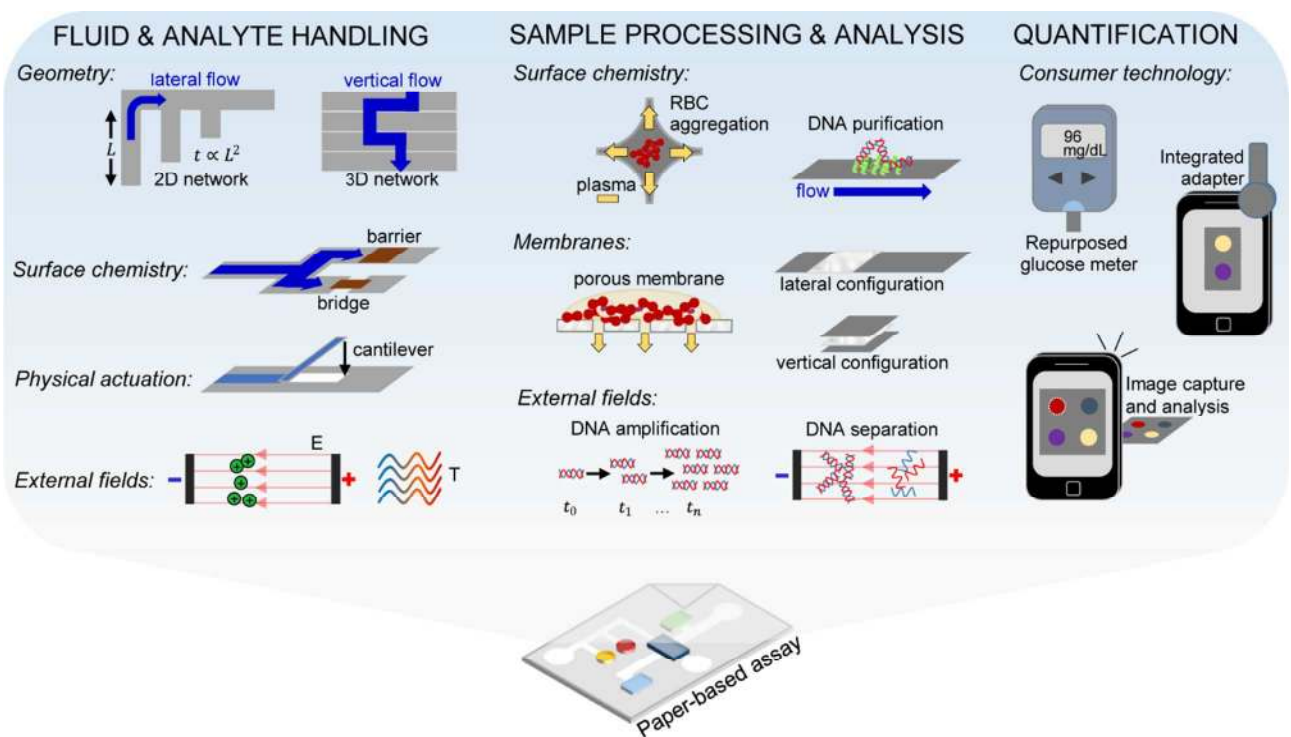


Figure 1. Overview of possible analytical capabilities employed in paper-based assays. A generalized paper-based assay with strategies for fluid and analyte handling, sample processing and analysis, and quantification.

Paper-based technologies have rapidly advanced in the last decade, incorporating multiple complex functions within a single device - a turning point in paper-based diagnostics.^{18,25–27} Figure 1 illustrates the numerous analytical capabilities that can be incorporated in paper-based assays. Here, we examine advances in paper-based microfluidics for global health. While these advances could find application in a spectrum of global health related issues, our discussion is centered on medical diagnosis of infectious diseases. We refer interested readers to more detailed reviews on paper-based analytical devices for environmental, food, and water analysis.^{28–30} Recent reviews of paper-based microfluidics cover – to varying degrees – fluid transport in paper, fabrication

1
2
3 methods, detection and readout strategies, and diagnostic applications.^{18,31–40} Specifically, there has
4
5 been focused discussion on fabrication, flow control, and detection methods,^{31,34,35,38,40} with limited
6
7 discussion of applications. Reviews including various potential applications^{18,32,33,36,37,39} miss
8
9 pivotal advancements from the last few years. For example, the emergence of molecular testing in
10
11 paper broadens potential applications into the wide arena of nucleic acid-based diagnostics and
12
13 warrants a fresh, comprehensive outlook.
14
15
16

17
18 This review is organized as follows. In section 2, we present foundational theory on fluid
19
20 transport in paper, with a focus on key enabling physical mechanisms and recent theoretical models
21
22 that better predict flow in modified paper (e.g., wax-patterned paper) and under thermal effects such
23
24 as evaporation. In section 3, we examine the many basic operations now used to manipulate fluid
25
26 and analyte transport in paper-based assays. Advances in fluid and analyte handling have enabled
27
28 analytical capabilities in paper comparable to conventional laboratory methods. In section 4, we
29
30 assess paper-based strategies for complex sample processing and analysis; focusing on strategies
31
32 that present new application opportunities and improve the practicality of paper-based assays for
33
34 field deployment. In section 5, we highlight the application of paper-based diagnostics in emerging
35
36 health applications, including male fertility testing and wearable diagnostics. We conclude the
37
38 review with future outlook and remaining challenges, namely remaining barriers in translation and
39
40 commercialization.
41
42
43
44
45

46 47 2 FLUID TRANSPORT IN PAPER

48
49 Fluid transport in paper is a passive process enabled by capillary action. Capillary action or wicking
50
51 within the paper matrix is a result of the interplay between cohesive and adhesive forces. Cohesive
52
53 forces, such as surface tension, arise due to intermolecular attraction between fluid molecules at the
54
55 liquid-air interface, while adhesive forces (i.e., van der Waals force) result from intermolecular
56
57
58
59
60

attraction at the liquid-fiber interface. The surface properties of the paper matrix dictate adhesion and consequently, the degree of wetting (physically represented by the fluid contact angle at the liquid-fiber interface). This section presents classical models for imbibition in paper and alternative models that take into consideration effects including evaporation, geometry and wetting characteristics.

2.1. Classical Models

Fluid transport in paper can be modeled using the Lucas-Washburn equation, which was originally derived to describe one-dimensional capillary flow in a parallel bundle of cylindrical tubes.⁴¹ It has been extended to fluid transport in porous paper⁴² (Figure 2), and relates wetted length to wicking time:

$$l(t) = \sqrt{\frac{\gamma r \cos \theta}{2\mu}} t \quad (1)$$

where $l(t)$ is the distance travelled by the fluid front under capillary pressure, γ is the liquid-air surface tension, r is the effective pore radius of the paper matrix, θ is the liquid-fiber contact angle, μ is fluid viscosity, and t is time. Equation (1) assumes constant cross-sectional area, uniform pores, no impurities within the paper matrix, unlimited reservoir volume, and no effect on wicking from patterned hydrophobic channel walls. Any violation of these conditions can result in deviations between experimental observations and the analytical expression. Most notably, the assumption of a straight pores of uniform cross-section is a significant deviation from the reality of typical paper substrates. Scanning electron microscope images of the fiber network of common paper materials, chromatography paper⁴³ and nitrocellulose membrane,⁴⁴ are shown in Figure 2c.

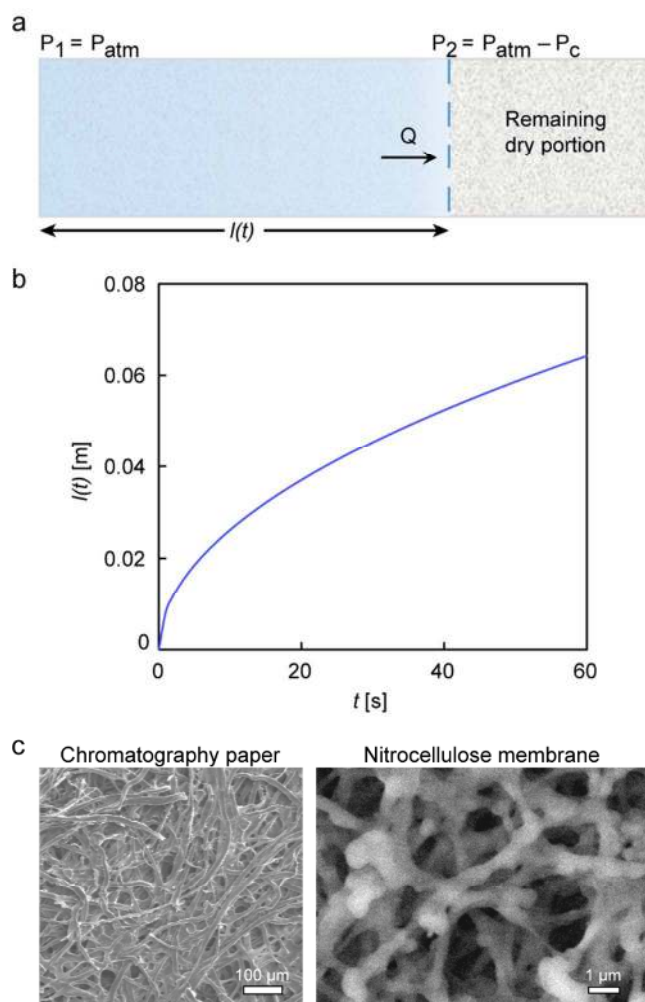


Figure 2. Fluid transport in paper. (a) The Lucas-Washburn equation is used to model fluid transport in paper. Wetted length, $l(t)$, is directly proportional to wicking time and a function of fluid and material properties. P_{atm} is atmospheric pressure and P_c is capillary pressure. (b) Representative curve of wetted length versus time for water wicked by Whatman Grade 1 Qualitative Filter Paper at 25 °C: $\gamma = 72$ mN/m, $r = 11$ μm , $\theta = 30^\circ$, and $\mu = 0.89$ mPa·s. (c) Scanning electron microscope images of the pore space of common paper materials, chromatography paper and nitrocellulose membrane. Images reprinted with permission from refs 43 and 44. Copyright 2016 MDPI and 2015 American Chemical Society.

Treating paper as a porous medium, Darcy's law has also been used to model fluid transport in paper. It is a phenomenologically derived equation that describes flow through porous media.⁴⁵ It can be used to characterize wicking rate (flow rate) in paper⁴² and is expressed as:

$$Q = -\frac{\kappa WH}{\mu L} \Delta P \quad (2)$$

where Q is the volumetric flow rate, κ is the permeability of the paper, WH is the cross-sectional area perpendicular to flow, μ is fluid viscosity, L is the length of the paper, and ΔP is the pressure difference along the length of the paper. For a paper-based system with n -connected sections of varying geometry, the volumetric flow rate through the fluidic circuit can be modeled using an electrical circuit analogy (Figure 3):

$$Q = -\frac{\Delta P}{\sum_i^n \frac{\mu L_i}{\kappa W_i H_i}} \leftrightarrow I = \frac{\Delta V}{\sum_i^n R_i} \quad (3)$$

where Q is the volumetric flow rate which is equivalent to electric current I , $\frac{\mu L_i}{\kappa W_i H_i}$ is the fluidic resistance of the i th section (a function of fluid/paper properties and geometry) which is analogous to Ohmic resistance R , and ΔP is the pressure difference across the fluidic circuit, analogous to the electric potential difference ΔV . In keeping with the analogy, the properties of series and parallel electrical circuits can be applied to their equivalent fluidic circuits. For example, flow rate in a series fluidic circuit is the same along the each section (i.e., $Q = Q_1 = Q_2 = \dots = Q_n$), where the equivalent fluidic resistance is equal to $R_1 + R_2 + \dots + R_n$.

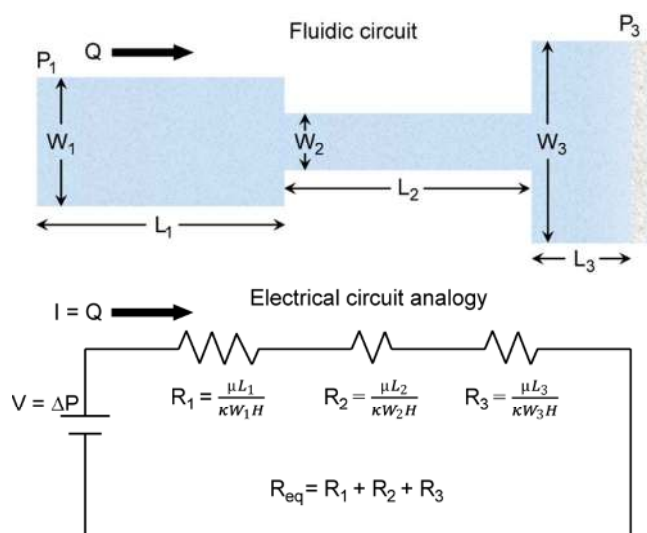


Figure 3. Electrical circuit analogy (Ohm's law) for fluid transport in a paper-based fluidic circuit. Darcy's law is used to model the volumetric flow rate in each section. The equivalent resistance for the fluidic circuit is the sum of all the resistances in series.

2.2. Alternative Models

Paper-based assays are typically used in ambient conditions, where evaporation critically affects fluid transport. Camplisson *et al.*⁴⁶ developed a modified form of equation (1) to account for fluid evaporation:

$$l(t) = \sqrt{\frac{\gamma r \phi h \cos \theta}{4 \mu q_0} \left(1 - e^{-\frac{2 q_0 t}{\phi h}}\right)} \quad (4)$$

where $l(t)$ is wetted length, r is the effective pore radius of the paper matrix, ϕ is paper porosity, h is the thickness of the paper, θ is the liquid-fiber contact angle, μ is fluid viscosity, and q_0 is evaporation rate defined as the volume of evaporated liquid per unit area of wetted channel and time t .

To date, most models of imbibition in paper apply a constant width and thickness constraint during wicking. Recently, Elizalde *et al.*⁴⁷ developed and experimentally validated a modified form of equation (1) that addresses transport in paper with non-uniform cross-sections. They provide an implicit equation for imbibition in arbitrarily shaped paper, predicting the time t needed to fill the paper for an arbitrary cross-section $A(l)$ and wetted distance $l(t)$:

$$\frac{\kappa R_0}{\mu} \int_0^l A(l') dl' + \int_0^l \left[A(l') \int_0^{l'} \frac{dx}{A(x)} \right] dl' = Dt \quad (5)$$

where κ is the permeability of the paper, R_0 is the initial load, μ is fluid viscosity, and D is a diffusive coefficient defined as $\kappa \Delta P / \mu$ (not to be confused with diffusion coefficient or diffusivity⁴⁸) A schematic of the flow domain used in the model is shown in Figure 4. For imbibition in paper with constant cross-sectional area, equation (5) reduces to equation (1). Table 1 summarizes the relationships between wetted length and time for constant cross-sectional area, and linearly and non-linearly varying cross-sectional areas. It is important to note that equation (5) holds under the condition that flow is in the Stokes regime (i.e., Reynolds number $\ll 1$, gravity is neglected).

Capillary pressure, curvature of the liquid-air interface, and contact angle are also assumed to be constant. Overall, these works provide a method to predict flow behavior in arbitrarily shaped paper-based assays, extending the predictive power of the classical Lucas-Washburn equation.

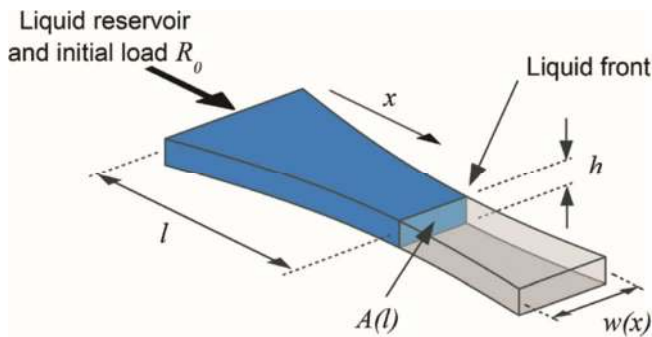





Figure 4. Schematic used to model imbibition in paper-based devices with arbitrary cross-sections. Reprinted with permission from ref 47. Copyright 2015 The Royal Society of Chemistry.

Table 1. Equations of for imbibition length as a function of time in arbitrarily shaped paper.⁴⁷

Cross-sectional area $A(x)$	Paper shape (Top view)	Equation $l(t)$
Constant, A_0		$\frac{l^2}{2} = Dt$
Linearly varying, $A_0(1 + ax)$		$\frac{(1 + al)^2}{2} \left[\ln(1 + al) - \frac{1}{2} \right] + \frac{1}{4} = a^2 Dt$
Non-linearly varying, $A_0(1 + ax)^2$		$\frac{1}{6} [(1 + al)^3 - 1] - \frac{1}{2} [(1 + al)^2 - 1] = a^2 Dt$

While cross-sectional areas available to flow can be set by the paper geometry, they are more commonly set by hydrophobic sealing boundaries such as wax. Hong and Kim⁴⁹ developed a modified form of equation (1) to account for contact angle variations due to hydrophobic barriers, using the model in Figure 5a. They consider the paper-based assay as a network of parallel capillaries. For a capillary next to a hydrophobic barrier, it has a different contact angle (θ_b) then

capillaries in the bulk. This contact angle must be greater than that of the capillaries in the bulk ($> 90^\circ$) to prevent imbibition through the boundary. Solving a force balance for the paper channel with θ_b in consideration leads to the following expression:

$$l(t) = k \sqrt{\left(1 + \beta \frac{d}{\phi^{\frac{1}{3}} w} \frac{\cos \theta_b}{\cos \theta}\right) \frac{\sigma}{\mu} t} \quad (6)$$

where $l(t)$ is wetted length, k and β are experimentally determined constants, ϕ is paper porosity, d is pore diameter, w is channel width, θ is contact angle in the bulk, θ_b is contact angle at the boundary, σ is surface tension, μ is fluid viscosity, and t is time. Equation (6) indicates that imbibition is slower in channels with hydrophobic boundaries since $\theta_b > 90^\circ$, as shown in Figure 5b. Additionally, imbibition in patterned paper depends on the width of the channel, which is not captured by the classical Lucas-Washburn equation. This width dependency has also been observed by others.^{50,51}

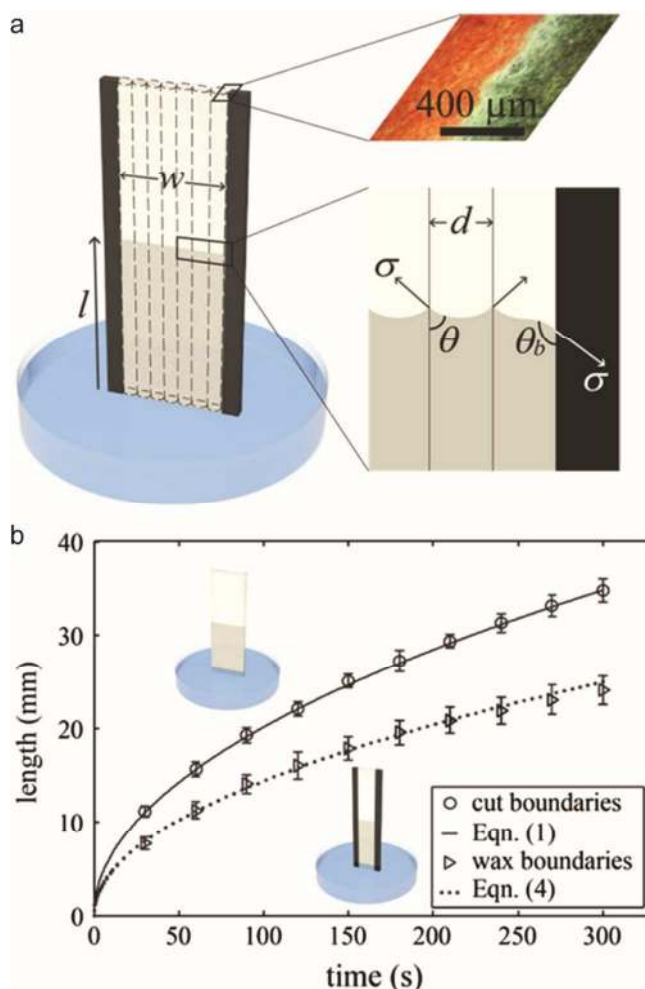


Figure 5. Imbibition in paper channels with and without hydrophobic boundaries. (a) Schematic used to model imbibition in paper-based assays with wax boundaries. (b) Flow in channels with boundaries is much slower than that in channels without boundaries. Reprinted with permission from ref 49. Copyright 2015 Springer.

For large strips of paper (widths $> 5 \text{ mm}$), Walji and MacDonald⁴³ observed a similar width dependency for wetted length (i.e., wicking speed increases with increasing channel width), however, in the absence of patterned hydrophobic boundaries. The authors also investigated the effects of surrounding conditions on imbibition, such as temperature and humidity – critical parameters for field deployability. Specifically, they observed an increase in wicking speed with increasing temperature. The increase in wicking speed can be attributed to a decrease in fluid viscosity as temperature rises. Given the same experimental conditions, humidity did not

significantly affect imbibition speed in the paper strip. Importantly, Walji and MacDonald explored the influence of machine direction (or fiber orientation in the paper matrix) on imbibition, which has not previously received attention as a parameter affecting wicking. They demonstrated that fiber alignment can have substantial impact on wicking speed, with a 30% increase when flow is parallel to the aligned fibers as compared to flow in the perpendicular direction (Figure 6). This work and those described above have extended our understanding of fluid transport in paper and now provide a number of models to inform the design of paper-based diagnostic assays.

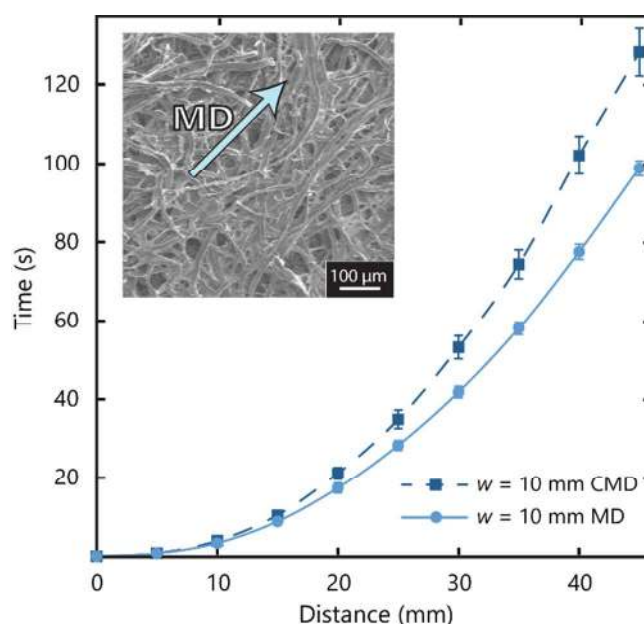


Figure 6. Effect of fiber alignment on imbibition in paper. Wicking speed in the direction of fiber alignment or machine direction is 30% faster than that in the orthogonal, cross machine direction. Reprinted with permission from ref 43. Copyright 2016 MDPI.

There is a rich parallel body of literature on transport of gases and liquid water in carbon paper-based electrodes for energy applications, namely fuel cells⁵² and electrolyzers.⁵³ Permeation of reactant gas in the through-plane vs. in-plane directions has been studied extensively, with in-plane and through-plane permeability ranging from 5 to 10 Darcy's for conventional fuel cell materials.^{54,55} In fuel cell applications hydrophobic coatings are also used, albeit more uniformly to discourage water saturation and promote gas transport.⁵⁶⁻⁵⁸

3 BASIC OPERATIONS FOR DIAGNOSTICS

Paper is the ideal platform for global health diagnostics owing to its low-cost and ultimately, its inherent ability to wick fluids. Fluid transport by wicking eliminates the need for expensive peripheral pumping instrumentation, which aligns well with the ‘simple and low-cost’ mantra for paper-based diagnostics. However, wicking alone is not sufficient for achieving the complex fluid and analyte handling tasks required for bioanalytical assays, such as the enzyme-linked immunosorbent assay or ELISA. Conventional ELISA consists of multiple washing and incubation steps, where timing is of crucial importance. Similar control and timed processing is needed in paper-based assays to achieve a reliable readout. This section examines the strategies developed for programmed sample and reagent delivery, and analyte manipulation (i.e., concentration, mixing, and separation).

3.1. Two-dimensional Flow

The most direct method to control imbibition in paper is by manipulating the geometry of the assay. Yager and colleagues demonstrated timing and sequential processing in their two-dimensional paper networks by simply exploiting Lucas-Washburn wicking behavior.^{42,59,60} Equation (1) in section 2 states that $t \propto L^2$ for paper strips of constant width and thickness. Sequential delivery of fluids can be achieved then by connecting a series of paper legs (Figure 7).

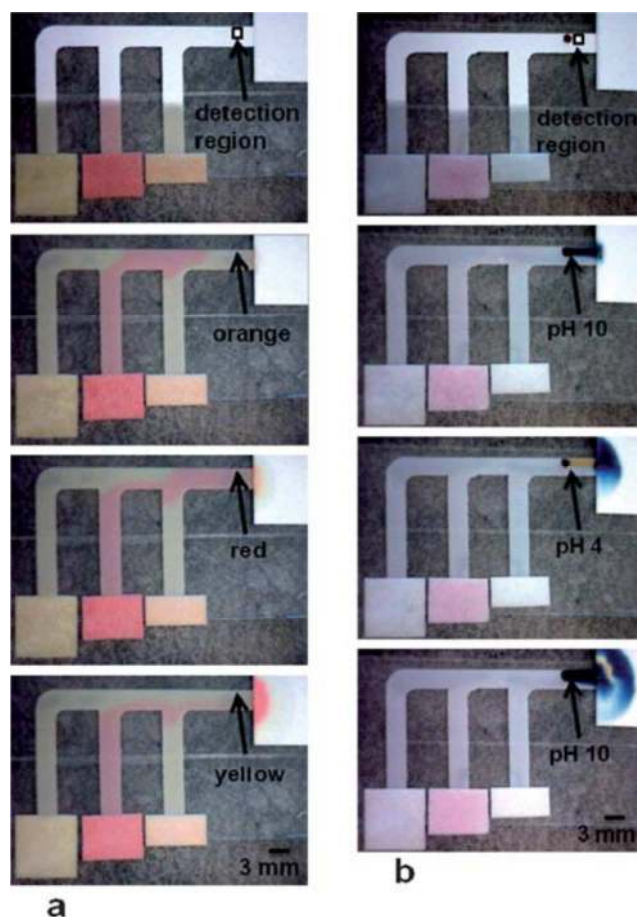


Figure 7. Sequential delivery of reagents in two-dimensional paper networks with paper legs connected in series. (a) Arrival of colored fluids at different times. (b) Arrival of pH solutions at different times. Reprinted with permission from ref 59. Copyright 2010 The Royal Society of Chemistry.

The control of imbibition using legs with expanding and contracting widths was also demonstrated.⁴² Wicking speed in a constant width leg decreases when the leg expands abruptly into a larger width and conversely, it increases when the leg contracts into a smaller width, as per conservation of mass. Using this principle, simple networks can be designed to achieve timed multistep reactions (Figure 8). Importantly, the sequential processing is baked into the device geometry and requires no external control or infrastructure, reducing cost and complexity.

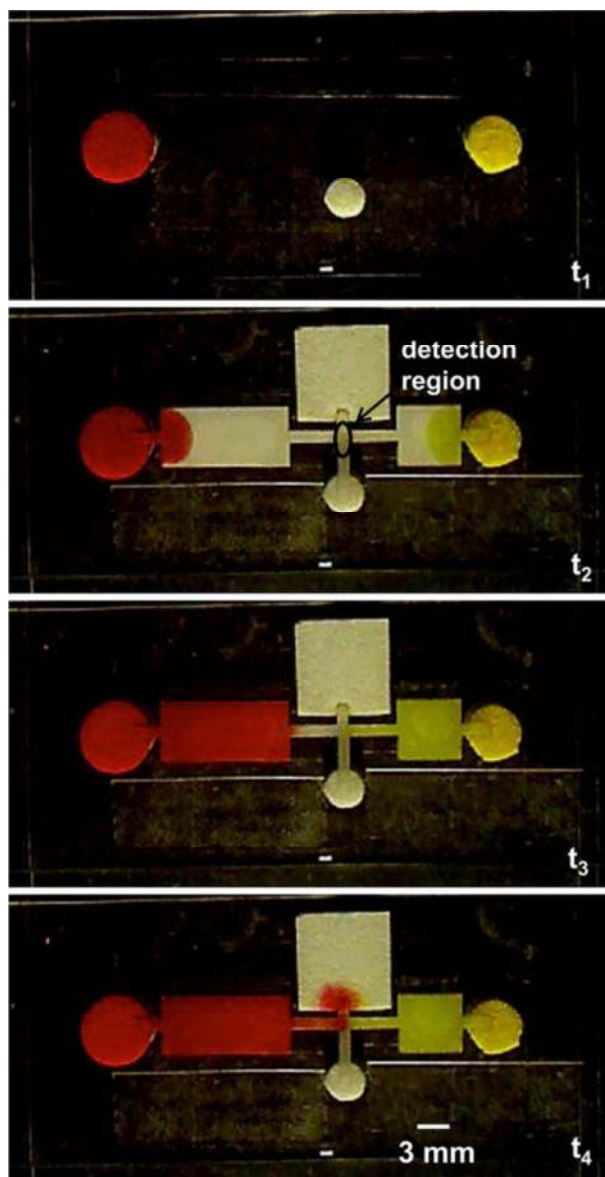


Figure 8. Sequential delivery of reagents to a detection region using expanding and contracting legs. At t_1 the sources pads are filled with fluids. The paper network is placed in contact with the source pads at $t_2 = 9$ s. Controlled delivery to the detection region is observed at $t_3 = 2.3$ min and $t_4 = 9.0$ min. Reprinted with permission from ref 42. Copyright 2011 Springer.

The development path for two-dimensional paper networks has been towards simple semi-automated paper-based assays for disease diagnosis.^{25,61–63} Fridley *et al.*⁶² developed a system for malaria diagnosis, with legs for sample preparation, washing, and signal enhancement. A limit of detection (LOD) of 3.6 ng/mL is achieved for the malaria antigen PfHRP2, which is within the range reported for conventional ELISA (0.1 – 4 ng/mL) and ~25-fold lower than that of commercial

rapid tests. An advantage of their system is that reagents are directly dried in the paper-based assay, enabling their long term storage without refrigeration. An operator simply adds sample and buffer to designated regions to reconstitute the dried reagents, and the assay subsequently runs itself (Figure 9). More in-depth analyses on drying and immobilizing reagents in paper are available and provide pertinent guidelines for assay deployability,^{64–66} including for instance maintaining devices with dried reagents in low humidity.

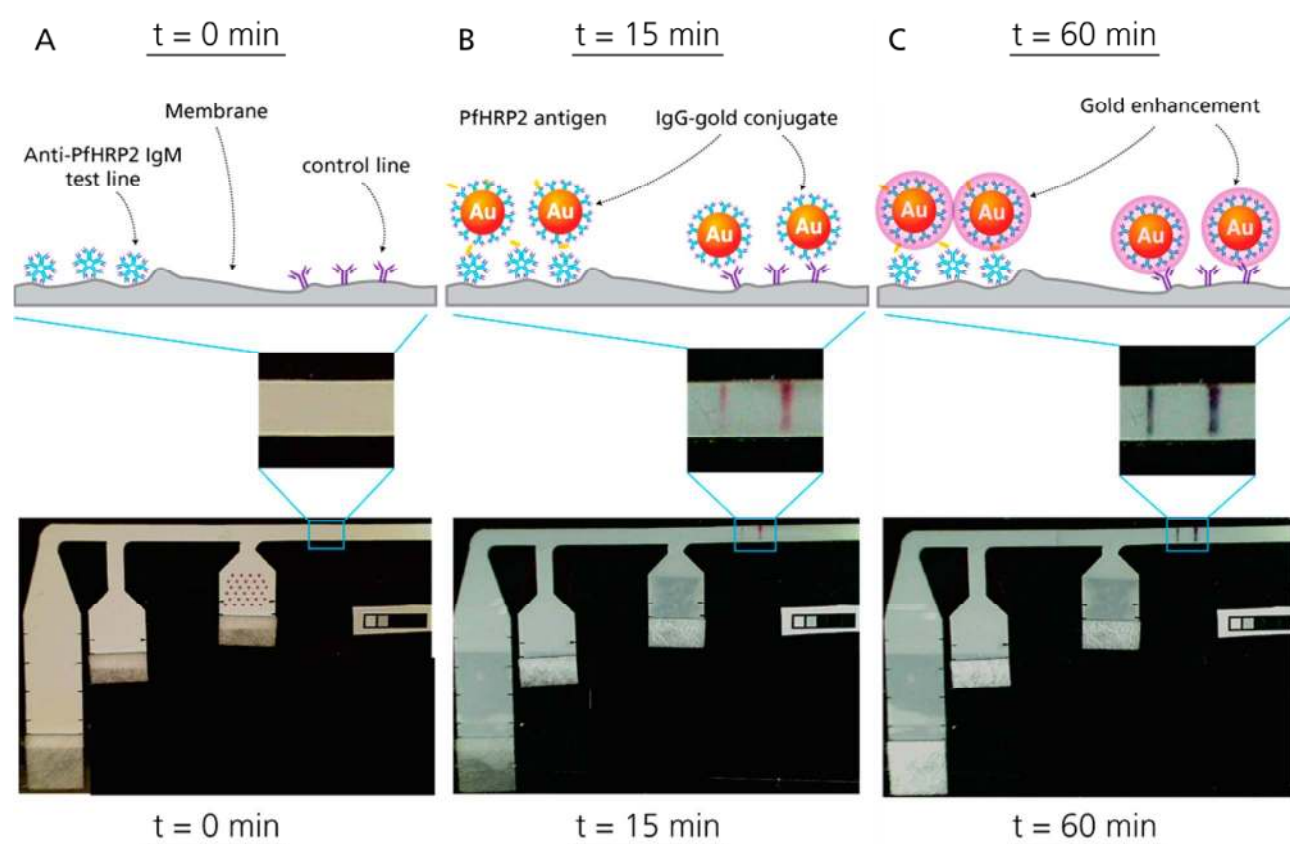


Figure 9. Schematics and images of a two-dimensional paper network for malaria diagnosis. All reagents necessary for carrying out the assay are pre-dried into the paper network. (A) Sample spiked with malaria antigen PfHRP2 (30 μ L) is applied to the right-most leg of the network. Buffer (100 μ L) is applied to the middle and left-most legs, following sample addition. (B) Initial signals appear after 15 min. (C) Signal amplification (3.2-fold) is achieved after 60 min. Reprinted with permission from ref 62. Copyright 2014 American Chemical Society.

3.2. Three-dimensional Flow

Three-dimensional (3D) paper networks can be realized by stacking⁶⁷ and folding (based on the principles of origami)⁶⁸ multiple fluidic layers or by controlling the penetration depth of melted wax in a single sheet of paper.^{69,70} Adding a third dimension provides vertical flow across different layers in addition to lateral flow within each layer. This added capability allows fluid to be delivered to a large array of reaction sites within a compact area. The 3D design also facilitates integration of different device elements, such as filtration membranes⁷¹ and electrodes.⁷² These elements can be sandwiched between layers within 3D μ PADs, adding functionality without compromising their compact size.

3.2.1. Stacked 3D μ PADs

Martinez *et al.*⁶⁷ first demonstrated the stacked design for 3D μ PADs with layers of paper and tape. Various configurations were realized based on the stacking arrangement of individual layers and their patterned fluidic features. An example device is shown in Figure 10. This device has a top layer with four inputs stacked on a bottom layer with an array of 1,024 detection spots. Fluid is routed from each input into a designated region, as indicated by the different colors. The authors also demonstrated their approach for more practical applications such as measuring glucose and protein concentrations in sample.

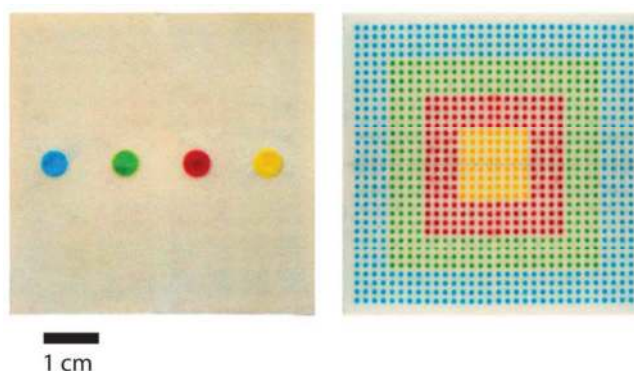


Figure 10. A three-dimensional μ PAD with four input sources in the top layer (left), which cover 1,024 detection spots in the bottom layer (right). Sample from each source is routed to specific

regions of the array. Reprinted with permission from ref 67. Copyright 2008 National Academy of Sciences.

The stacked 3D μ PAD concept was further developed to enable programmable fluid logic, where flow is initiated by manually depressing a “on” button in the device with a stylus or a ballpoint pen.⁷³ Pressing the button closes a gap between two vertically aligned channels in separate layers, allowing fluid to wick from one channel to the other. This strategy enables programmable and selective measurement of target analytes in a given sample. Figure 11 shows a urinalysis device that can selectively measure glucose, protein, ketones, and nitrite. Depending on the desired readout, the relevant button is pressed and sample wicks into the corresponding detection spot. Since the inception of 3D μ PADs, many variations of the stacked design have been and continue to be developed for biochemical,^{71,74,75} immunological,^{76–78} and nucleic acid testing.^{79,80}

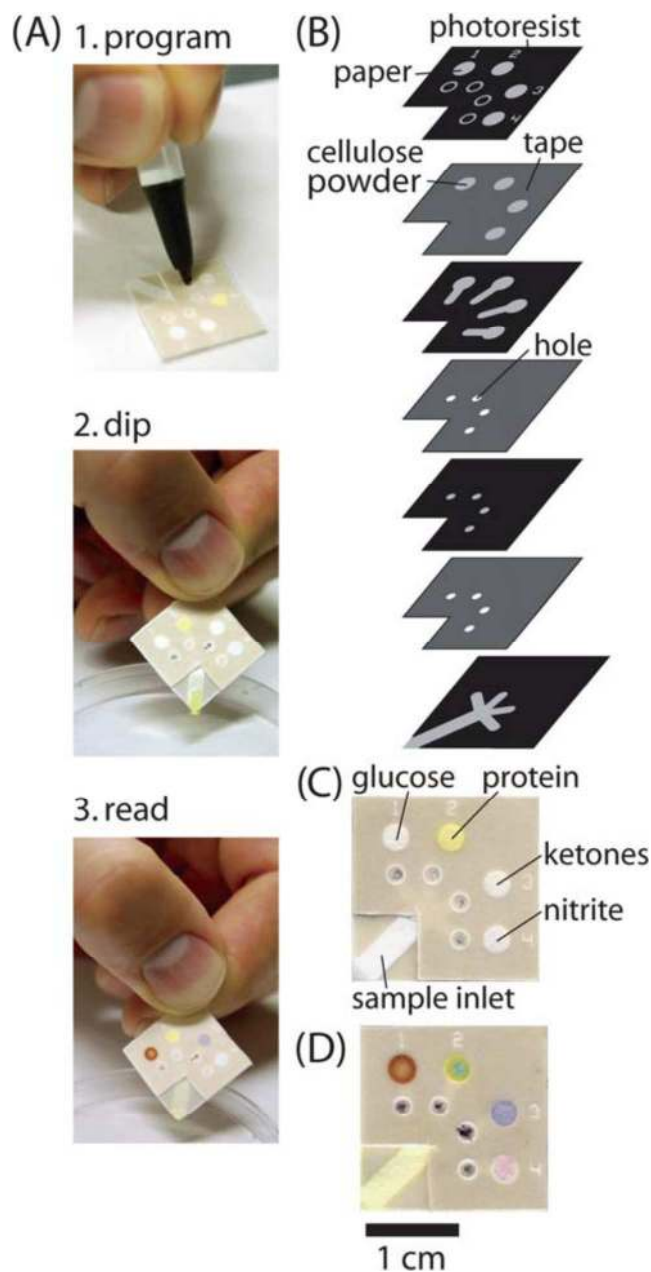


Figure 11. Programmable 3D μ PAD for urinalysis. (A) The device is programmed by pressing the relevant buttons for the desired readouts. Sample is collected and colorimetric signals are subsequently generated in the detection spots. (B) Exploded view showing layers of the device. (C) Device showing readout for protein. (D) Device showing readout for all four target analytes. Reprinted with permission from ref 73. Copyright 2010 The Royal Society of Chemistry.

3.2.2. Origami-based 3D μ PADs

Folding paper into intricate shapes, or origami, is also a popular method for making 3D μ PADs.

The main advantages of literally turning the page, as compared to layer-by-layer stacking include (i)

reduced fabrication time (i.e., multiple layers of a device are patterned in a single sheet of paper), (ii) added precision when aligning features in separate layers, and (iii) the ability to disassemble/unfold the device to analyze individual layers. Liu and Crooks⁶⁸ first introduced these devices as 3D origami-based paper analytical devices or 3D oPADs (Figure 12) and demonstrated their applicability for simple glucose and protein analysis. Many variations of the origami design have been developed for bioanalysis since its inception.^{81–86}

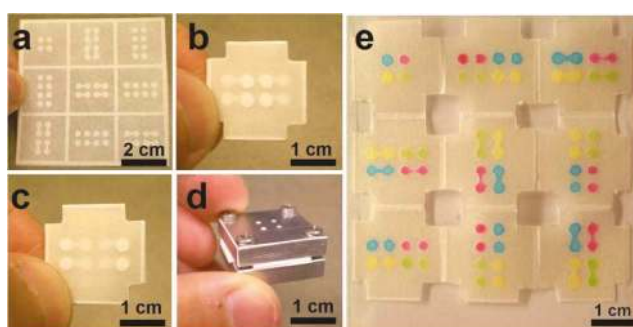


Figure 12. Paper-based device assembled via folding or origami. Multiple layers are patterned into a single sheet of paper, reducing fabrication time. Folding also enables precise alignment of features and the ability to disassemble the device for analysis of individual layers. Reprinted with permission from ref 68. Copyright 2011 American Chemical Society.

Govindarajan *et al.*⁸¹ demonstrated that complex sample preparation, such as DNA extraction, could be achieved by sequentially folding tabs with dried reagent (activated by addition of buffer) over an extraction region (Figure 13). They were able to extract a bacterial load of 33 CFU/mL from *E. coli* spiked in porcine mucin without using peripheral instrumentation, which is within the LOD for commercial systems (e.g., Cepheid GeneXpert). Extracted DNA from the field can be saved and transported for further analysis in a centralized laboratory or directly interfaced with downstream detection technologies (e.g., nucleic acid rapid test).

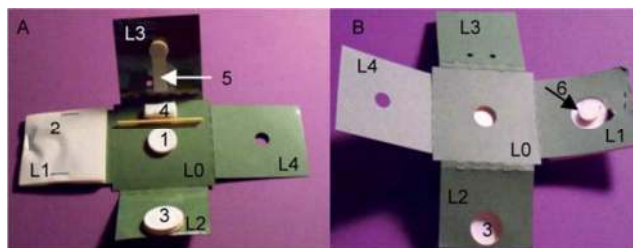


Figure 13. An oPAD for point-of-care nucleic acid extraction. (A) Front side of device with four tabs (L1-L4) that are folded in succession above and below the base layer (L0). Device components include a (1) DNA filter, (2) waste absorption pad, (3) sample loading pad, and (4) lysis buffer pad, (5) buffer channel, and (6) contact pad (shown in B). (B) Back side of device. Reprinted with permission from ref 81. Copyright 2012 The Royal Society of Chemistry.

In general, each tab in an oPAD represents a switch or valve that houses a single reaction, which is activated by folding the tab onto a target region. Therefore, the complexity of the device (i.e., number of tabs or user operations) depends on the desired application. Typically, researchers try to minimize the number of reaction steps to improve the user-friendliness of the device. Robinson *et al.*⁸⁶ recently developed a one-fold activated oPAD for point-of-care monitoring of phenylalanine in whole blood in the context of the metabolic disease phenylketonuria. Whole blood is loaded onto a plasma membrane, separated plasma wicks into two downstream pads with enzymatic reagents, and a third pad is then folded on top to generate a colorimetric signal that can be quantified with an imaging source such as a scanner or mobile phone. The entire process can be completed within 8 minutes, providing relevant data within the clinical range of phenylalanine levels (1 – 9 mg/dL).

Origami-based 3D assays are particularly useful for electrochemical testing where sample is typically incubated and measured between multiple electrodes. Li and Liu⁸⁷ developed an origami-based electrical impedance spectroscopy device capable of quantifying HIV p38 antigen in human serum as low as 300 fg/mL, which is > 33 times lower than commercial p38 antigen testing kits. This ultralow detection capability is uniquely enabled by zinc oxide nanowires that are directly grown in the origami-based device (Figure 14).

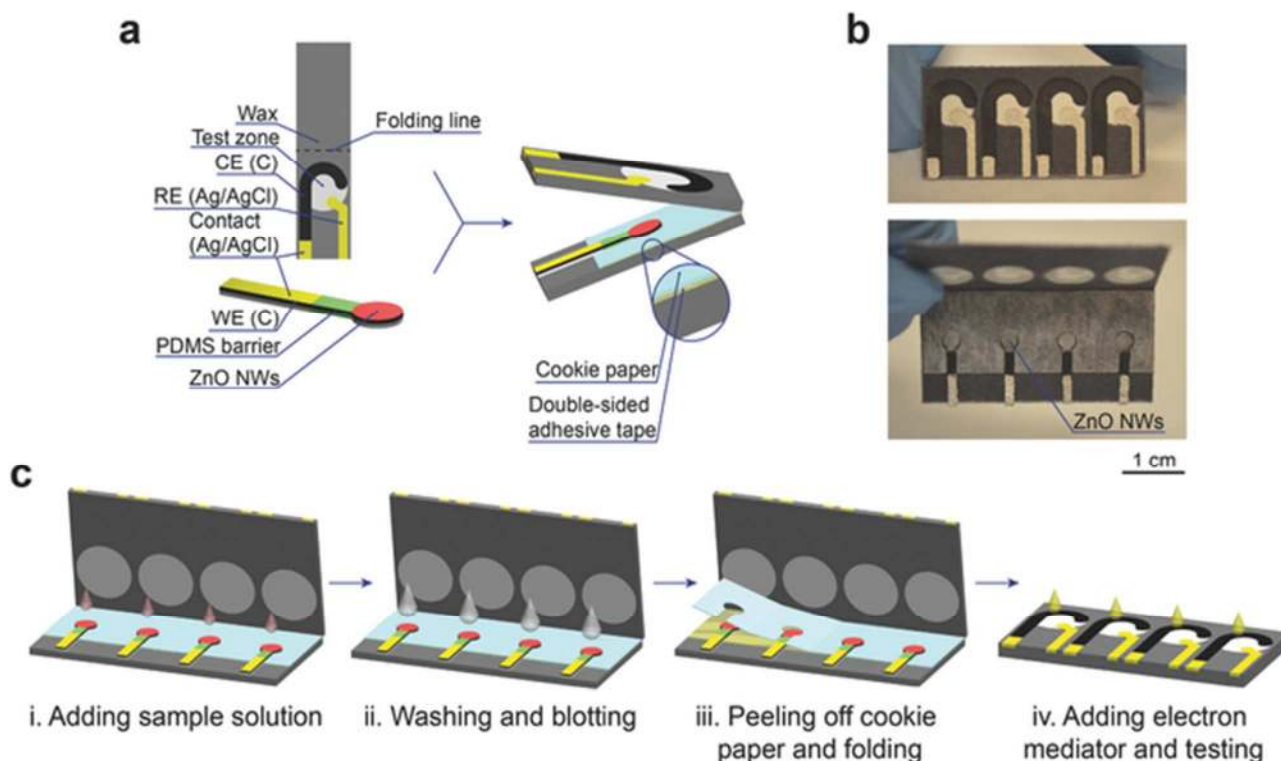


Figure 14. An origami-based electrochemical impedance spectroscopy assay for ultrasensitive analyte detection. a) Schematic of device with relevant electrochemical components. Zinc oxide nanowires are directly grown in the assay to improve the immobilization of probes. b) Images of folded and unfolded assembled devices. c) Testing protocol using the assay. Reprinted with permission from ref 87. Copyright 2016 Wiley-VCH Verlag GmbH & Co.

3.2.3. Single-sheet 3D μ PADs

In addition to stacking and folding, 3D μ PADs have also been created in single sheets of paper by controlling the density of deposited wax on the paper (i.e., penetration depth through the thickness of the paper when the wax is melted). When compared to stacking and folding, this approach reduces fabrication time and material, and removes any potential for user alignment error. However, single sheet integration may not achieve the same level of multiplexing possible with stacking and folding given the smaller volume per device. Li and Liu,⁶⁹ and Renault *et al.*⁷⁰ first demonstrated this concept around the same time using different methods for controlling density. In their work, Li and Liu⁶⁹ varied the color of patterned wax, where regions with lighter colored wax (low density)

have low penetration and similarly, regions with darker colored wax (high density) have high penetration (Figure 15). Renault *et al.*⁷⁰ employed double-sided wax printing to achieve 3D channels. Three types of microchannels were conceptualized: an open-channel which is the standard for μ PADs, a hemichannel, and a fully enclosed channel (Figure 16). Both hemichannels and fully enclosed channels reduce fluid evaporation during wicking, which is critical for limited sample volumes ($< 100 \mu\text{L}$). Fully enclosed channels also reduce the risk of contamination from the external environment.

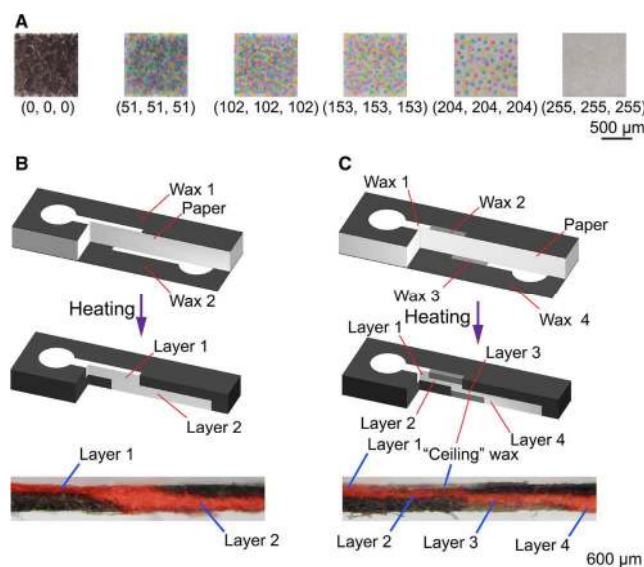


Figure 15. Three-dimensional channel networks formed in a single sheet of paper by varying wax density (color). (A) Wax printed at different RGB values ranging from black to grayscale. (B) Two-layer channel. (C) Four-layer channel. Reprinted with permission from ref 69. Copyright 2014 Springer.

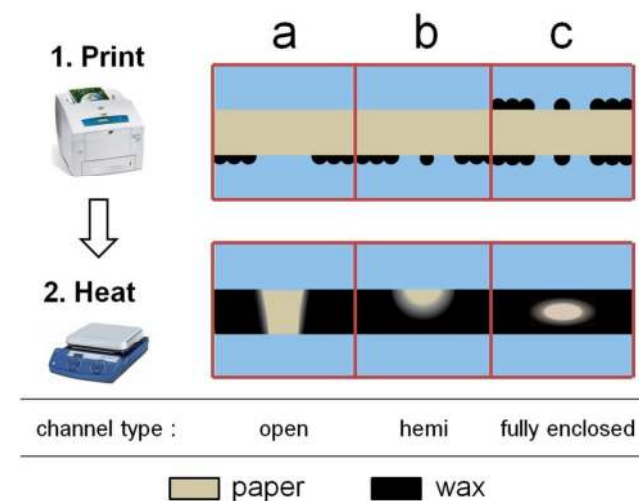


Figure 16. Three-dimensional channel networks formed in a single sheet of paper using double-sided wax printing: (a) open channel, (b) hemichannel, and (c) fully enclosed channel. Reprinted with permission from ref 70. Copyright 2014 American Chemical Society.

Jeong *et al.*⁸⁸ recently developed a “digital” assay using the single-sheet 3D channel approach to measure bovine serum albumin (BSA) and glucose levels in sample (Figure 17). Detection of both analytes is enabled by colorimetric signals generated when BSA and glucose react with pre-embedded reagents in their respective regions. BSA concentration is quantified by simply counting the number of bars that change to blue, where more bars indicate higher BSA concentration (e.g., one bar for 0.1 mg/mL and four bars for 1.0 mg/mL). This approach does not require external equipment, such as readers, to quantify target analytes, and the clockwise readout resembles the speedometer which is intuitive for users. The work exemplifies the potential of 3D μ PADs for sophisticated analysis in an easy-to-use compact format.

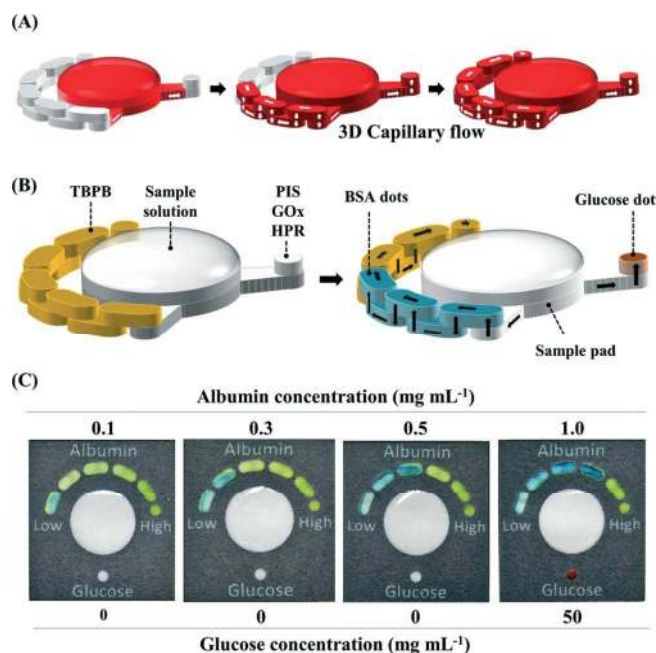


Figure 17. A “digital” assay using 3D channels in a single sheet of paper. (A) Schematic of three-dimensional flow in the assay to measure bovine serum albumin (BSA) and glucose levels in a sample. Detection of both analytes is enabled by colorimetric readout, where quantification of BSA is achieved by counting the number of blue colored bars. (B) The BSA detection region is pre-embedded with tetrabromophenol blue, which generates a blue color upon reaction with BSA. Similarly, the glucose detection region is treated with a mixture of potassium iodide, glucose oxidase, and horseradish peroxidase to give a red color in the presence of glucose. (C) Images of the assay after sample addition. The number of blue bars increases with increasing BSA concentration, up to four bars for 1.0 mg/mL of BSA. A red signal is generated when 50 mg/mL of glucose is present in the sample. Reprinted with permission from ref 88. Copyright 2015 The Royal Society of Chemistry.

3.3. Open Channel Flow

As described in section 2, imbibition in paper follows the Lucas-Washburn behavior, where wicking speed is intrinsically slow ($t \propto L^2$). Slow wicking imposes a practical constraint on the length of paper that can be wetted within a reasonable time period for testing (~10-15 min). To increase wicking speed in paper channels, paper matrix can be removed from the patterned channels such that the open space increases the effective pore diameter of the channel (i.e., $t \propto \frac{1}{r}$ from equation (1) in section 2).^{46,89–91} Faster wicking channels have also been created by sandwiching paper channels between two sheets of plastic.^{92,93}

Renault *et al.*⁸⁹ combined open channels with standard paper channels, forming a hybrid channel with capillary pressure-driven flow. Wicking in the hybrid channel followed Lucas-Washburn behavior, however, the rate of transport was substantially enhanced by the addition of the open channel (i.e., increase in effective pore radius r of the overall hybrid channel), as shown in Figure 18. Similar flow rate enhancement was observed in the razor-scored channels developed by Giokas *et al.*⁹¹ and the two-ply channels by Camplisson *et al.*⁴⁶

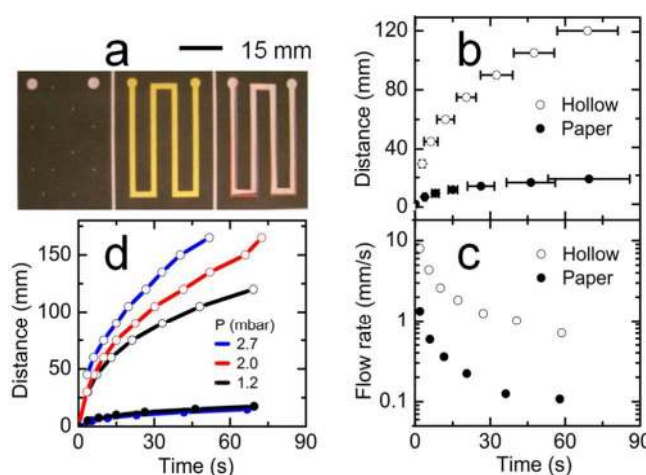


Figure 18. Hollow channels enable faster flow rates and better distance coverage. (a) Image of device with a port layer (left), a standard paper channel layer (middle), and hollow channel layer (right). The device is assembled by folding the right layer on top of the middle layer followed by the left layer. (b-c) Comparison of wetted distance and flow rate in the device with and without hollow channels. (d) Wetted distance for different applied pressures (sizes of fluid droplets applied to the ports). Reprinted with permission from ref 89. Copyright 2013 American Chemical Society.

Pressure-driven flow can also be achieved in open channels and behaves similar to that in open channels in polymer substrates. Glavan *et al.*⁹⁰ demonstrated pressure-driven flow in omniphobic open channels to create a number of iconic microfluidic devices including a serial diluter and droplet generator (Figure 19). To rectify flow in their device, open channels were simply folded or unfolded at specific regions to valve on and off flow. Time delays were also created by varying the length of space between open channels that still contained porous matrix. One caveat of the approach, however, is the requirement of an external pumping source to drive flow since the

paper assays are non-wetting. In general, the use of open channels in paper to improve wicking speed is counter-intuitive and somewhat redundant. Open channel polymeric microfluidic devices already provide a viable avenue for achieving fast flow rates. It is not clear these types of paper-based channels will find practical utility for diagnostics.

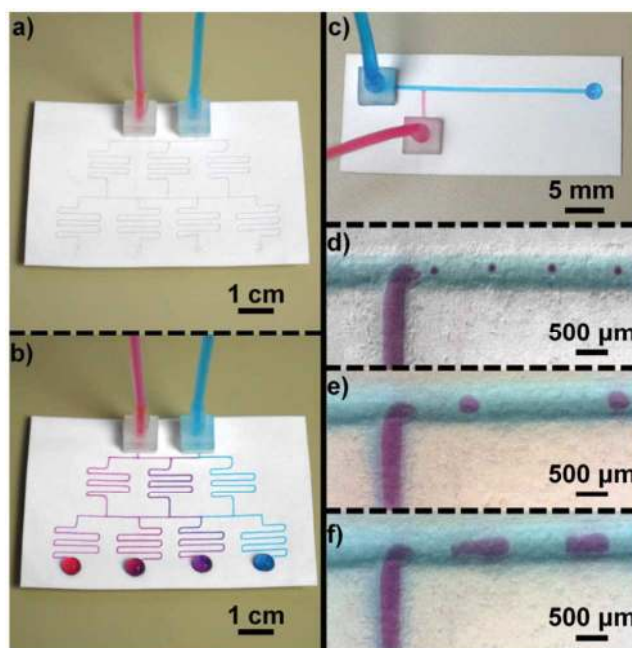


Figure 19. Pressure-driven flow in omniphobic hollow channels for (a-b) serial dilution and (c-f) droplet generation. Reprinted with permission from ref 90. Copyright 2013 The Royal Society of Chemistry.

3.4. Time Delays

While cross-section geometry, permeability and paper orientation can be varied to control fluid advance to some degree, many multistep diagnostic applications have more complex timing requirements. Time delays are often essential to precisely control the onset and offset of reactions and ultimately, to automate multistep assays. This subsection examines the chemical and physical strategies that have been used to achieve controlled delays in paper-based assays.

3.4.1. Chemical-based Delays

Chemical-based delays are created by chemically treating the paper matrix to alter its permeability. These chemicals can be dissolved when sample is added or are permanently embedded in the matrix to rectify flow. Two types of time delays have been developed using dissolvable substances: (1) a barrier embedded in a paper channel that allows downstream flow after it is dissolved and (2) a bridge that connects two paper channels and stops flow after it is dissolved.

Lutz *et al.*⁹⁴ demonstrated the barrier concept using dried sugar in paper. Sugar is non-reactive and thus, does not generally affect assay chemistries. However, the addition of sugar into the assay may limit the type of analyte that can be measured. For example, sugar-based time delays are a non-starter for the many assays related to glucose. The authors developed a multistep two-dimensional paper network for detecting malaria antigen in serum using the approach (Figure 20). The length of each time delay was determined by the concentration of sugar dried in each leg. The only required user steps were adding reagents to designated loading pads and folding the device. Upon folding, reactions were sequentially activated by the sugar delays without user intervention. As noted by Professor George Whitesides, this approach is inexpensive and has added benefits in terms stabilizing proteins in a dried state.⁹⁵ The bridge concept was also demonstrated by both Houghtaling *et al.*⁹⁶ and Jahanshahi-Anbuhi *et al.*⁹⁷ around the same time. Both groups used a bridge to connect two paper channels, shutting off flow once it was dissolved (Figure 21). This type of delay is useful for automated sample metering when there is an abundant source. The size of the bridge provides control for the volume of sample to be metered.

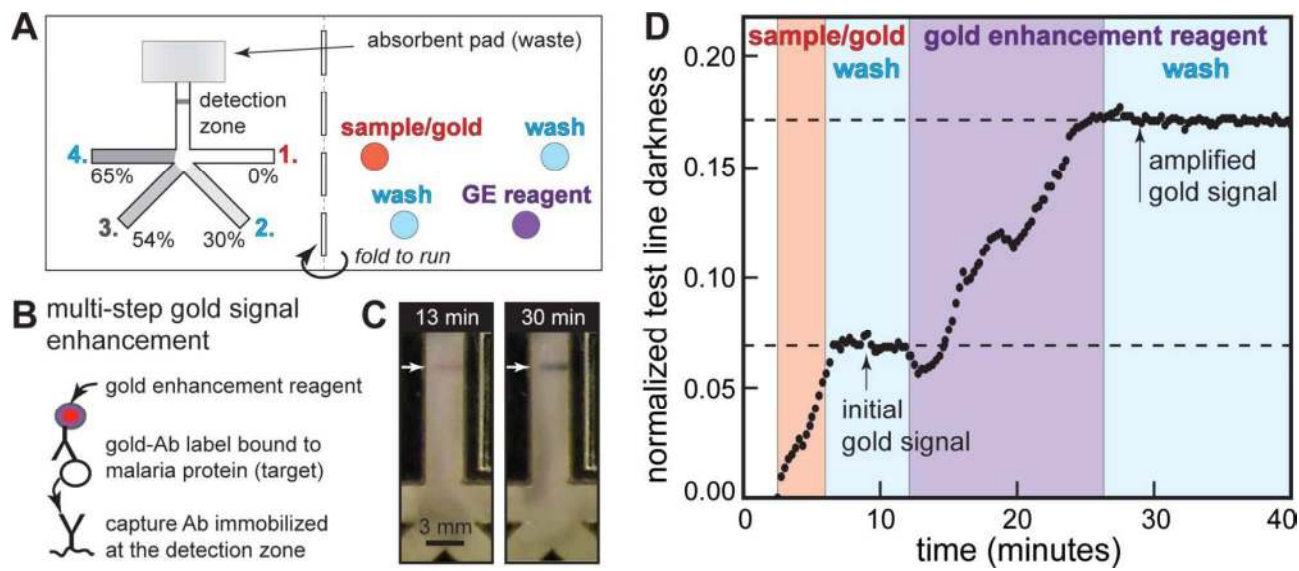


Figure 20. Dissolvable sugar delays for timing fluid delivery in a multistep two-dimensional paper network for malaria antigen detection in serum. (A) Schematic of the network. Each reaction leg has a different concentration of dried sugar to precisely control the arrival of reagent. (B) Schematic of the immunochemistry and signal enhancement used in the assay. (C) Images of original signal after 13 min. and amplified signal after 30 min. (D) Signal intensity vs time with shaded regions indicating specific reactions. Reprinted with permission from ref 94. Copyright 2013 The Royal Society of Chemistry.

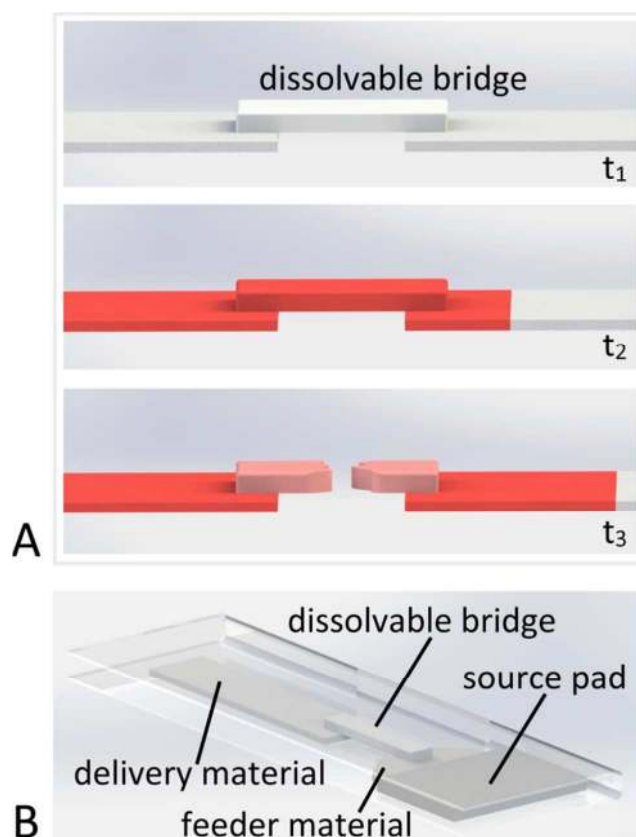


Figure 21. Dissolvable bridge connecting two paper channels. (A) Flow is shut off after the bridge dissolves. (B) Schematic of an assay with a dissolvable bridge for metering sample volume. Reprinted with permission from ref 96. Copyright 2013 American Chemical Society.

In addition to dissolvable substances, wax has been used to permanently tune the permeability of paper for timing purposes. The wax approach is, perhaps, more streamlined than others since most paper-based assays are already commonly defined by wax printing. Noh and Phillips⁹⁸ used paraffin wax to meter samples in a 3D μ PAD. Timing and sample metering in the device were achieved by patterning a metering layer with varying amounts of wax. Flow through a port layer to a bottom analysis layer was then modulated by a middle metering layer. The authors cleverly leveraged this approach for time-dependent quantification of biomarkers (Figure 22).^{99,100} Other groups have also used wax to alter paper permeability for timing fluid transport, leveraging parameters unique to wax printing such as color¹⁰¹ and brightness¹⁰² to control the amount of wax embedded in the paper matrix.

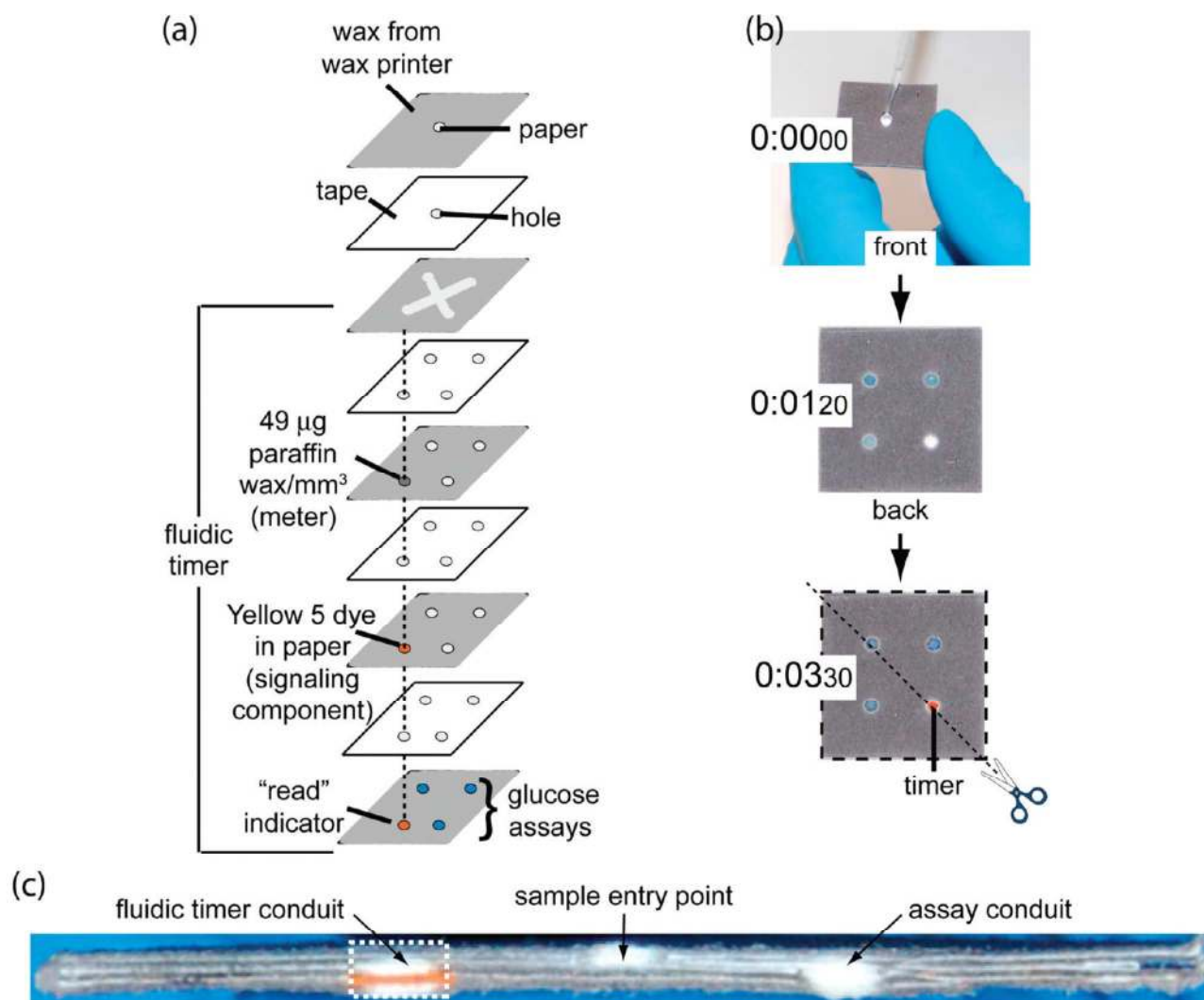


Figure 22. A time-dependent assay for measuring glucose. (a) Exploded view of the layers of the assay. (b) Sample is added to a central reservoir. The blue dots indicate positive results for glucose in the sample. The assay is completed when the orange dot appears. (c) Cross-section of the fluidic timer. Reprinted with permission from ref 99. Copyright 2010 American Chemical Society.

Moreover, chemicals such as alkyl ketene dimer have been patterned in paper to create semi-permeable valves.¹⁰³ Thiol-ene 'click' chemistry¹⁰⁴ has been used to create fluidic diodes in paper.¹⁰⁵ The diode consists of two terminals (anode and cathode) separated by a hydrophobic gap (Figure 23). The anode is treated with a surfactant that gets reconstituted during flow. The

surfactant adsorbs into the hydrophobic gap, reducing surface tension in this region to allow flow toward the cathode.

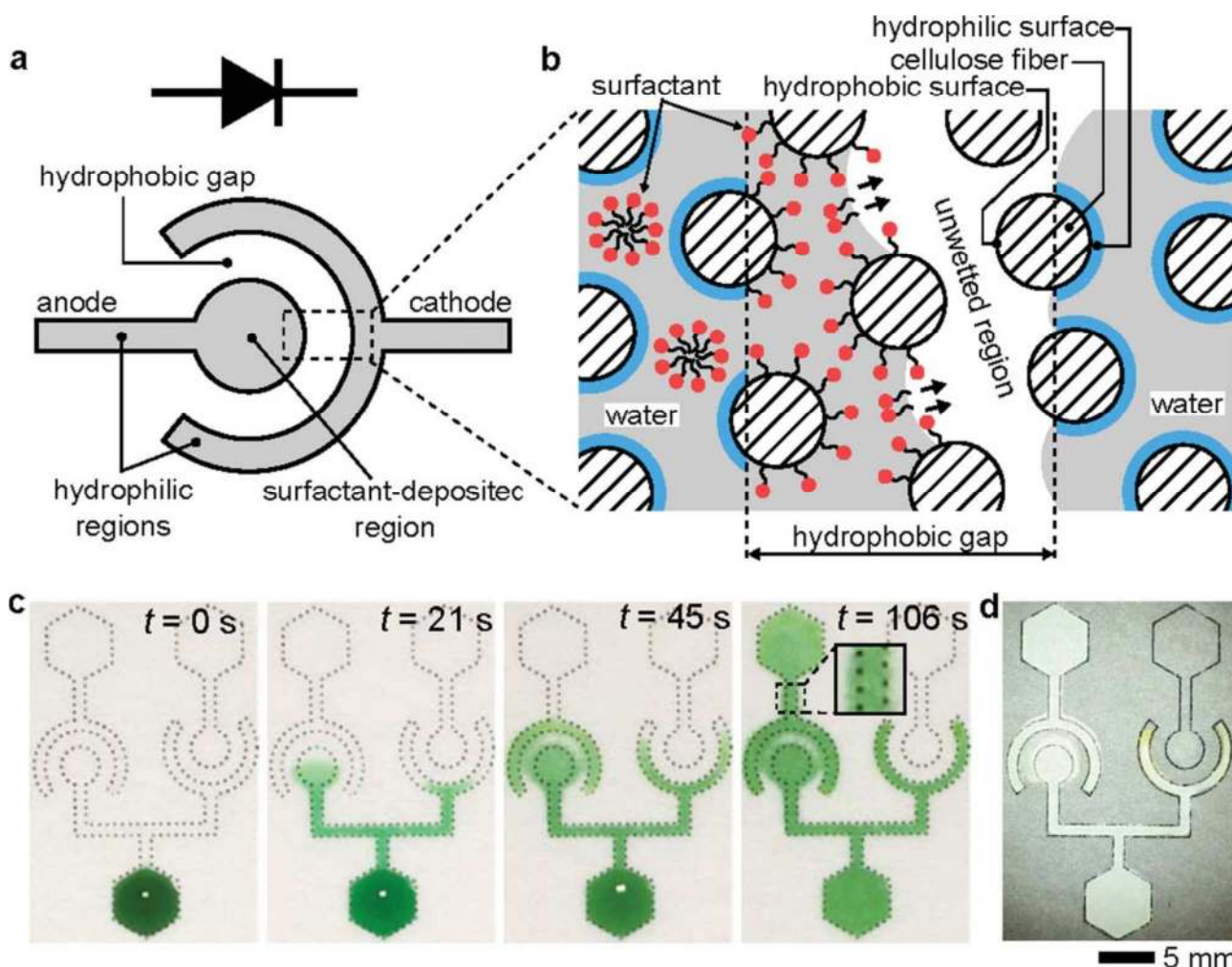


Figure 23. A two terminal diode in paper. (a) Schematic of the diode consisting of an anode, cathode, and hydrophobic gap. (b) Mechanism of fluid transport across the diode. Surfactant in the anode is reconstituted during flow, which adsorbs into the hydrophobic gap. Surface tension in the gap is subsequently reduced, allowing flow towards the cathode. (c) Time series of the diode in operation. (d) Regulation of human serum delivery with the diodes. Reprinted with permission from ref 105. Copyright 2012 The Royal Society of Chemistry.

Laser direct writing has also been used to fabricate time delays.¹⁰⁶ The method involves patterning paper with photopolymer followed by targeted polymerization via laser. He *et al.*¹⁰⁶ developed two types of time delays using this strategy – a solid barrier that partially penetrates

through the thickness of the paper and a porous barrier through the entire thickness. In both cases, the permeability of the polymerized region is substantially reduced, increasing fluidic resistance and slowing flow in that region. Similar to wax printing, laser direct writing is a precise and rapid fabrication technique that can streamline the design of multiple fluidic features (i.e., channels and time delays) without the post-writing addition of chemicals.

3.4.2. Physical Delays

In comparison to chemical-based strategies, physical modification of the paper matrix does not require additional reagents and provides more flexibility in designs for rectifying flow. Potential reactivity of samples to the patterned chemicals is also less of a concern. Toley *et al.*¹⁰⁷ used cellulose absorbent pads as shunts to delay flow in paper channels. The effect is similar to increasing the cross-sectional area, but introducing an additional material allows much larger time delays independent of the planar device design. Shunts were placed in direct contact with channels, creating a parallel flow path and delaying fluid delivery to its target region (Figure 24). Using the electrical circuit analogy noted earlier, the shunt becomes a parallel resistor to the channel and adds resistance to the overall fluidic circuit. Flow rate in the circuit can be tuned by changing the size of the shunt, and time delays ranging from 3 to 20 min have been realized.¹⁰⁷ The authors recently extended their shunt method to include expandable and movable pads for fluid switching and rerouting capabilities.¹⁰⁸ A complete valving toolkit was developed to include on-switches, off-switches, and flow-diversion switches. All switches were activated by an expandable sponge that connects or disconnects different channels depending on the switching mechanism. These valving systems do not require external actuation or chemicals to function. They can also be pre-programmed to automate multistep diagnostic protocols.

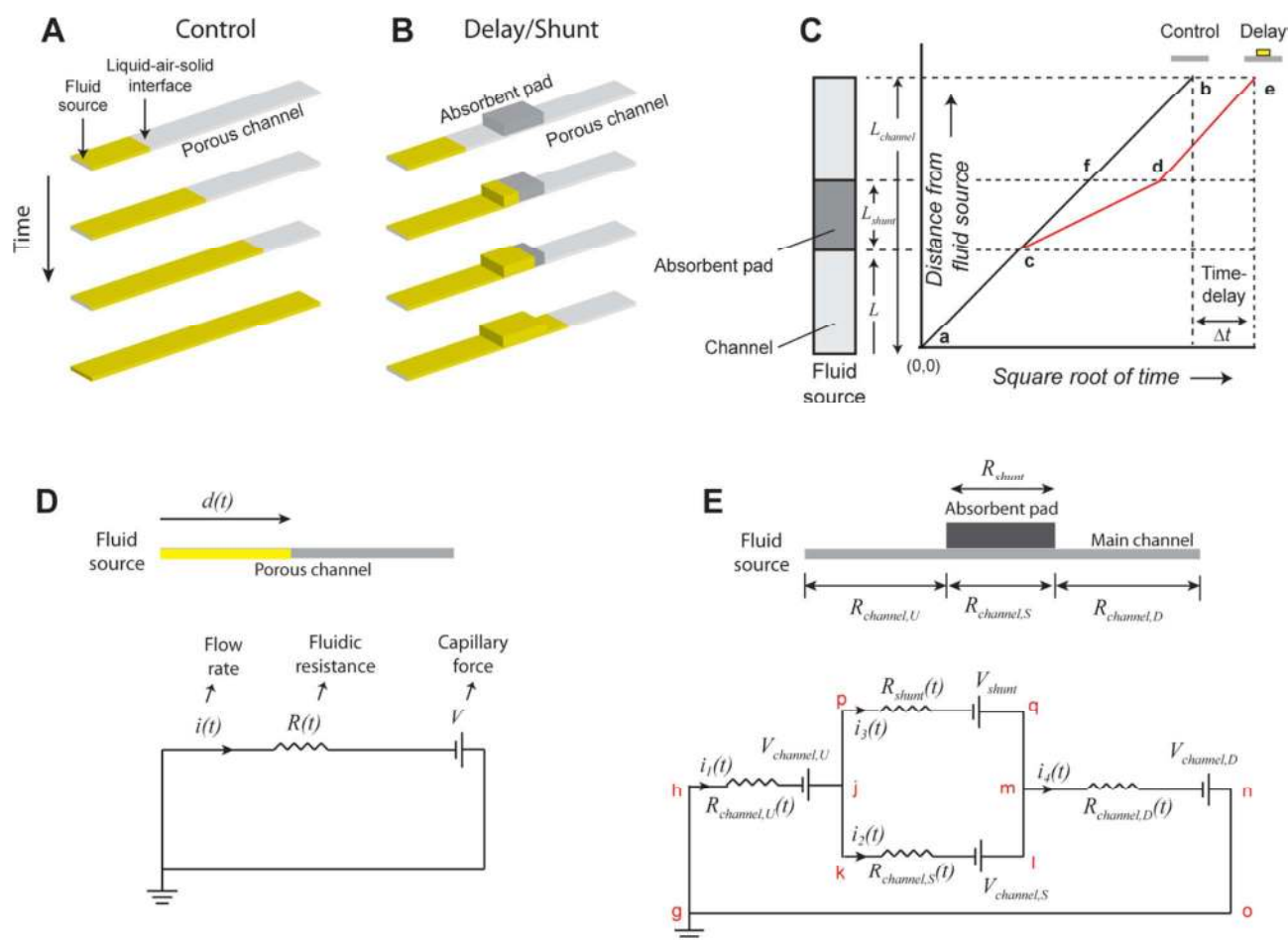


Figure 24. Timing fluid transport in paper-based assays with shunts. (A) Schematic of flow in a standard paper channel. (B) Schematic of flow in a paper channel with a shunt. (C) Idealized plot of distance vs time showing time delay when a shunt is used. Electrical circuit analogy for a standard (D) channel and (E) a channel with a shunt. The shunt is a parallel resistor to the channel and adds resistance to the overall circuit. Reprinted with permission from ref 107. Copyright 2013 American Chemical Society.

Researchers have also directly modified physical parameters of the paper matrix, such as porosity, to rectify flow. Shin *et al.*¹⁰⁹ demonstrated that time delays can be easily manufactured in paper by compressing the matrix in specific regions, effectively reducing the porosity and increasing fluidic resistance of that region. Flow rate in the compressed region can be tuned by the degree of compression applied to the region during fabrication, analogous to compression of carbon paper in electrochemical applications.¹¹⁰ Using this compression strategy, Park *et al.*¹¹¹ developed a multistep assay to detect *Escherichia coli* O157:H7 and *Salmonella typhimurium*. The device only

required an initial dipping step by the user to introduce sample into the assay. All processing and readout steps were then automated via the time delays.

3.5. Hydrogel-based Transport and Storage

Hydrogels are hydrophilic polymeric networks capable of absorbing large volumes of fluid. Natural, synthetic, and hybrid hydrogels have been used extensively in biomedical applications, mainly as scaffolds for engineered tissue constructs and vehicles for drug delivery.^{112–115} Fluid retention in hydrogels is largely dependent on their bulk structure, which can be tailored to specific applications. Once swollen, hydrogels can be triggered to collapse via external stimuli (e.g., temperature, pH, UV-irradiation), releasing their encapsulated contents. This capacity for controlled storage and delivery of fluids has prompted a number of groups to exploit hydrogels for flow control, and reagent storage and delivery in paper-based assays.^{116–120} Other stimuli-responsive gels, such as ionogels – polymer gels that contain ionic liquids, have also been used as passive pumps for fluid delivery.¹²¹

For controlled fluid delivery, Niedl and Beta¹¹⁶ synthesized temperature-sensitive *N*-isopropylacrylamide (NIPAM) hydrogel pads as dynamic fluid reservoirs. The gel pads were placed in contact with paper-based assays, where fluid delivery was achieved by collapsing the gel. Gel collapse was triggered by heating the gel above its lower critical solution temperature, 31 °C. The rate of collapse was controlled by adding acrylamide to the NIPAM hydrogel, where pure NIPAM gels collapsed instantaneously and NIPAM-acrylamide composites collapsed gradually over time (Figure 25). The addition of acrylamide increased the degree of hydrogen bonding with water molecules in the gel matrix, effectively reducing the rate of fluid release. The overall practicality of this method will depend on the robustness of the hydrogels in real-world conditions, where temperatures can fluctuate drastically in short periods of time. Evaporation is also an inherent

caveat of hydrogels, affecting its structural stability. Thus, precise temperature-based flow control may be difficult to achieve in the range of temperatures expected in practice.

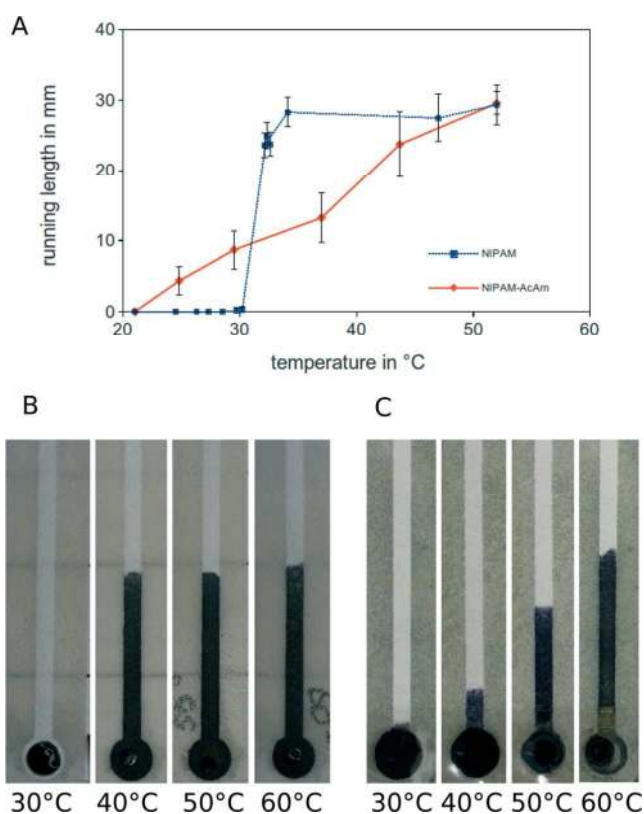


Figure 25. Temperature-sensitive hydrogels for flow control in paper-based assays. (A) Plot showing instantaneous release of encapsulated fluid for the pure NIPAM gel (blue line) and gradual release for the NIPAM-acrylamide gel (red line). Images comparing the rate of collapse and wetting in paper channels at different temperatures for the (B) NIPAM and (C) NIPAM-acrylamide gels. Reprinted with permission from ref 116. Copyright 2015 The Royal Society of Chemistry.

Similarly, Akyazi *et al.*¹²¹ directly polymerized ionogel reservoirs into their paper-based devices for passive pumping. Fluid added to a reservoir was first absorbed by the ionogel and gradually released into a downstream paper channel upon gel saturation. Wicking in the channel was controlled by using ionogels with different swelling rates, achieved by incorporating different ionic liquids within the gel matrices (Figure 26). Although effective at delivering fluids in a controlled manner, the reactivity of the ionic liquids used to form the ionogels remains a concern.

Common biological targets, such as proteins and nucleic acids, are polar molecules that can potentially react with the ionic liquids causing unwanted reactions. Further characterization with biological samples is needed to confirm the practicality of ionogels for paper-based diagnostics.

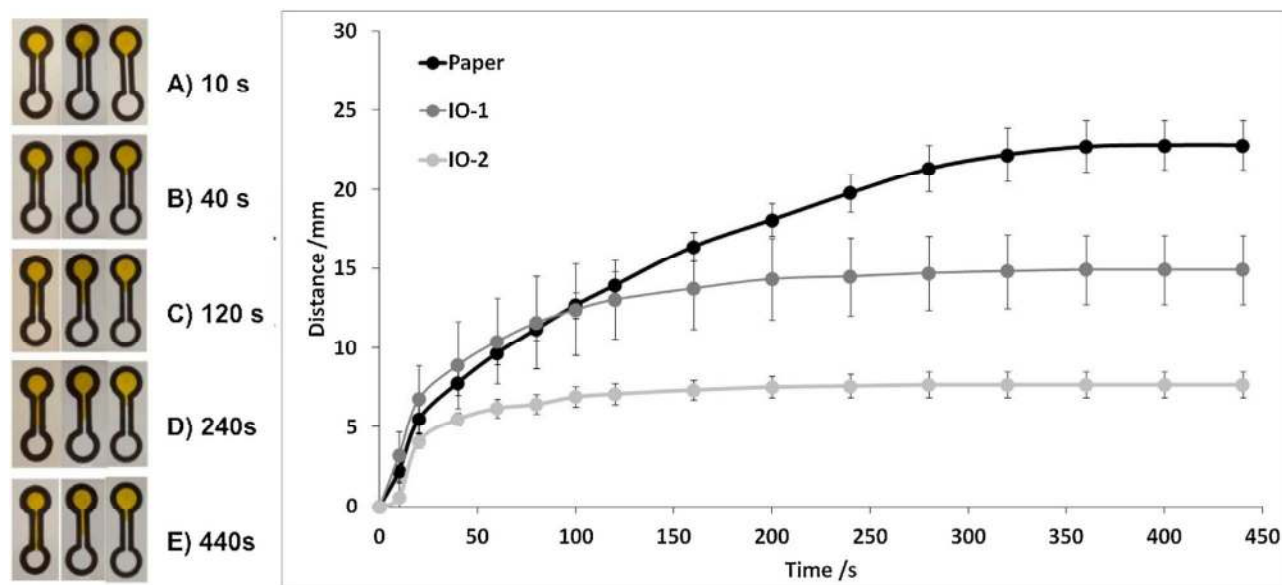


Figure 26. Ionogels directly polymerized into paper-based assays for passive pumping. (A-E) Time series of images showing wicking in the paper-based assays. Left images – pristine paper. Middle images – ionogel 1 (IO1). Right images – ionogel 2 (IO2). Plot showing wicking distance versus time for pristine paper, IO1, and IO2. Different swelling rates between IO1 and IO2 result in different wicking speeds in the paper channel. Reprinted with permission from ref 121. Copyright 2016 Elsevier.

Yang and colleagues demonstrated the regulation of flow and reagent release in paper-based assays using aptamer-crosslinked hydrogels.^{118–120} These hydrogels are composed of a linker-aptamer that binds to target DNA in the sample and also to polyacrylamide polymers crosslinked with complimentary short DNA sequences. Hydrogel polymerization occurs when unbound linker-aptamer hybridizes to the crosslinked polymer. Conversely, target DNA binding to linker-aptamer prevents hybridization and gel polymerization. Two separate strategies for flow regulation were demonstrated, either relying on maintaining or transitioning the hydrogel to solution phase: 1) target-aptamer binding prevents hydrogel polymerization, allowing downstream flow (hydrogel

remains in solution phase),¹¹⁸ and 2) target-aptamer binding collapses pre-polymerized hydrogel, allowing flow and releasing encapsulated reagents (hydrogel transitions to solution phase).^{119,120}

Figure 27 illustrates the working principle of the first strategy.

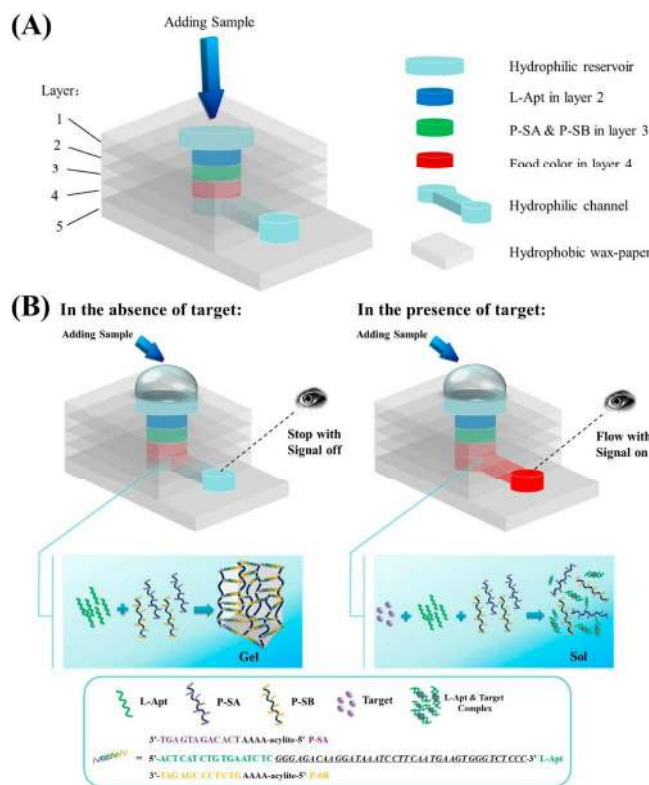


Figure 27. Aptamer-crosslinked hydrogels for flow regulation in 3D paper-based assays. (A) Schematic of the different layers of the 3D paper-based assay. (B) Addition of a sample without targets induces hybridization between aptamers and crosslinked polymers and subsequently, hydrogel polymerization. The polymerized hydrogel blocks downstream flow. Conversely, target binding to aptamers prevents hybridization and polymerization, allowing downstream flow to respective readouts. Reprinted with permission from ref 118. Copyright 2015 American Chemical Society.

In the context of reagent storage, hydrogels offer several advantages over dried reagents in the paper matrix. Namely, gel encapsulation of sensitive and expensive reagents reduces environmental degradation and improves the stability of the reagents. Mitchell *et al.*¹¹⁷ demonstrated the capability of *N,N'*-methylenebisacrylamide-cross-linked poly(*N*-isopropylacrylamide) gels for the storage of small molecules, enzymes, antibodies, and DNA. The

enzyme horseradish peroxidase was stored up to 35 days with no significant loss in activity. Gel-based storage minimizes potential biological contamination and can achieve similar robustness as paper-based devices packaged with dessicant.¹²² The thermostability of the hydrogels, however, was not directly addressed. Varying temperatures could prove detrimental to the stability of the stored reagents.

3.6. Externally Actuated Structures

Paper-based assays have been designed with externally actuated features to modulate flow. Manually actuated structures include movable arms and slip layers that connect one fluidic region to another when activated.^{76,78,123–125} The paper-based slip layer concept is based on the earlier SlipChip,¹²⁶ a glass-based microfluidic device with two sliding plates. This approach is particularly advantageous when high-throughput and parallel processing is required. For example, fluid can be simultaneously delivered to a large array of reservoirs (Figure 28a) or sequentially delivered to multiple channels at the same time (Figure 28b).¹²⁴ Liu *et al.*⁷⁶ demonstrated a multistep ELISA in a 3D μ PAD with a slip layer. Sample introduced to the slip layer was sequentially maneuvered into contact with reagent zones, detecting rabbit IgG as a proof-of-concept analyte. More recently, a slip-based 3D μ PAD was developed for the detection of human norovirus. The device was activated by slipping a layer containing sample and buffer onto downstream processing layers (Figure 29). An impressive LOD of 9.5×10^4 copies/mL of human norovirus was achieved, which is up to 100-fold lower than commercial lateral flow assays.⁷⁸

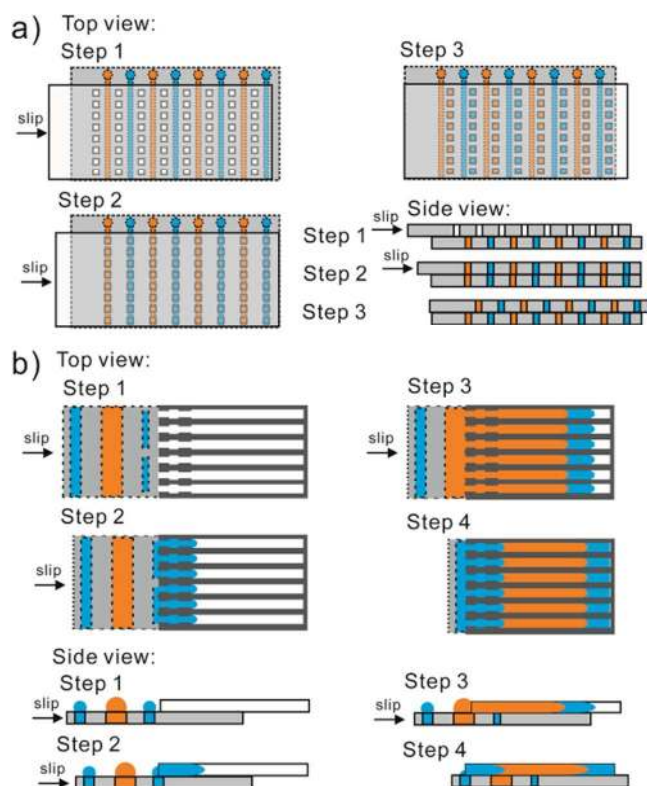


Figure 28. High-throughput and parallel processing in paper-based assays with a slip layer. (a) Simultaneous delivery of fluid to a large array of reservoirs in parallel. (b) Sequential delivery of fluid to multiple channels at the same time. Reprinted with permission from ref 124. Copyright 2013 American Chemical Society.

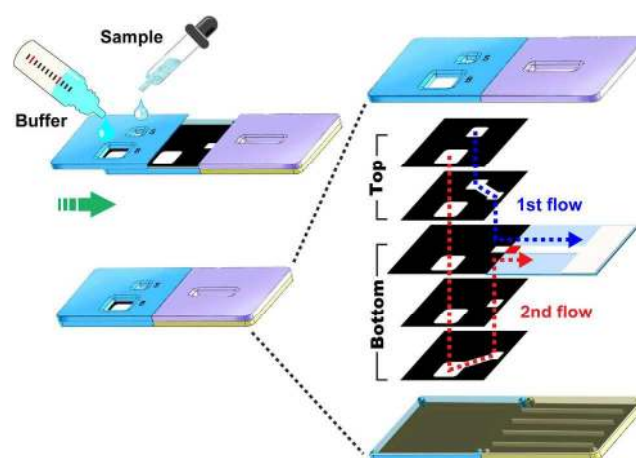


Figure 29. A slip-based 3D μ PAD for the detection of human norovirus. Sample and buffer are introduced onto the slip layer. The device is activated by sliding the layer onto downstream processing layers. Analyte processing and signal enhancement are sequentially automated by fluidic controls in the assay. Reprinted with permission from ref 78. Copyright 2016 Nature Publishing Group.

External electromagnets have also been used to actuate ferromagnetic paper cantilevers as valves.¹²⁷ The opening and closing of the cantilever is controlled by a timing channel that triggers the electromagnet. An ionic salt bridge acts as an on-switch for electrodes directly patterned in the timing channel. When fluid wets the salt bridge, the electrical circuit closes and activates the electromagnet. Although more precise than manually actuated structures, the additional electromagnetic components increase the complexity of device fabrication. Such external hardware requirements also reduce the ultimate affordability of the assay, undermining a key motivating advantage of the paper-based approach.

3.7. Analyte Concentration during Wetting

Despite the many advantages of paper-based assays, poor detection sensitivity remains an issue. A commonly used approach for enhancing detection sensitivity is colorimetric signal enhancement. The most common colorimetric labels used in lateral flow assays and paper-based microfluidic assays are gold nanoparticles. Gold nanoparticles can be readily attached to different affinity reagents (e.g., antibodies) and produce an intense red color due to their localized surface plasmonic resonance.¹²⁸ Accordingly, strategies for enhancing color signal intensity typically involve increasing the optical density of gold nanoparticles in the readout. Commercial gold enhancement solution is available and has been applied to paper-based assays.^{61,62,129} Using this solution, 6-fold improvement in signal intensity¹²⁹ and 4-fold improvement in the LOD of bovine serum albumin have been achieved.⁶¹ Hu *et al.*¹³⁰ improved the optical density of gold nanoparticles in their assay by forming gold nanoparticle aggregates. These aggregates were conjugated with probes to capture HIV sequences in sample, achieving a 2.5-fold improvement in LOD. A number of other techniques based on enhancing gold nanoparticles are also available in the literature.^{131–134}

1
2
3 Recently, a polymerization-based amplification strategy was developed using a light
4 responsive hydrogel (Figure 30).¹³⁵ The hydrogel solution contained photoinitiators bound to
5 affinity reagents for specific biomolecules. Application of light triggered polymerization of the
6 hydrogel, producing a highly contrasted color change in the presence of target analytes. The authors
7 applied their approach to the detection of malaria antigen in serum, achieving a LOD of 7.2 nM.
8 Other methods for analyte concentration during wetting include the use of volatile solvents and
9 aqueous two-phase flow. In the work by Yu and White,¹³⁶ target analytes were concentrated in a
10 lateral flow assay by the evaporative wicking of a solvent, achieving 24-fold improvement in the
11 signal readout. Chiu *et al.*¹³⁷ developed a two-phase solution system to concentrate analytes in the
12 salt-rich portion of the solution. Using this approach, they achieved a 10-fold improvement in the
13 LOD of the protein transferrin.
14
15
16
17
18
19
20
21
22
23
24
25
26
27
28
29
30
31
32
33
34
35
36
37
38
39
40
41
42
43
44
45
46
47
48
49
50
51
52
53
54
55
56
57
58
59
60

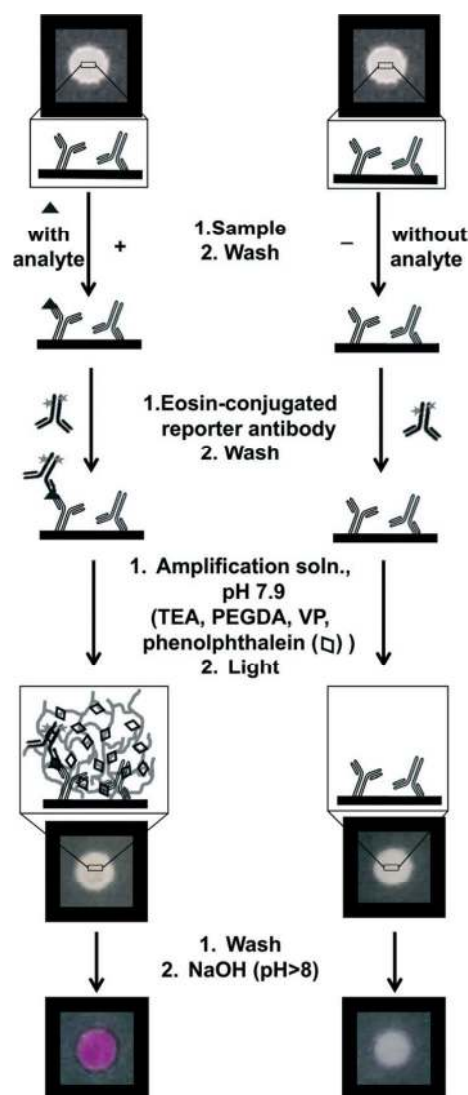


Figure 30. Polymerization-based amplification of colorimetric signal readout in paper. Hydrogel containing photoinitiators bound with affinity reagents are added to the device after sample introduction. Dosing with light activates polymerizes the hydrogel and produces a sharp color change in the presence of target analytes. Reprinted with permission from ref 135. Copyright 2014 The Royal Society of Chemistry.

3.8. Post-wetting Analyte Concentration

The strategies described in section 3.7 demonstrate concentration of analytes beyond the current capabilities of conventional lateral flow assays. However, they rely on capillary action generated in the remaining dry portions of the paper matrix. Once a paper-based assay is saturated, further analyte concentration is generally not possible with these approaches. To achieve post-wetting

manipulation, the most relevant available techniques are those that apply external fields (e.g., acoustic, thermal, and electric fields).

Surface acoustic waves (SAWs) have been used to deliver sample from a paper-based assay into a mass spectrometer¹³⁸ and to uniformly mix fluids in paper.¹³⁹ For mixing in paper, SAWs atomize fluid at the end of a Y-channel via acoustic signals generated by a transducer (Figure 31). Atomization creates a negative pressure gradient in the channel, drawing and uniformly mixing fluid at the same time. The SAW approach outperformed capillary flow-based mixing, albeit at the expense of added complexity. Taking a different approach, Wong *et al.*¹⁴⁰ demonstrated that analyte concentration can be achieved by continuously evaporating fluid from the end of a wetted paper channel via localized heating. Using this approach, the authors were able to concentrate a tuberculosis biomarker, lipoarabinomannan, up to 20-fold without compromising its detectability.

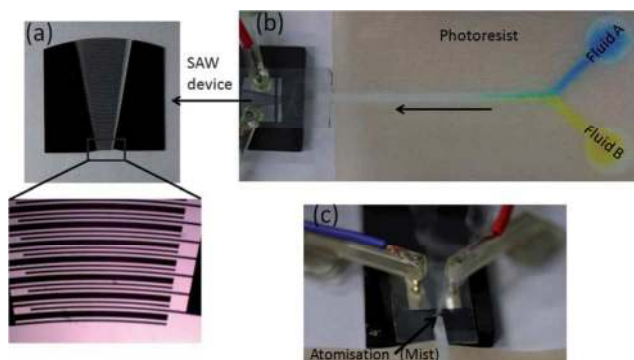


Figure 31. Application of surface acoustic waves (SAWs) to uniformly mix fluids in paper. (a) Transducer to generate SAWs. (b) Atomization of fluid in the Y-channel creates a negative pressure, drawing fluid toward the transducer. Fluids A and B are uniformly mixed. (c) Image of atomized fluid. Reprinted with permission from ref 139. Copyright 2012 The Royal Society of Chemistry.

The first of several electrokinetic phenomena to be applied in paper was electrophoresis dating back to the 1950s.²¹ Several other electrokinetic methods have been translated to paper, including isotachopheresis and ion concentration polarization. Isotachopheresis or ITP can be

1
2
3 leveraged to concentrate and separate ionic compounds based on an ion mobility gradient.¹⁴¹ A
4
5 similar technique to ITP called field amplification stacking, which also relies on an ionic gradient,
6
7 has also been demonstrated for sample preconcentration in paper-based assays.^{142,143} ITP has been
8
9 used extensively in traditional microfluidic devices for biomolecular detection, concentration, and
10
11 separation.^{7,144–146} Moghadam *et al.*¹⁴⁷ first demonstrated the ITP concept in paper and concentrated
12
13 a fluorescent tracer up to 900-fold as proof-of-concept. They applied their method to a lateral flow
14
15 assay or detecting IgG (Figure 32), improving the LOD by two orders of magnitude with analytical
16
17 sensitivity comparable to laboratory-based ELISA.¹⁴⁸ Around the same time, Rosenfeld and
18
19 Bercovici¹⁴⁹ developed a similar ITP approach to concentrate analytes in paper-based assays,
20
21 achieving up to 1000-fold signal amplification of a fluorescent tracer.
22
23
24
25
26
27
28
29
30
31
32
33
34
35
36
37
38
39
40
41
42
43
44
45
46
47
48
49
50
51
52
53
54
55
56
57
58
59
60

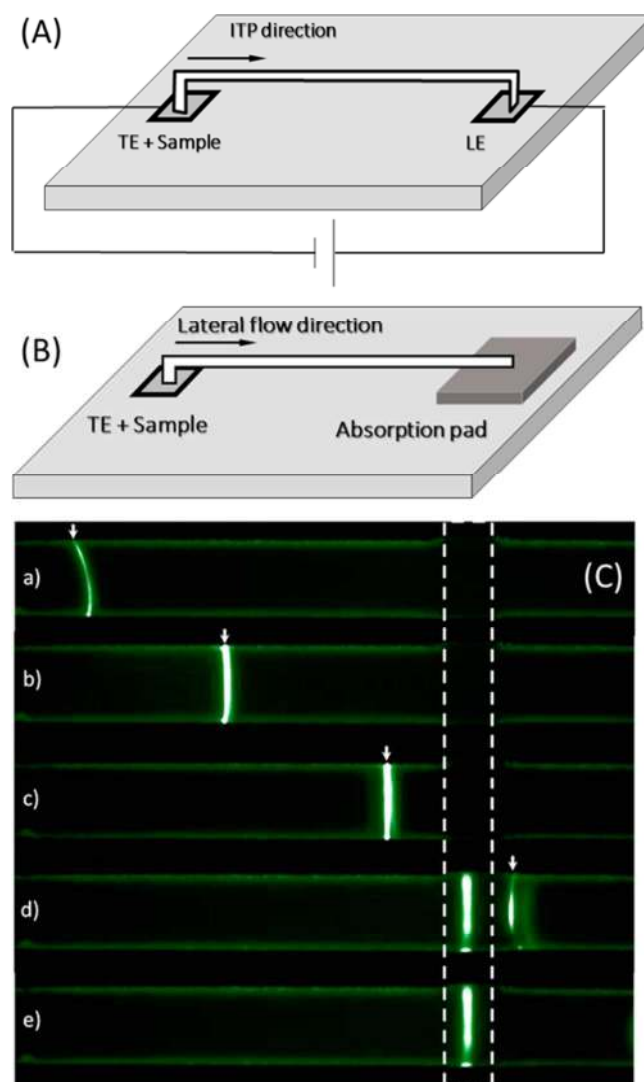


Figure 32. Isotachophoretic concentration in a lateral flow assay. (a) Schematic of setup for ITP focusing. (b) Schematic of a lateral flow assay without ITP, as a control experiment. (c) Time series of ITP focusing of Alexa Fluor 488 IgG. Reprinted with permission from ref 148. Copyright 2015 American Chemical Society.

Recently, Li *et al.*¹⁵⁰ developed an ITP *o*PAD for DNA focusing (Figure 33). A slip layer designates the starting boundary for sample focusing. Single stranded DNA (ssDNA) was concentrated after 4 min, reaching a concentration factor up to 100-fold. In comparison to the lateral flow format for ITP, the *o*PAD design reduces the overall length of the assay, enabling high electric field generation with low voltage sources (e.g., two nine volt batteries). This design improves the portability of ITP devices and is more conducive for field deployment.

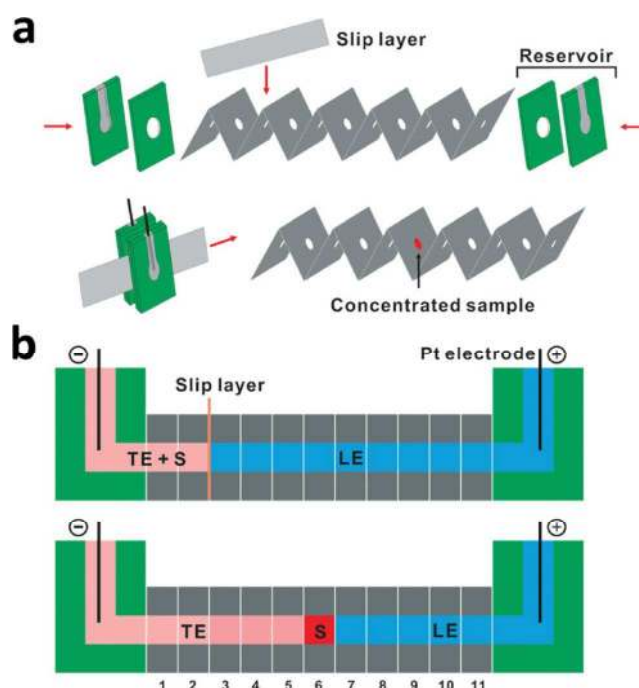


Figure 33. Low voltage isotachopheretic concentration of DNA in an oPAD. (a) The device consists of a slip layer to form the starting boundary for sample focusing and an oPAD sandwiched between buffer reservoirs in plastic. Width averaged concentration profiles. (b) Continuous accumulation of the tracer over time. (c) Images of the focused tracer at different locations in the paper channel. Reprinted with permission from ref 150. Copyright 2015 The Royal Society of Chemistry.

Another electrokinetic phenomenon that has been successfully deployed in paper is ion concentration polarization (ICP).^{44,151–155} ICP occurs at the interface of ion-selective nanochannels and microchannels, where an applied electric field causes the formation of ion depletion and enrichment zones.^{156,157} These ICP effects have been leveraged for water desalination,^{158,159} biomolecular concentration,^{160,161} and separation^{162,163} in traditional microfluidic devices. Gong *et al.*¹⁵¹ first demonstrated the feasibility of ICP in paper-based assays for concentration and directional transport of target analytes (Figure 34). Fluorescent tracers were concentrated up to 40-fold and the LOD for FITC-labeled bovine serum albumin was improved by 5-fold. The direction of analyte transport could also be controlled by switching the electrode configuration of the device. This approach has been extended to simultaneously concentrate and separate DNA and proteins in

biological matrices.^{44,164} A number of different configurations of paper-based ICP have also been demonstrated, including faradaic ICP and origami-based ICP assays.^{152,153,165–167} Importantly, ICP transport can be achieved through battery-power¹⁶⁸ and analysis of generated data is possible with a smartphone.¹⁶⁹ These added capabilities increase the potential of paper-based ICP assays for field use; however, the added cost of supporting equipment may prove testing unfeasible in resource-limited regions. More traditional electrophoretic separation methods have also been developed for paper-based assays.^{170–172}

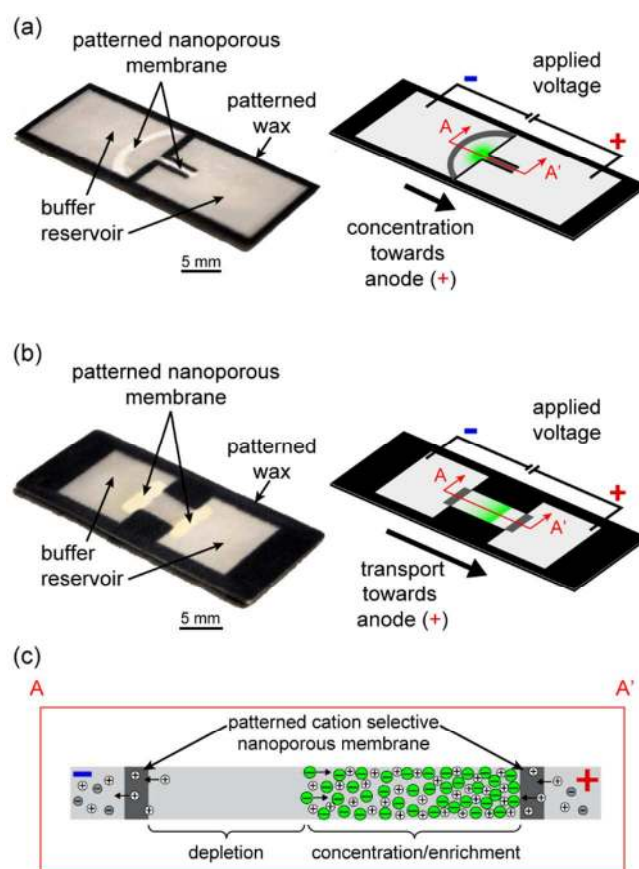


Figure 34. Ion concentration polarization focusing and directional transport in paper. (a) Schematic of device and operation for focusing analytes. (b) Schematic of device and operation for directional transport of analytes. (c) ICP phenomenon under applied voltage. Reprinted with permission from ref 151. Copyright 2014 American Chemical Society.

Although external fields provide advanced fluid and analyte handling capabilities, there are several caveats. The most obvious caveat is the requirement of peripheral equipment, such as transducers, heaters, voltage supplies and associated power sources to generate the desired field. The added equipment increases total cost, reduces ease-of-use and narrows the application field. Inexpensive heaters and electronics (e.g., disposable chemical heaters¹⁷³ and battery-powered voltage sources^{147,168,174}) have shown some success with polymeric microfluidic devices, but remain untested for paper-based assays. Specific to electrokinetic assays, Joule heating can be detrimental to analysis, where uncontrolled fluid evaporation dries the paper matrix and hinders analyte transport. This effect was observed previously during successive cycles of transporting analytes in paper-based ICP.¹⁵¹ Different strategies have been employed to temporarily mitigate evaporation, including the use of cover slips, wax-patterning, and large fluid reservoirs.^{147,149,151} More robust strategies will be needed to control evaporation in the high temperature and humidity conditions typical of resource-limited settings.

4. SAMPLE PROCESSING AND ANALYSIS

The diagnostic testing pipeline is a multistep process, consisting of sample collection, preparation, and analysis. Conventional methods for sample collection include the syringe and needle, vacutainer, lancet, and transfer pipette, which are not well-suited to point-of-care settings in terms of safety and disposal. Sample preparation typically involves a number of extraction, washing, and incubation steps, making the overall process time- and resource-intensive. Moreover, downstream analysis of purified samples relies on sophisticated instrumentation (e.g., plate readers, sequencers). Simplified paper-based strategies for sample collection, preparation, and analysis can expedite analysis and patient treatment. This section highlights and examines the strategies that improve field deployability.

4.1. Sample Collection

Sample collection or world-to-assay interfacing is a frequently overlooked aspect of paper-based assay design. There has been substantial work on improving downstream analytical capabilities in paper with limited improvement in getting the sample to the assay. The gold standard for transferring sample for commercial rapid tests is the transfer pipette or capillary tube, while the single-channel pipette is typically used for proof-of-concept demonstrations. Both methods increase the risk of exposure to infectious samples and would have limited practicality in point-of-care settings where stringent biosafety protocols are needed.

Researchers have recently started to integrate lancets and needles to streamline sample collection and analysis in one device.^{175,176} Li *et al.*¹⁷⁶ developed a device consisting of a finger press-activated microneedle for sample collection and paper-based components for plasma separation and analyte detection (Figure 35). Downstream analysis in the device was automated upon initial activation of the microneedle. The device was successfully tested on a live rabbit specimen, whereby blood was collected from an artery in the rabbit's ear, and glucose and cholesterol levels were measured in the separated blood plasma. Overall, the authors demonstrated a reliable method for whole blood collection and downstream sample processing in a single device. However, the safety of the device was not adequately addressed. For instance, the microneedle is always exposed, increasing the risk for accidental needle stick. Further optimization in terms of safety is needed to improve the practicality of the device for field use.

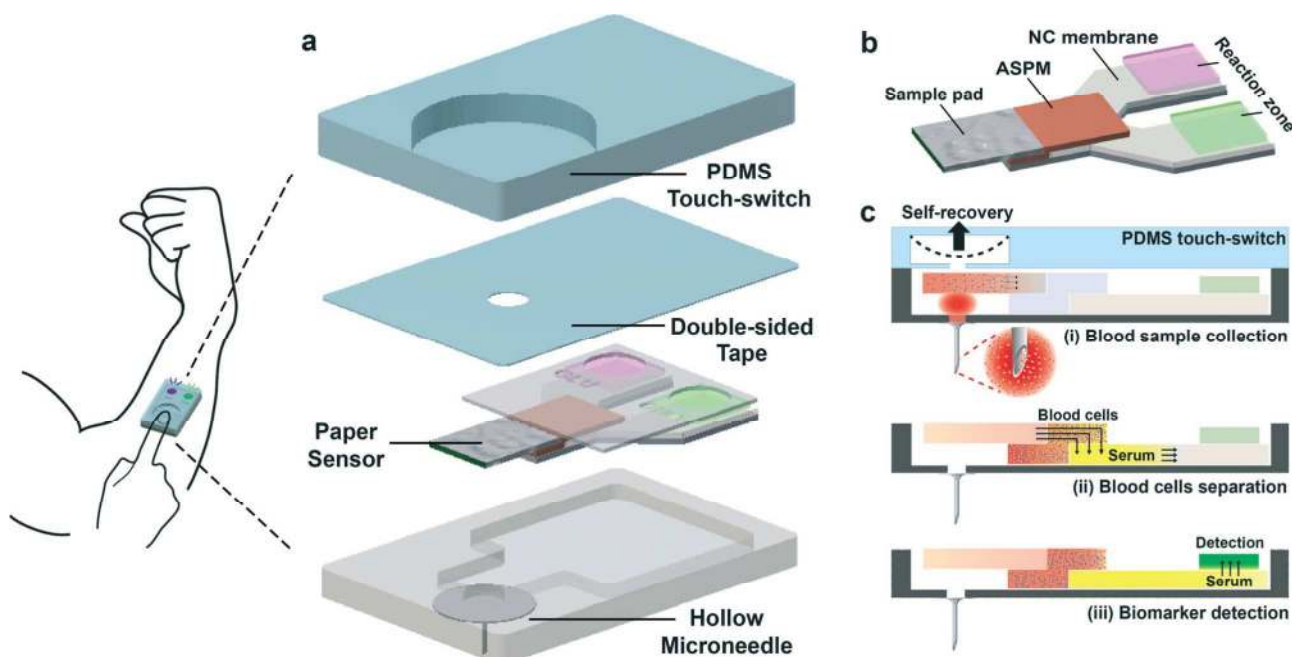


Figure 35. A paper-based device with an integrated microneedle for sample collection. (a) Exploded view of the components of the device. (b) Schematic of the paper-based test. (c) Schematic operation of the device via finger press. Reprinted with permission from ref 176. Copyright 2015 The Royal Society of Chemistry.

In terms of future technical innovation for paper-based sample collection, the microneedle patch is a low hanging fruit that has yet to be picked. Microneedle patches have been primarily developed for transdermal drug delivery.^{177–179} They have also been applied as sample collectors.¹⁸⁰ In a paper-based format, a microneedle patch could seamlessly interface as a sample collection layer within a 3D paper-based assay. Regardless of the final configuration of the envisioned device, these patches offer the potential for simple, integrated sample collection.

4.2. Complex Sample Preparation and Analysis

Nutrient and oxygen transport via whole blood is vital to maintaining homeostasis in the human body. Whole blood also carries a myriad of biochemical, immunological, and molecular biomarkers upregulated during infection, providing targets for disease diagnosis, treatment, and monitoring. Simple solutions for processing whole blood in the field would expedite diagnosis and ultimately,

1
2
3 improve patient outcomes. This subsection examines paper-based strategies for complex sample
4 processing that can be used in the field.
5
6
7

8 4.2.1. Whole Blood Processing 9

10 A typical blood sample from a venipuncture can range up to 10 mL. Large sample volumes are
11 needed for routine diagnosis to accommodate panels of tests and to ensure sufficient capture of rare
12 analytes (e.g., low copies of viral nucleic acid during onset of infection). Centrifugation is the gold
13 standard for processing milliliter-scale sample volumes, separating plasma from blood cells for
14 downstream analysis. The electrical power requirements and high cost of conventional centrifuges,
15 however, restrict their utility to centralized labs. Battery-powered centrifuges are commercially
16 available (e.g., Separation Technology Centrifuge Hematastat Ii 100-100), but have hefty prices
17 tags costing up to several thousand USD per machine. In response to the need for low-cost and
18 portable centrifugation technology, the diagnostics community has developed strategies that
19 leverage a ubiquitous power source: human hand-power. Everyday objects, such as an egg beater¹⁸¹
20 and a salad spinner,¹⁸² have been modified as hand-powered centrifuges for point-of-care whole
21 blood processing. These unconventional solutions could be employed as upstream processing
22 modules to downstream paper-based assays, enabling milliliter-scale sample volume processing and
23 analysis in the field.
24
25
26
27
28
29
30
31
32
33
34
35
36
37
38
39
40
41
42
43

44 In the context of channel-based microfluidics, hydrodynamic plasma separation has been the
45 traditional approach for processing large blood sample volumes.^{183–185} This approach leverages the
46 Zweifach-Fung effect^{186,187} to skim plasma into bifurcation channels from whole blood that is
47 continuously pumped into a main feed channel. Although effective, the continuous pumping
48 requirements and clogging issues of hydrodynamic separation systems limit their practicality for
49 field use. Centrifugal microfluidic platforms also have the capability to process whole blood at
50
51
52
53
54
55
56
57
58
59
60

milliliter-scale volumes^{188–190} and can incorporate paper-based assays directly into the platform for downstream analysis.^{191,192} These disc-based platforms have potential for field use as they can be operated with a portable optical drive and an accompanying tablet or laptop.

Paper-based centrifugation is now possible. Recently, Bhamla *et al.*¹⁹³ developed an ultralow-cost (~20 cents) hand-powered paper centrifuge based on the physics of a whirligig toy; i.e., circular disks that spin by winding and unwinding strings attached to their centers. In its current design, the paper centrifuge can achieve rotational speeds up to 125,000 rpm, which encompasses the performance range of conventional centrifuges. Its utility for plasma separation from whole blood was demonstrated using two capillary tubes filled with blood collected from a finger prick, which are placed into plastic holders attached to the paper disk (Figure 36). Plasma was separated from 8 μ L of whole blood per tube in 1.5 minutes. Although not explicitly demonstrated in this first work, processing of milliliter-scale sample volumes can be potentially achieved by attaching several microcentrifuge tubes to the disks. Ultimately, the paper centrifuge extends the processing capabilities of paper-based technologies, reducing the infrastructure and cost barriers to (large volume) whole blood processing in the field.

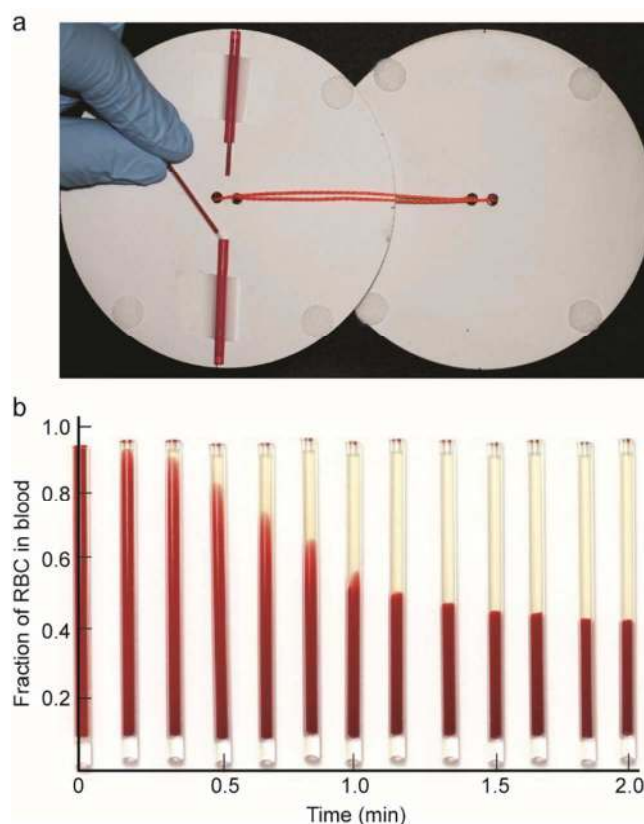


Figure 36. A paper centrifuge for whole blood processing based on the physics of a whirligig toy. (a) Paper centrifuge loaded with two capillary tubes filled with 8 μL of blood per tube. (b) Separation of plasma and red blood cells over time. Full separation is achieved after 1.5 minutes at a hematocrit of ~ 0.45 . Adapted with permission from ref 193. Copyright 2017 Nature Publishing Group.

Filtration is another approach for whole blood processing. Paper-based substrates are well-suited for filtration given their intrinsic wicking behavior. Milliliter-scale filtration can also be achieved by simply increasing the surface area of the paper assay.¹⁹⁴ Paper-based filtration can be achieved by red blood cell (RBC) aggregation combined with size exclusion^{195–199} or solely by size exclusion.^{71,194,200–202} For the former approach, Yang *et al.*¹⁹⁷ developed a device embedded with agglutination antibodies (anti-A, B). Upon addition of whole blood, RBCs aggregate and are immobilized within the paper matrix, while plasma wicks into surrounding detection zones (Figure 37). Similarly, Ge *et al.*¹⁹⁶ used anti-D antibodies to agglutinate RBCs for plasma separation in their

origami-based immunoassay. The agglutination methods demonstrate effective plasma separation comparable to conventional centrifugation, however, the specific antibodies employed may not be applicable to all human blood types. Moreover, the cost of agglutination-based assays can be high if multiple antibodies are required per device. A more universal approach to RBC aggregation has been demonstrated by leveraging salt solutions. Nilghaz and Shen¹⁹⁹ developed a salt functionalized separation device that generates an osmotic pressure gradient upon addition of whole blood, which subsequently induces red blood cell crenation and aggregation.

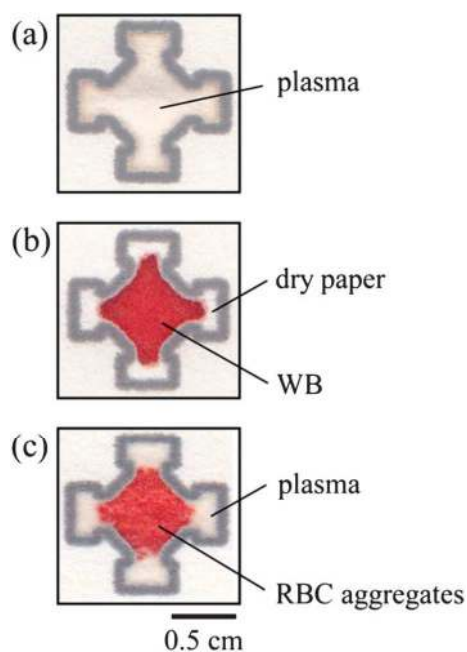


Figure 37. Plasma separation in paper using red blood cell (RBC) agglutination. (a) Plasma extracted by conventional centrifugation and added to the assay. (b) Whole blood applied to an untreated assay. (c) Plasma separation in paper treated with agglutination antibodies. RBCs aggregate and plasma wicks into surrounding detection zones. Reprinted with permission from ref 197. Copyright 2012 The Royal Society of Chemistry.

Plasma separation membranes can be integrated as an upstream component in lateral flow assays or as a layer in 3D μ PADs. Songjaroen *et al.*²⁰⁰ developed a hybrid assay consisting of a porous filtration membrane connected in the lateral flow configuration with chromatography paper. The assay was strategically patterned with wax such that the sample zone resided in the filtration

membrane and the detection zones in the paper. Based on size exclusion, blood cells are trapped in the membrane with plasma transported to the detection zones. For the 3D μ PAD configuration, Vella *et al.*⁷¹ incorporated a filtration membrane on top of a detection layer, covering three separate detection zones. Successful detection of target biomarkers in all three zones was achieved via application of a single 15 μ L finger prick-based blood sample. This approach has been rigorously tested in the clinic.⁷⁴ In comparison to the lateral flow format, the 3D format offers the advantages of faster reaction times due to shorter transport distances and smaller material footprint as a result of stackable fluidic layers. Several groups have also used filtration membranes as components in plastic microfluidic devices.^{194,201,202}

4.2.2. Nucleic Acid Analysis

Molecular testing is a cornerstone of modern medical diagnostics, routinely used for forensics,²⁰³ genetics,²⁰⁴ and disease diagnosis.²⁰⁵ Conventional nucleic acid analysis techniques, such as polymerase chain reaction (PCR), are considered the gold standard in infectious disease diagnosis, providing much lower LODs than serological-based tests at the onset of infection. However, the high complexity of nucleic acid testing generally requires a number of supporting instrumentation. Practical methods for nucleic acid purification and analysis in paper would have transformative implications for point-of-care molecular diagnostics.

Govindarajan *et al.*⁸¹ demonstrated an origami-based approach to extract and purify pathogenic bacterial DNA. Although low-cost and suitable for processing raw samples without complex instrumentation, the overall process requires the operator to complete ten manual steps, potentially increasing the risk of user error. Paper-based membranes, such as the Fusion 5 membrane, have been integrated in a plastic device for DNA extraction and amplification.⁷⁹ Fluid handling for the device still relied on laboratory syringe pumps and the amplification process

required a conventional thermal cycler. Recently, Byrnes *et al.*²⁰⁶ devised a clever strategy to purify and concentrate DNA in a single step using a chitosan-based lateral flow assay (Figure 38). Below pH 6.3, the primary amine groups on chitosan become protonated, suitable for capturing negatively charged target DNA. When target DNA flows through the chitosan embedded region, they are immobilized and concentrated (up to 13-fold here). DNA is subsequently eluted for downstream processing by increasing the pH to above 6.3, at which the charge on chitosan returns to neutral. This work is particularly exciting because the approach greatly simplifies the sample preparation needed for DNA analysis and demonstrates potential to be directly integrated in existing lateral flow assays.

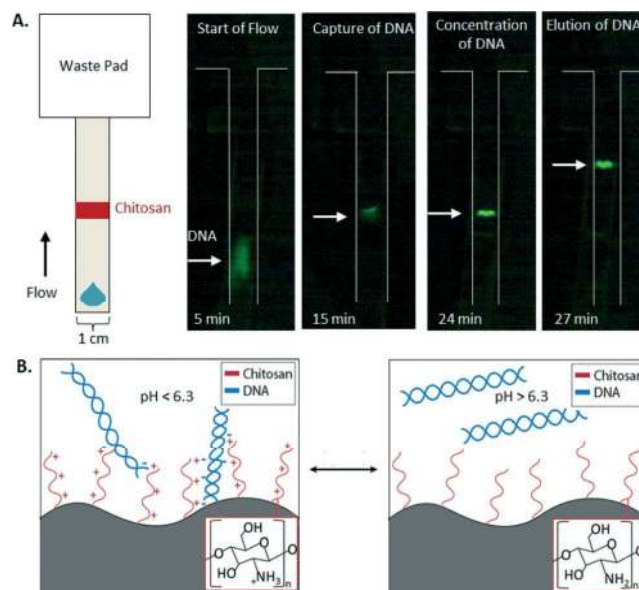


Figure 38. DNA purification and concentration in a chitosan-based lateral flow assay. (A) Schematic of the assay. Images of DNA capture, concentration, and elution. (B) Schematics of chitosan chemistry for capturing DNA under different pH. Reprinted with permission from ref 206. Copyright 2015 The Royal Society of Chemistry.

Following extraction and purification of DNA, PCR is usually performed to amplify and detect target sequences. Advancements in PCR reaction chemistry have led to transformative isothermal amplification methods for point-of-care diagnostics,²⁰⁷ which are much more amenable

1
2
3 to paper-based assays than traditional thermal cycling. A number of groups have demonstrated
4
5 isothermal nucleic acid amplification in paper-based assays using loop-mediated isothermal
6
7 amplification (LAMP),^{80,208–210} isothermal helicase dependent amplification,²¹¹ recombinase
8
9 polymerase amplification,²¹² and rolling circle amplification.²¹³ These methods have enabled the
10
11 translation of a powerful laboratory-based analytical technique to simple paper-based assays,
12
13 broadening their overall diagnostic capabilities. The low amplification temperature (65° C) has also
14
15 led to innovative use of unconventional heating sources, such as disposable chemical heaters,^{173,211}
16
17 ultimately improving assay deployability.
18
19
20

21
22 Connelly *et al.*⁸⁰ developed a “paper machine” for molecular diagnosis of *E. coli* from
23
24 human plasma (Figure 39). The approach uses a magnetic device with a magnetic slip layer
25
26 containing paper discs for sample processing and analyte detection. Operation of the device consists
27
28 of sliding the magnetic slip layer through the device, stopping at designated regions for sample
29
30 preparation, isothermal DNA amplification, and endpoint detection via a smartphone. An important
31
32 feature of the device is its capability to process whole cells (i.e., cell lysis is integrated in the paper-
33
34 based device), which has not been previously demonstrated. The authors achieved an analytical
35
36 sensitivity of one copy of double stranded (dsDNA) for *E. coli* using their approach.
37
38
39
40
41
42
43
44
45
46
47
48
49
50
51
52
53
54
55
56
57
58
59
60

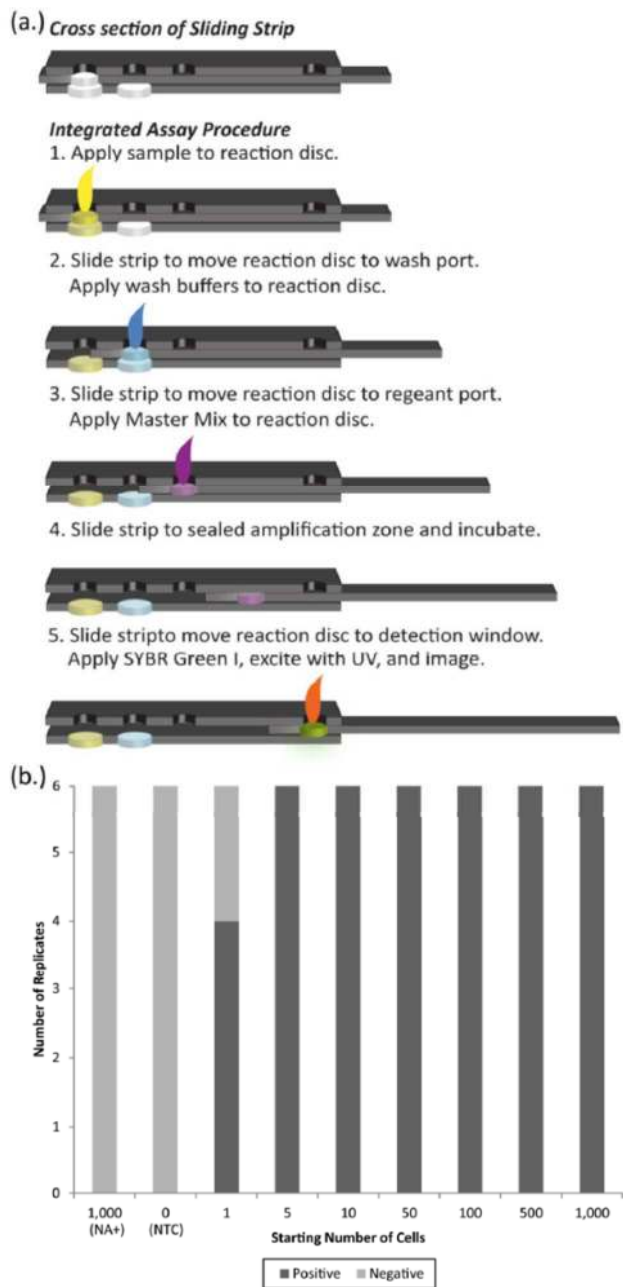


Figure 39. A “paper machine” for molecular diagnostics. (a) Operation of the device for nucleic acid analysis, showing steps for sample introduction, washing, amplification and detection. (b) Detection of *E. coli* spiked in human plasma. Reprinted with permission from ref 80. Copyright 2015 American Chemical Society.

Direct nucleic acid analysis has also been demonstrated in paper. Instead of relying on thermal amplification to detect target sequences, ICP was leveraged to simultaneously concentrate and separate hepatitis B viral (HBV) DNA sequences in human serum (Figure 40).⁴⁴ The approach

achieved a LOD of 150 copies/mL and resolved four specific regions of the HBV genome. Similar electrokinetic transport (i.e., isotachopheresis) has been applied to increase the sensitivity of DNA hybridization assays in polymeric microfluidic devices,^{214–217} achieving up to 8.2-fold higher signal than conventional hybridization.²¹⁷ Although not explicitly demonstrated in the ICP work above, such analytical capability is achievable with ICP-based DNA concentration in paper. ICP-based hybridization would add a powerful tool to the paper-based DNA testing toolbox and complement existing amplification-based detection strategies.

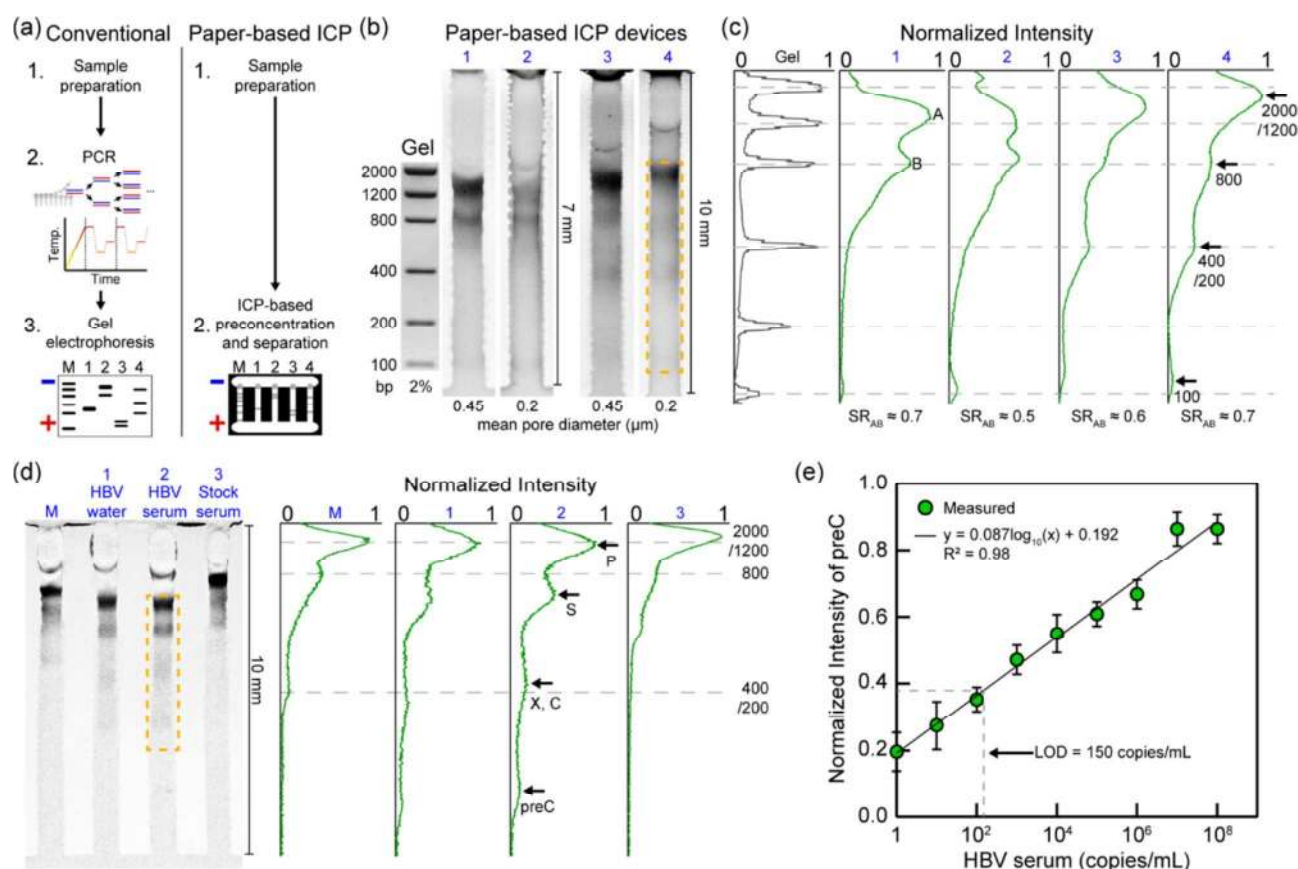


Figure 40. Direct DNA analysis with ICP in paper. (a) Comparison of conventional and ICP-based approaches. (b) Simultaneous concentration and separation of HBV DNA sequences. (c) Intensity profiles of the analyzed sequences. (d) Comparison of direct HBV DNA analysis in water and serum. Intensity profiles of the separations. (e) Calibration curve for HBV DNA detection using the precore (preC) region of the viral genome. The LOD is determined to be 150 copies/mL. Reprinted with permission from ref 44. Copyright 2015 American Chemical Society.

4.3. Integrated Analysis

The development of paper-based assays, to date, has largely focused on assays with single capabilities; for example, an assay designed for analyte concentration only concentrates analytes. This modular approach increases the complexity of testing as multiple single assays would be needed to complete a test. Process integration (i.e., the assembly of sample collection, sample preparation, and analysis into a single platform) can improve ease-of-use and expedite analysis.

Gong *et al.*¹⁷⁵ developed an integrated device for HBV testing in the format of a pen, inspired by the ubiquitous ball-point pen. The pen-based device was divided into two compartments: one compartment housed the sample collection mechanism (a standard lancet embedded in tubing for finger prick) and the other contained a paper-based platform comprised of a collection pad, filtration membrane for plasma separation, and lateral flow test strip for biomarker detection. Here, the familiarity of the pen format improved ease-of-use and patient familiarity while offering an established route to scale, leveraging the massive existing supply chain for consumer pens.

The advances in paper-based nucleic acid analysis described in section 4.2.2 have culminated into integrated paper-based laboratories for molecular testing. Rodriguez *et al.*²⁰⁹ developed a foldable paper-based NAAT capable of performing extraction, amplification, and detection of DNA/RNA targets. The diagnostic functionality of the device is demonstrated via analysis of human papillomavirus 16 DNA from clinical cervical specimens. Target detection is achieved in less than 1 hour with a LOD of 10^4 DNA copies. Lafleur *et al.*²¹⁸ recently developed the first autonomous fully integrated nucleic acid amplification test (NAAT) based on 2D paper networks (Figure 41). The NAAT does not require peripheral instrumentation or manual sample processing in comparison to existing commercial integrated NAATs^{219–221} and NAAT kits.²²² The

integrated device contains a world-to-assay interface for a sample collection swab used to collect nasal fluid. Upon sample introduction via the interface, sample processing, amplification, and detection are automated by the device. As proof-of-concept, the device was used to detect methicillin-resistant *Staphylococcus aureus*, achieving a LOD of $\sim 5 \times 10^3$ genomic copies. Given the potential high impact of the NAAT technologies described here, the major challenge of implementing them in the field will be finding cost-effective heating sources for the amplification process. The next phase of development for these systems should focus on innovating the supporting elements around the paper-based assay such that cost and operational complexity remain low.

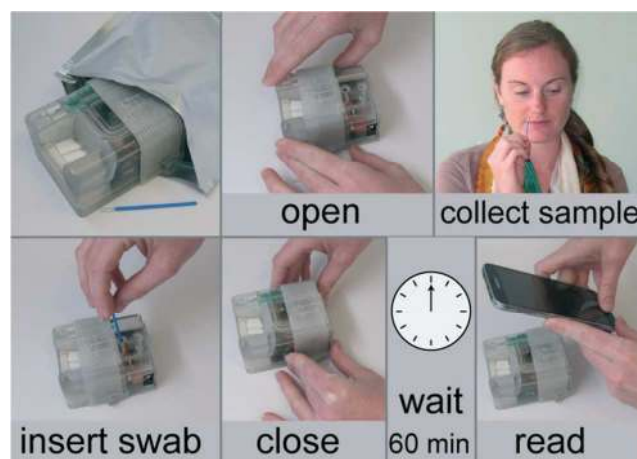


Figure 41. An autonomous fully integrated nucleic acid amplification test. Upon introduction of a collected sample (e.g., nasal swab) to a world-to-chip interface, sample processing, amplification, and detection is automated by 2D paper networks housed in the device. Quantitation of results can be further achieved with a smartphone application. Reprinted with permission from ref 218. Copyright 2016 The Royal Society of Chemistry.

4.4. Quantitative Electrochemical Analysis

The glucose monitoring system for diabetes is the gold standard in commercially available electrochemical paper-based diagnostic platforms. The system consists of an electrochemical paper strip and a reader that quantifies blood glucose level in the strip. The conventional glucose meter

has also been repurposed to measure cholesterol, lactate, and alcohol in paper strips.²²³ Electrochemical sensing can achieve lower detection limits than colorimetric detection and therefore, it is an ideal approach for quantitative paper-based analysis. Electrochemical paper-based analytical devices (ePADs) were first demonstrated by Dungchai *et al.*²²⁴ and have grown exponentially in number since their initial work.^{72,223–230}

A number of electrochemical sensing techniques have been realized in ePADs, including amperometry, voltammetry, potentiometry, electrochemical impedance, and capacitance.³⁸ Electrodes form the basis of these techniques, where a typical ePAD consists of three electrodes: a working electrode, a counter electrode, and a reference electrode. Together, these electrodes transduce chemical signals into measurable electrical signals. Thus, there has been extensive research on electrode development; in particular, focusing on electrode material type (e.g., carbon- and metal-based electrodes) and fabrication strategies.^{231,232} Recently, Li *et al.*²³³ demonstrated direct writing of electrodes into paper using a ballpoint pen-like device modified to contain carbon ink. This strategy provides a simple and low-cost means to fabricate ePADs directly in the field.

Paper-based electrochemical sensors have been applied to environmental and biological testing. In the context of bioanalytical applications, they have been used for biochemistry, immunosensing, nucleic acid testing, and cellular analysis applications.^{231,232} Wang *et al.*²³⁴ developed a 3D ePAD with structures that “pop-up” when unfolded, as similar to pop-up greeting cards (Figure 42). This design enables precise control over timing of reactions by connecting and disconnecting fluidic layers in the pop-up structure when folded and unfolded, respectively. Samples are also well-contained when the structure is folded, minimizing exposure to infectious agents. The assay was coupled to a commercial glucometer for quantitative readout. In a proof-of-concept experiment, devices were used to measure beta-hydroxybutyrate (BHB) spiked in human

whole blood, the biomarker for diabetes ketoacidosis. A LOD of 0.3 nM was achieved, which is comparable to the LOD of 0.12 nM for commercial BHB test strips.

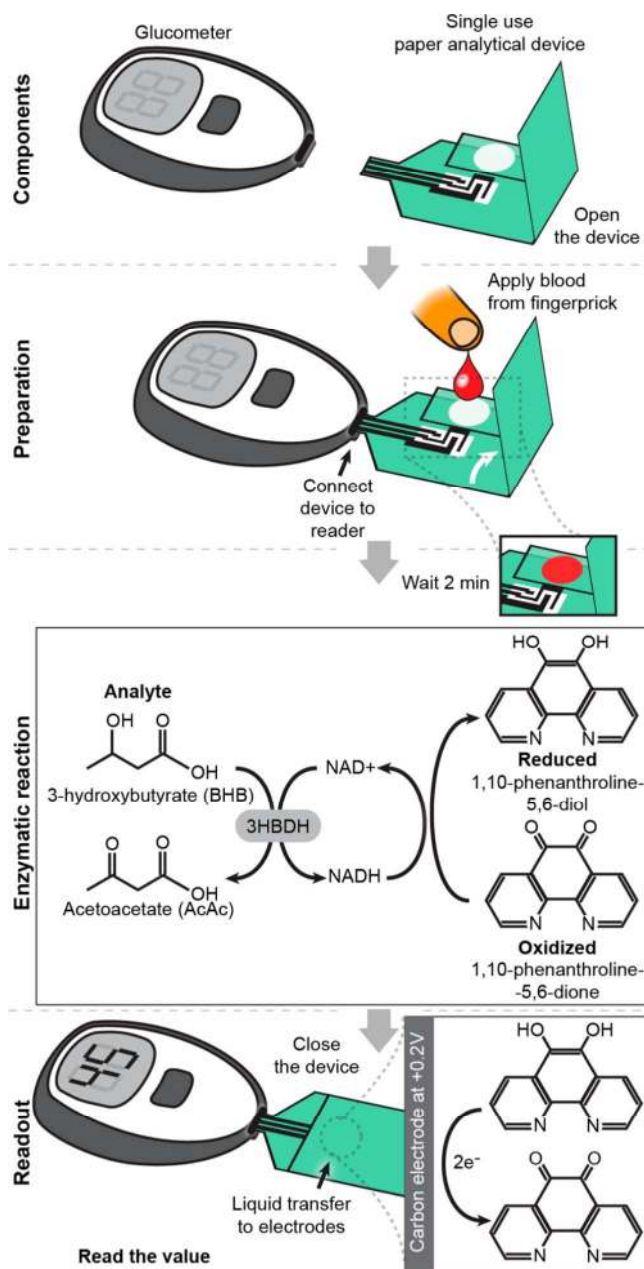


Figure 42. A paper-based “pop-up” assay for assessing diabetic ketoacidosis. Schematic shows the components and operation of the assay-reader combination. Following sample collection and preparation, the reader outputs a value for beta-hydroxybutyrate in the sample, the biomarker for diabetes ketoacidosis. Reprinted with permission from ref 234. Copyright 2016 American Chemical Society.

In the context of practical application, there have been successful demonstrations of ePADs as portable sensors that can be adapted to existing commercial glucometers.^{223,234} They are well-positioned, in this regard, for field use. Continued development of ePADs, however, should focus further on improving electrode configurations and materials to address sensitivity issues. Safe and reliable methods to collect and introduce sample into ePADs are also needed, possibly with inspiration from examples in section 4.1. Finally, the capability of ePADs to analyze different types of biological matrices would also broaden their utility.

4.5. Quantitative Analysis with Consumer Technology

An exciting advancement in paper-based assay development has been their integration with mobile phones (e.g., camera phones and smartphones).^{235–240} Mobile phone technology is particularly attractive as analytical systems owing to their advanced computing and imaging power, vast market base, and familiarity (to both the end user and manufacturer). They are quickly becoming a quintessential component for quantitative point-of-care diagnostics. The most basic use of phones for quantitation is image acquisition of colorimetric readouts.^{241,242} Captured images can be processed with an in-phone application, on a separate computer, or delivered to a central database. A more integrated strategy includes leveraging accessories that attach to the phone for quantitation of signals in paper-based assays.^{243–247} Commercial lateral flow assay readers for iPhones (Detekt Biomedical LLC) and Android phones (Holomic LLC) are also available. Lee *et al.*²⁴⁷ developed the Nutriphone – an iPhone adaptor with a paper-based test strip and an accompanying application for measuring serum vitamin D levels (Figure 43). Colorimetric analysis of vitamin D concentrations on the test strip produced results equivalent to conventional ELISA, demonstrating the applicability of the system for sensitive self-diagnosis of micronutrient levels.

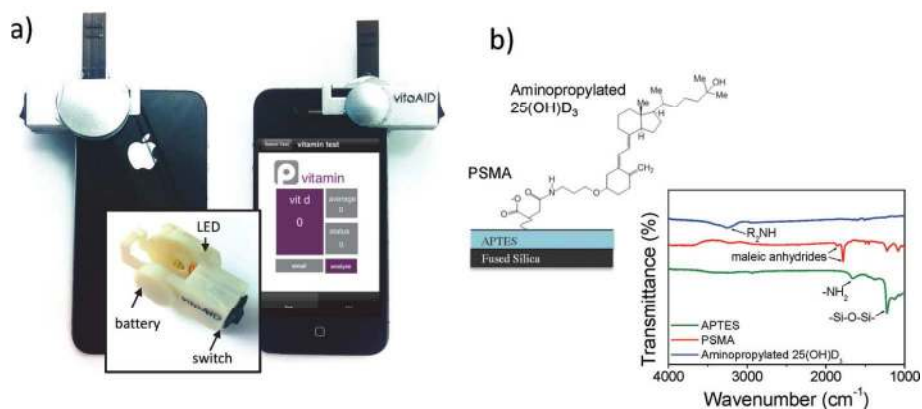


Figure 43. The NutriPhone: A paper-based adaptor for vitamin D monitoring coupled to an iPhone for quantitation. (a) Image of system and in-phone application used for analysis. (a) Assay chemistry and signal detection via the iPhone. Reprinted with permission from ref 247. Copyright 2014 The Royal Chemical Society.

Fluorescence imaging on mobile phones has also been developed,²⁴⁸ enabling analytical measurements in paper-based assays that rival benchtop fluorescence microscopes. Thom *et al.*²⁴⁸ developed a paper-based assay with an integrated fluidic battery to power an on-chip fluorescent assay for detecting and measuring β -D-galactosidase. The assay was coupled to a smartphone with a fluorescence imaging adapter, allowing measurement of β -D-galactosidase concentrations down to 700 pM. Portable fluorescent readers are also commercially available; for example, the HRDR-300 Fluorescent Reader from Holomic LLC.

In the advancement of smartphone applications for paper-based assays, developers need to keep in mind possible limitations of these technologies – in addition to those specific to the use of paper. For instance, the availability of higher end smartphones can vary from country to country, limiting the availability of more powerful computing and imaging capabilities in certain areas. Infrastructure for centralized databases to store diagnostic information may also be too costly and not feasible for resource-limited regions. Moreover, the use of smartphones and other consumer technologies needs to reflect their demand; that is, simple camera phones are well-suited for low volume testing (e.g., one-time screening applications) whereas more sophisticated smartphones are

1
2
3 better suited for high volume quantitative monitoring. Many of these challenges will be overcome
4
5 with time, and further penetration of highly capable smartphones globally. Overall, there is
6
7 tremendous potential for portable quantitative analysis with the paper-consumer technology
8
9 combination. In terms of supporting infrastructure, smartphones are undoubtedly the partner-of-
10
11 choice for paper-based diagnostics.
12
13
14

15 16 5. EMERGING APPLICATIONS 17

18
19 In the context of global health, paper-based diagnostics has focused primarily on infectious disease
20
21 detection and monitoring. While these established application areas are both vast and critically
22
23 important, there are a number of other areas of application where paper-based microfluidics can
24
25 make impact. Specifically, we envision a wide variety of emerging applications in more niche
26
27 health and health monitoring applications, as well as accompanying the trend toward ubiquitous
28
29 sensing and wearables. The most technically and commercially productive routes will be in
30
31 applications that can (a) leverage the tremendous paper-based diagnostics tool box already
32
33 developed for disease, and (b) afford a high margin for associated development, compensating for a
34
35 smaller overall market size. We highlight two illustrative examples here, male infertility
36
37 assessment and wearable diagnostics.
38
39
40
41
42

43 44 5.1. Male Infertility 45

46
47 Infertility affects more than 70 million couples worldwide with male-factor infertility accounting
48
49 for half of the cases.^{249,250} Conventional techniques for male fertility testing (i.e., semen analysis)
50
51 include counting chambers, computer-assisted sperm analysis,²⁵¹ and vitality assays.²⁵² Like most
52
53 laboratory-based methods, these techniques are time- and resource-intensive. Test results can also
54
55 be subjective,²⁵³ and patient compliance is low due to embarrassment and anxiety.²⁵⁴ Both
56
57
58
59
60

1
2
3 traditional^{255–258} and paper-based^{44,122,259–262} microfluidic devices have been developed to address
4
5 these gaps. The paper-based assays are comparatively more portable and convenient in terms of
6
7 operation, making them ideal for self-diagnosis.
8
9

10 Commercial paper-based semen tests are currently limited to providing information on a
11
12 single semen parameter, such as total concentration for the SpermCheck® assay²⁵⁹ and sperm
13
14 motility for the Fertell® assay.²⁶⁰ In efforts to expand the capabilities of paper-based semen tests for
15
16 home testing, Matsuura *et al.*²⁶¹ developed a colorimetric assay to assess both total sperm
17
18 concentration and motility. Total sperm concentration was measured using a methylene blue dye
19
20 derivative that stains DNA in the nuclei of sperm cells. Motility was observed using a yellow 3-
21
22 (4,5-dimethylthiazol-2-yl)-2,5-diphenyl tetrazolium salt (MTT), which converts to purple formazan
23
24 by metabolically active sperm. The degree of spread by purple formazan in the assay was measured
25
26 and used to determine motility. A potential caveat of the assay is that non-motile, but metabolically
27
28 active sperm can be transported by capillary action in the assay and thus, artificially overestimate
29
30 the actual number of motile sperm in the sample. Nosrati *et al.*¹²² developed a 3D paper-based assay
31
32 to address this issue and to provide more intuitive parameters on sperm health. In their work, live
33
34 sperm concentration, motile sperm concentration, and motility were quantified using the MTT assay
35
36 (Figure 44). Live and motile sperm concentrations are better indicators of male fertility potential, as
37
38 compared to total sperm concentration which does not distinguish live, dead, or motile sperm
39
40 populations. The critical advantage of this assay, however, is that motile sperm must swim in a
41
42 viscous buffer through a porous membrane to reach a detection area embedded with MTT. In this
43
44 manner, only motile sperm are quantified, reducing the error associated with flow in a 2D assay.
45
46
47
48
49
50
51
52
53
54
55
56
57
58
59
60

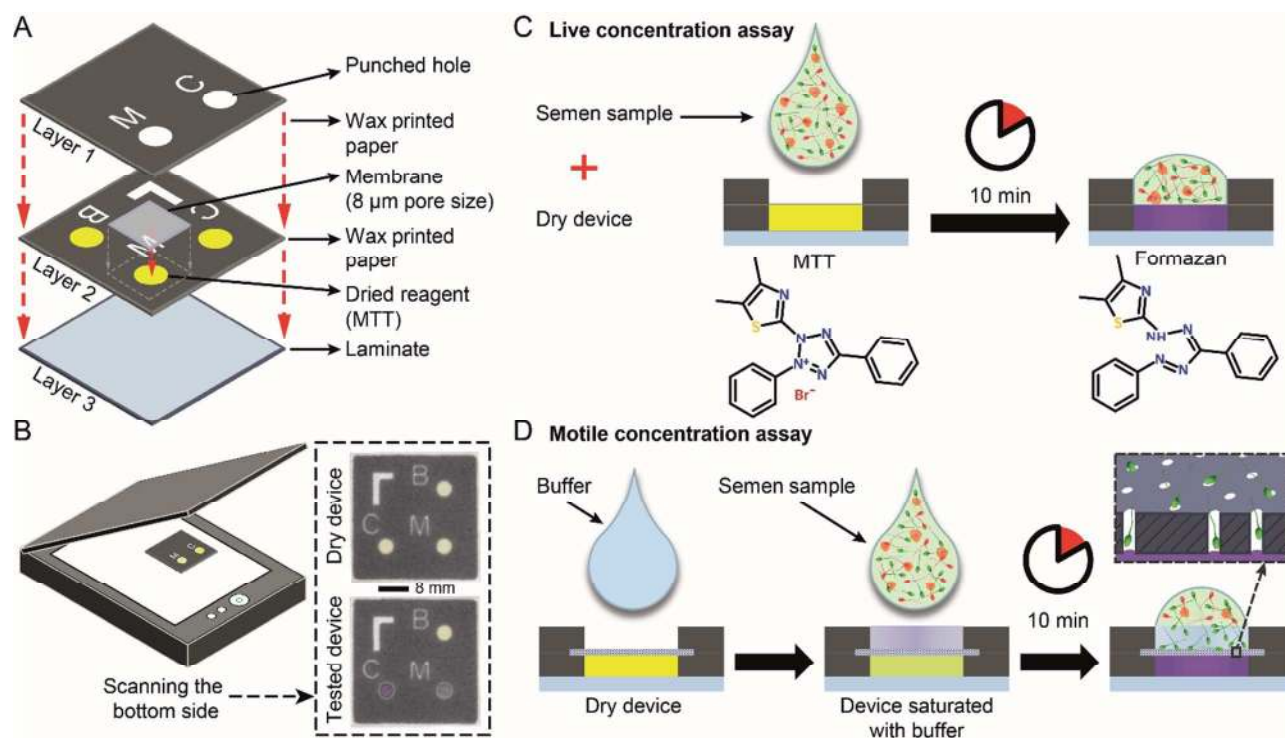


Figure 44. 3D paper-based assay for measuring live and motile sperm concentration, and sperm motility. (A) Exploded view of the assay. (B) Colorimetric signals are imaged with a desktop scanner. Representative pristine and tested assays are shown in the dashed box. (C) Schematic of the working principle for the live concentration readout. (D) Schematic of the working principle for the motile concentration readout. Motility is determined as the ratio of motile to live sperm. Reprinted with permission from ref 122. Copyright 2016 American Association for Clinical Chemistry.

Sperm DNA integrity is a crucial indicator of sperm health and the genetic well-being of offspring.²⁶³ The clinical gold standard for DNA integrity analysis is the sperm chromatin structure assay.^{264,265} Two paper-based approaches have been developed for quantifying DNA integrity based on the concentration and separation capabilities of paper-based ICP.^{44,262} Importantly, both approaches provide identical clinical outcomes for patients as the clinical gold standard. Overall, current paper-based technologies for male fertility testing have shown promise for quantitative analysis of parameters critical to sperm health and male fertility potential. They offer similar opportunity of self-testing for men that home pregnancy and ovulation tests have offered women, and ultimately, provide a panel of complimentary personalized fertility tests.

5.2. Wearable Diagnostics

Wearable technology has become popular in recent years and has important implications for next generation point-of-care diagnostics and personalized medicine. Consumers are now able to monitor their own basic health (e.g., heart rate, sleeping pattern, diet) on a daily basis with fitness trackers from companies like Fitbit, Garmin, and Apple. In academia, Google Glass has been directly adapted as an imaging instrument for lateral flow assays. Feng *et al.*²⁶⁶ used the Glass for qualitative and quantitative measurement of HIV and prostate cancer biomarkers, respectively (Figure 45). The overall system provided a hands-free means to detect target analytes, store information on a centralized server, and track the spatiotemporal pattern of tests in real-time.

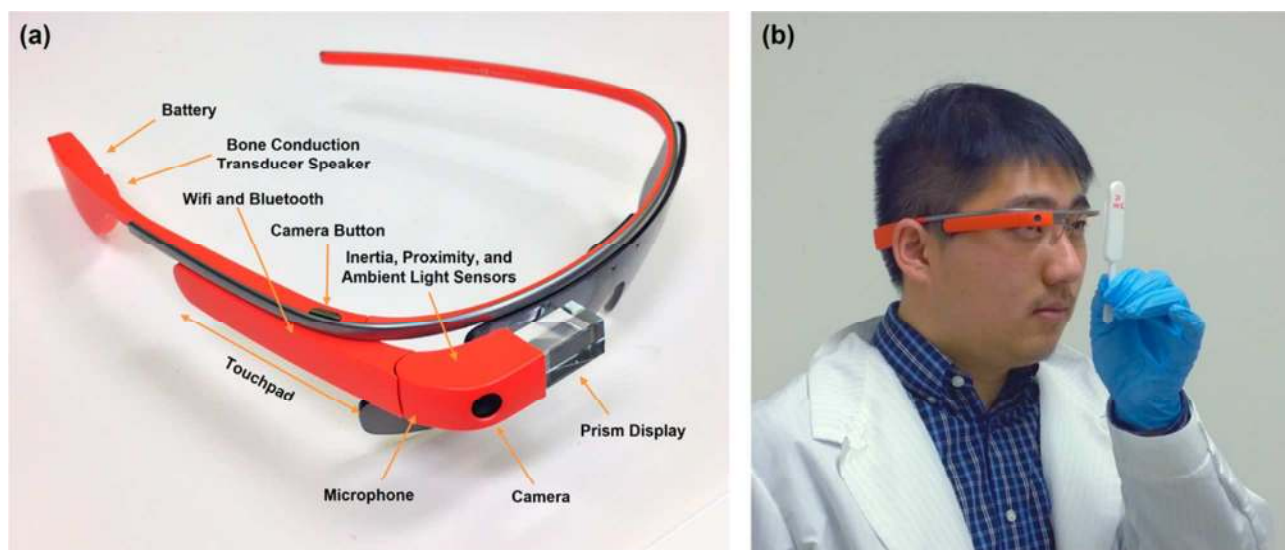


Figure 45. Wearable technologies such as the Google Glass for paper-based analysis. a) Google Glass and its components. (b) Analysis of a lateral flow assay. Acquired images can be processed by the Glass and stored on a centralized database. Reprinted with permission from ref 266. Copyright 2014 American Chemical Society.

Growing interest in wearable technologies has inspired a research base in flexible sensors.^{267–270} These sensors are typically attached to skin by an adhesive and noninvasively monitor levels of target analytes in bodily fluids such as sweat. Paper has been demonstrated as a

1
2
3 viable platform for the development of wearable flexible sensors.^{271–276} Mu *et al.*²⁷¹ developed a
4
5 paper-based skin patch for screening cystic fibrosis (Figure 46). Their approach translates standard
6
7 sweat-based testing to a paper-based format. The paper-based patch is attached to the skin and
8
9 directly measures levels of anions in sweat. The performance of the patch correlated well to the
10
11 clinical standard ($R^2 = 0.98$). In addition to sweat-based monitoring, Güder *et al.*²⁷⁶ developed a
12
13 paper-based respiration sensor to monitor breathing patterns (Figure 47). The sensor converts
14
15 changes in humidity caused by inhalation and exhalation to a measurable electrical signal. It is
16
17 directly integrated into a medical facemask that can be worn by a patient. Together with a
18
19 smartphone application, the paper-based electrical respiration sensor provides an inexpensive
20
21 method to quantify the basic health of patients.
22
23
24
25
26

27 The current proof-of-concept demonstrations of wearable paper-based sensors show promise
28
29 and opportunity for simplifying basic health monitoring that typically rely on complex
30
31 instrumentation. The transition to simple wearables greatly enables self-diagnosis, having potential
32
33 for broad dissemination. Continued efforts in design and testing should expand the available sample
34
35 reservoir to include more information-rich sample types, such as blood. For instance, a paper-based
36
37 skin patch could be stacked on a microneedle patch that automatically meters blood from a patient
38
39 and delivers blood plasma to the paper-based detection patch. It would also be worthwhile to
40
41 explore the possibilities of interfacing paper-based assays directly with consumer fitness trackers
42
43 for improved convenience. Although further development is crucial for more robust, stand-alone,
44
45 repeat-use systems, paper-based diagnostics is well positioned within the more general trend toward
46
47 distributed sensing – as relevant to the full range of emerging artificial intelligence powered big-
48
49 data solutions, and the related internet of things. Sensor requirements in such distributed sensing
50
51
52
53
54
55
56
57
58
59
60

applications are very similar to those of the global health applications that shaped the paper-microfluidics field.

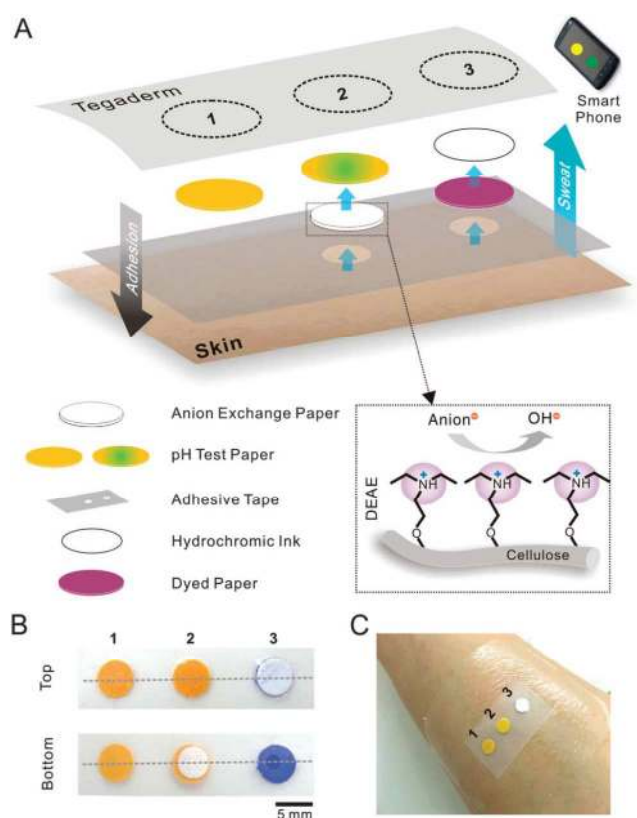


Figure 46. A paper-based skin patch for screening cystic fibrosis. (A) Schematic of the patch with three detection regions. Region 1 contains a pH test paper as an imaging reference. Region 2 contains a stack of an anion exchange paper and a pH test paper for measuring sweat anions. Region 3 contains a colorimetric sensor that becomes transparent when sufficient sweat volume wicks into the device. (B) Top and bottom images of the skin patch. (C) A skin patch attached to the skin of the inner forearm. Reprinted with permission from ref 271. Copyright 2015 The Royal Society of Chemistry.

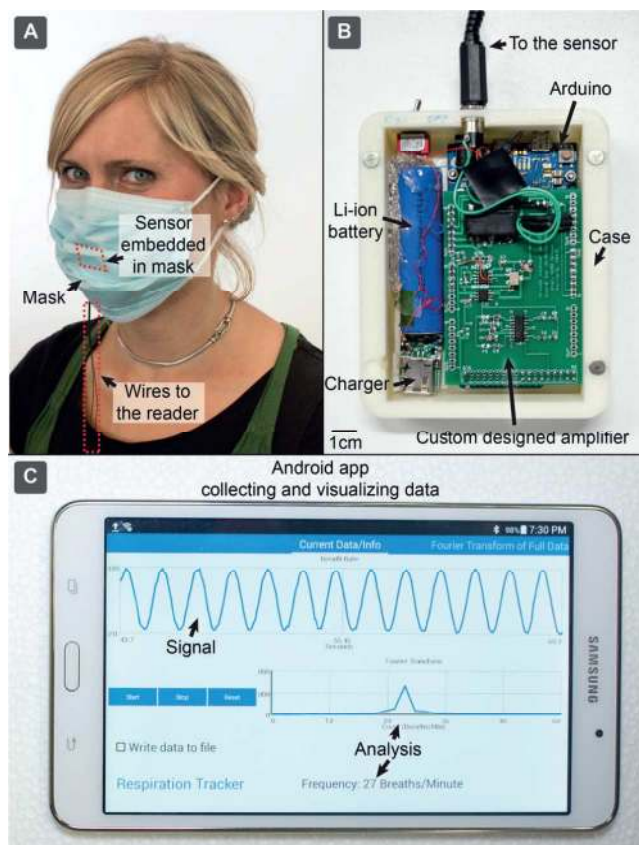


Figure 47. A wearable paper-based electrical respiration sensor. A) The paper-based sensor is embedded in a medical facemask and connected to a reader. B) Image of the data acquisition unit. C) Image of the tablet running the application to capture incoming data. Reprinted with permission from ref 276. Copyright 2016 Wiley-VCH Verlag GmbH & Co.

6. CONCLUSIONS AND OUTLOOK

The field of paper-based microfluidics has made enormous strides since its inception. There is now a formidable toolbox of advanced strategies for fluid and analyte manipulation in paper-based assays. Every step of the diagnostic pipeline has been demonstrated in a paper-based format, from sample collection to analysis. Through clever engineering, analytical techniques that could only be performed in laboratories, such as nucleic acid amplification, can now be executed in the palm of one's hand. Moreover, smartphone technology is expanding the analytical power of paper-based assays, as well as their accessibility in the developing world. As paper-based technologies continue

to mature, our collective efforts should address the key remaining challenges of translation and commercialization, as summarized below.

6.1. Path to Translation and Commercialization

The most promising near-term opportunity for translation is paper-based nucleic acid testing. It is the “killer application” that has potential to transform the diagnostics landscape in both developing and developed countries. There has been substantial progress in translating nucleic acid sample preparation²⁰⁶ and amplification^{80,209} to paper-based formats, with recent demonstration of a fully autonomous paper-based molecular testing platform.²¹⁸ The main barrier for advancing these technologies and keeping costs down is the requirement of heating instrumentation for the amplification process. Low-cost chemical,¹⁷³ solar-powered,²⁷⁷ and external battery-powered heaters²¹⁸ have been used with some success. A more direct approach is, perhaps, the integration of paper-based batteries^{278,279} and electronics²⁸⁰ to realize an all-paper testing platform.

The remaining barriers to translation and commercialization for all paper-based diagnostic technologies are: 1) process integration, 2) manufacturing at scale, 3) clinical validation, 4) recognizing social impact, and 5) complying with regulatory policies. Process integration is the act of combining multiple basic operations into a single system, which simplifies overall operation and increases usability. Much of the past and current research in paper-based microfluidics has focused on developing standalone assays with single capabilities (e.g., an assay that only enriches DNA or an assay that only separates blood plasma). Integration of upstream and downstream diagnostic processes is often an afterthought.^{281,282} There have been several demonstrations of integrated sample collection, preparation, and analysis in a single paper-based platform.^{175,176,218} More work needs to move in this direction. The field is maturing at a rapid pace and there is now a vast toolbox

of capabilities at our disposal. Thus, we, as a community, can afford to focus more on practicality and ultimate impact, rather than novelty alone.

The capability to manufacture technology at scale (i.e., scalability) is essential for commercial success. Scalability should inform the device material, device design, and fabrication method necessary for commercial production. For example, common microfluidic materials used in academic labs, such as PDMS, are not suitable for mass production. While useful for prototyping and proof-of-concept studies, soft lithography is a slow fabrication process with low-throughput. Paper has an advantage over polymer microfluidic substrates in that there is an established manufacturing process for lateral flow assays that could be translated to paper-based microfluidics. Methods for fabricating paper-based assays are also more high-throughput, including inkjet printing, wax printing, laser writing, and photolithography.^{18,283–285} In general, scalability needs to be considered in the early stages of device development to ensure streamlined transition from prototype to final product.

Clinical validation is integral to translation. Patient samples can be drastically different on a day-to-day basis due to the patients' disease state and lifestyle; thus, they can exhibit very different behavior in devices compared to model samples used for proof-of-concept. Many researchers recognize the importance of patient testing and have started to address this issue.^{74,122,175,209} It is prudent, however, for researchers to follow the appropriate certification guidelines required for patient testing in their respective research labs. In the United States, all facilities that perform testing on human specimens must be properly certified under the Clinical Laboratory Improvement Amendments of 1988 (CLIA). CLIA certification can be waived for diagnostic tests that are simple and accurate enough as to minimize erroneous results. In our own work, clinical validation was performed in collaboration with the National Hospital of Tropical Diseases in Vietnam and was

1
2
3 regulated by the local Ministry of Health. In the event that patient samples are not readily available,
4
5 a good starting point is commercial matrices (e.g., animal or human blood) that have been
6
7 rigorously tested for infectious agents and pass the biosafety requirements of the facility. These
8
9 matrices can then be spiked with model analytes and assessed accordingly.
10
11

12
13 The social impact of technology is often overlooked by technology developers, but is just as
14
15 important as the technical and economic implications. Grand Challenges Canada, in association
16
17 with the Bill and Melinda Gates Foundation, are explicit in their expectation of “coordinated
18
19 application of scientific/technological, social and business innovation to develop solutions to
20
21 complex challenges.” This “integrated innovation” approach combines technology developers,
22
23 clinicians, public health experts, and manufacturers from all participating countries. This tight,
24
25 region-specific collaboration is maintained throughout the process from conceptual design, testing,
26
27 regulatory approval, and manufacturing and deployment – a best practice for ultimate impact in
28
29 global health.
30
31
32

33
34 A major barrier to commercialization is complying with regulatory policies. Medical
35
36 diagnostic tests are regulated by the Food and Drug Administration (FDA) in the United States, by
37
38 Health Canada in Canada, and by the European Commission in countries within the European
39
40 Union. These agencies categorize diagnostic tests by their intended use and risk to patients/users.
41
42 The FDA has a three class system (Class I, II, and III) with increasing risk and regulatory
43
44 controls,²⁸⁶ Health Canada uses four classes (Class I, II, III, and IV) with a set of 16 rules,²⁸⁷ and the
45
46 European Commission employs five classes (Class I-sterile, I-measure, IIa, IIb, and III).²⁸⁸ For
47
48 example, a paper-based assay for testing transmissible agents, such as HIV, is considered high risk
49
50 and would be classified as Class III by the FDA, Class IV by Health Canada subject to Rules 1-3,
51
52 and Class III by the European Commission. In addition to the regulatory controls associated with
53
54
55
56
57
58
59
60

each class, manufacturers must follow Good Manufacturing Practices and be ISO13485 certified. These guidelines ensure the quality of tests in all stages of the manufacturing process: fabrication, packaging, labelling, storage, installation, and service. We encourage researchers to consult the relevant medical device regulations early and often during technology development to expedite commercialization; that is, to design for regulatory approval in addition to function and low cost.

6.2. Final Comments

Particularly with summative recent advancements, we are optimistic that the continued development of paper-based diagnostics will have profound implications for global health. There is particular excitement surrounding integrated paper-based molecular testing, as these technologies will provide unprecedented analytical power in simple low-cost assays. One can imagine personalized mini-laboratories for disease monitoring (e.g., HIV anti-viral therapy) in the comfort of one's home, eliminating the need for travel to centralized hospitals – a major barrier that impedes access to healthcare in developing countries. These integrated systems would also have impact as rapid response systems for early diagnosis of emerging epidemics. Ultimately, such systems have the potential to revolutionize healthcare delivery and disrupt the current model of going to the doctor's office, receiving a diagnosis, and then waiting for treatment.

We encourage the community to explore applications beyond those of global disease diagnosis. There are many opportunities to advance this technology through a much wider array of applications in global health (food, water, and environmental testing) as well as the full range of energy production and process industries. The most commercially attractive avenues will be those that can leverage the established paper-based microfluidic toolbox developed for global health, while tapping high-margin markets that can support the necessary development costs. In addition to broadening the applicability of paper-based microfluidics, early commercial success in more niche

1
2
3 markets can set the stage for more significant investment in the ultimate large-volume, low-margin
4
5 market of global health. More broadly, we see paper-based diagnostics as well-positioned within
6
7 the general trend toward distributed sensing. That is, as artificial intelligence powered big-data
8
9 solutions multiply across sectors, so do their sensing requirements. Those technical and cost
10
11 requirements are very similar to those of the global health applications that continue to shape the
12
13 paper-microfluidics field.
14
15
16
17
18
19
20
21
22
23
24
25
26
27
28
29
30
31
32
33
34
35
36
37
38
39
40
41
42
43
44
45
46
47
48
49
50
51
52
53
54
55
56
57
58
59
60

AUTHOR INFORMATION

Corresponding Author
Email: sinton@mie.utoronto.ca

Notes
The authors declare no financial competing interests.

Biographies
Max Gong received his B.A.Sc. from University of Toronto in 2007, his M.A.Sc. from University of Guelph in 2010, and his Ph.D. from University of Toronto in 2015. During his doctoral studies, he was the recipient of an Alexander Graham Bell Canada Graduate Scholarship from the Natural Sciences and Research Council of Canada (NSERC). He is currently a Postdoctoral Fellow in Biomedical Engineering at the University of Wisconsin-Madison, supported by a NSERC Postdoctoral Fellowship.

David Sinton received his B.Eng. from University of Toronto in 1998, his M.Eng from McGill University in 2000, and his Ph.D. from University of Toronto in 2003. He holds the rank of Professor in Mechanical Engineering at the University of Toronto, where he holds the Canada Research Chair in Microfluidics and Energy. He is a Fellow of the American Society of Mechanical Engineers, a Fellow of the Engineering Institute of Canada, and the holder of an NSERC E.W.R. Steacie Memorial Fellowship.

ACKNOWLEDGEMENTS

The authors gratefully acknowledge an Alexander Graham Bell Canada Graduate Scholarship-Doctoral and a Postdoctoral Fellowship from the Natural Sciences and Engineering Research Council of Canada to M.M.G. The authors also gratefully acknowledge funding support of Grand Challenges Canada (5-02-02-01-01), the Natural Sciences and Engineering Research Council of Canada and the Canadian Institutes of Health Research through the CHRP program (18009-10), and the Canada Research Chairs Program (230931). Moreover, the authors thank Dr. Aaron Persad for his insightful suggestions for improving the scope and organization of the manuscript.

REFERENCES

- (1) Gates, B. The Next Epidemic - Lessons from Ebola. *N. Engl. J. Med.* **2015**, 372 (15), 1381–1384.
- (2) Whitesides, G. M. Cool, or Simple and Cheap? Why Not Both? *Lab Chip* **2013**, 13 (1), 11–13.
- (3) Gubala, V.; Harris, L. F.; Ricco, A. J.; Tan, M. X.; Williams, D. E. Point of Care Diagnostics: Status and Future. *Anal. Chem.* **2012**, 84, 487–515.
- (4) Yager, P.; Domingo, G. J.; Gerdes, J. Point-of-Care Diagnostics for Global Health. *Annu. Rev. Biomed. Eng.* **2008**, 10, 107–144.
- (5) Whitesides, G. M. The Origins and the Future of Microfluidics. *Nature* **2006**, 442 (July), 368–373.
- (6) Gervais, L.; De Rooij, N.; Delamarche, E. Microfluidic Chips for Point-of-Care Immunodiagnosics. *Adv. Mater.* **2011**, 23.
- (7) Culbertson, C. T.; Mickleburgh, T. G.; Stewart-James, S. A.; Sellens, K. A.; Pressnall, M. Micro Total Analysis Systems: Fundamental Advances and Biological Applications. *Anal. Chem.* **2014**, 86, 95–118.
- (8) Sackmann, E. K.; Fulton, A. L.; Beebe, D. J. The Present and Future Role of Microfluidics in Biomedical Research. *Nature* **2014**, 507 (7491), 181–189.
- (9) Jiang, H.; Weng, X.; Li, D. Microfluidic Whole-Blood Immunoassays. *Microfluid. Nanofluidics* **2011**, 10, 941–964.
- (10) Chen, L.; Manz, A.; Day, P. J. R. Total Nucleic Acid Analysis Integrated on Microfluidic Devices. *Lab Chip* **2007**, 7, 1413–1423.
- (11) Niemz, A.; Ferguson, T. M.; Boyle, D. S. Point-of-Care Nucleic Acid Testing for Infectious Diseases. *Trends Biotechnol.* **2011**, 29 (5), 240–250.
- (12) Bange, A.; Halsall, H. B.; Heineman, W. R. Microfluidic Immunosensor Systems. *Biosens. Bioelectron.* **2005**, 20, 2488–2503.
- (13) Harrison, D. J.; Manz, A.; Fan, Z.; Luedi, H.; Widmer, H. M. Capillary Electrophoresis and Sample Injection Systems Integrated on a Planar Glass Chip. *Anal. Chem.* **1992**, 64 (20), 1926–1932.
- (14) Bilitewski, U.; Genrich, M.; Kadow, S.; Mersal, G. Biochemical Analysis with Microfluidic Systems. *Anal. Bioanal. Chem.* **2003**, 377, 556–569.
- (15) Sia, S. K.; Whitesides, G. M. Microfluidic Devices Fabricated in Poly(dimethylsiloxane) for Biological Studies. *Electrophoresis* **2003**, 24 (21), 3563–3576.
- (16) Nunes, P. S.; Ohlsson, P. D.; Ordeig, O.; Kutter, J. P. Cyclic Olefin Polymers: Emerging Materials for Lab-on-a-Chip Applications. *Microfluid. Nanofluidics* **2010**, 9 (2), 145–161.
- (17) Roy, E.; Galas, J.-C.; Veres, T. Thermoplastic Elastomers for Microfluidics: Towards a High-Throughput Fabrication Method of Multilayered Microfluidic Devices. *Lab Chip* **2011**,

- 11 (18), 3193–3196.
- (18) Cate, D. M.; Adkins, J. A.; Mettakoonpitak, J.; Henry, C. S. Recent Developments in Paper-Based Microfluidic Devices. *Anal. Chem.* **2015**, 87 (1), 19–41.
- (19) Nilghaz, a.; Ballerini, D. R.; Shen, W. Exploration of Microfluidic Devices Based on Multi-Filament Threads and Textiles: A Review. *Biomicrofluidics* **2013**, 7 (2013), 0–16.
- (20) Martin, A. J. P.; Synge, R. L. M. A New Form of Chromatogram Employing Two Liquid Phases. *Biochem. J.* **1941**, 35 (12), 1358–1368.
- (21) Kunkel, H. G.; Tiselius, A. Electrophoresis of Proteins on Filter Paper. *J. Gen. Physiol.* **1951**, 35 (2), 89–118.
- (22) Chard, T. Pregnancy Tests: A Review. *Hum. Reprod.* **1992**, 7 (5), 701–710.
- (23) Martinez, A. W.; Phillips, S. T.; Butte, M. J.; Whitesides, G. M. Patterned Paper as a Platform for Inexpensive, Low-Volume, Portable Bioassays. *Angew. Chemie - Int. Ed.* **2007**, 46 (8), 1318–1320.
- (24) Rolland, J.; Mourey, D. Paper as a Novel Material Platform for Devices. *MRS Bull.* **2013**, 38 (4), 299–305.
- (25) Fu, E.; Liang, T.; Spicar-Mihalic, P.; Houghtaling, J.; Ramachandran, S.; Yager, P. Two-Dimensional Paper Network Format That Enables Simple Multistep Assays for Use in Low-Resource Settings in the Context of Malaria Antigen Detection. *Anal. Chem.* **2012**, 84 (10), 4574–4579.
- (26) Apilux, A.; Ukita, Y.; Chikae, M.; Chilapakul, O.; Takamura, Y. Development of Automated Paper-Based Devices for Sequential Multistep Sandwich Enzyme-Linked Immunosorbent Assays Using Inkjet Printing. *Lab Chip* **2012**, 126–135.
- (27) Fobel, R.; Kirby, A. E.; Ng, A. H. C.; Farnood, R. R.; Wheeler, A. R. Paper Microfluidics Goes Digital. *Adv. Mater.* **2014**, 26, 2838–2843.
- (28) Sicard, C.; Glen, C.; Aubie, B.; Wallace, D.; Jahanshahi-Anbuhi, S.; Pennings, K.; Daigger, G. T.; Pelton, R.; Brennan, J. D.; Filipe, C. D. M. Tools for Water Quality Monitoring and Mapping Using Paper-Based Sensors and Cell Phones. *Water Res.* **2015**, 70, 360–369.
- (29) Busa, L.; Mohammadi, S.; Maeki, M.; Ishida, A.; Tani, H.; Tokeshi, M. Advances in Microfluidic Paper-Based Analytical Devices for Food and Water Analysis. *Micromachines* **2016**, 7 (5), 86.
- (30) Meredith, N. A.; Quinn, C.; Cate, D. M.; Reilly, T. H.; Volckens, J.; Henry, C. S. Paper-Based Analytical Devices for Environmental Analysis. *Analyst* **2016**, 141 (6), 1874–1887.
- (31) Li, X.; Ballerini, D. R.; Shen, W. A Perspective on Paper-Based Microfluidics: Current Status and Future Trends. *Biomicrofluidics* **2012**, 6 (1), 11301.
- (32) Yetisen, A. K.; Akram, M. S.; Lowe, C. R. Paper-Based Microfluidic Point-of-Care Diagnostic Devices. *Lab Chip* **2013**, 13, 2210–2251.
- (33) Byrnes, S.; Thiessen, G.; Fu, E. Progress in the Development of Paper-Based Diagnostics for Low-Resource Point-of-Care Settings. *Bioanalysis* **2013**, 5 (22), 2821–2836.

- (34) Tomazelli Coltro, W. K.; Cheng, C. M.; Carrilho, E.; de Jesus, D. P. Recent Advances in Low-Cost Microfluidic Platforms for Diagnostic Applications. *Electrophoresis* **2014**, *35*, 2309–2324.
- (35) Hu, J.; Wang, S.; Wang, L.; Li, F.; Pingguan-Murphy, B.; Lu, T. J.; Xu, F. Advances in Paper-Based Point-of-Care Diagnostics. *Biosens. Bioelectron.* **2014**, *54*, 585–597.
- (36) Cheung, S. F.; Cheng, S. K. L.; Kamei, D. T. Paper-Based Systems for Point-of-Care Biosensing. *J. Lab. Autom.* **2015**, *20* (4), 316–333.
- (37) Lopez-Marzo, A. M.; Merkoci, A. Paper-Based Sensors and Assays: A Success of the Engineering Design and the Convergence of Knowledge Areas. *Lab Chip* **2016**.
- (38) Yang, Y.; Noviana, E.; Nguyen, M. P.; Geiss, B. J.; Dandy, D. S.; Henry, C. S. Paper-Based Microfluidic Devices: Emerging Themes and Applications. *Anal. Chem.* **2017**, *89* (1), 71–91.
- (39) Mahato, K.; Srivastava, A.; Chandra, P. Paper Based Diagnostics for Personalized Health Care: Emerging Technologies and Commercial Aspects. *Biosens. Bioelectron.* **2017**, *96*, 246–259.
- (40) Böhm, A.; Biesalski, M. Paper-Based Microfluidic Devices: A Complex Low-Cost Material in High-Tech Applications. *MRS Bull.* **2017**, *42* (5), 356–364.
- (41) Washburn, E. W. The Dynamics of Capillary Flow. *Phys. Rev.* **1921**, *17* (3), 273–283.
- (42) Fu, E.; Ramsey, S. a.; Kauffman, P.; Lutz, B.; Yager, P. Transport in Two-Dimensional Paper Networks. *Microfluid. Nanofluidics* **2011**, *10*, 29–35.
- (43) Walji, N.; MacDonald, D. B. Influence of Geometry and Surrounding Conditions on Fluid Flow in Paper-Based Devices. *Micromachines* . 2016.
- (44) Gong, M. M.; Nosrati, R.; San Gabriel, M. C.; Zini, A.; Sinton, D. Direct DNA Analysis with Paper-Based Ion Concentration Polarization. *J. Am. Chem. Soc.* **2015**, *137* (43), 13913–13919.
- (45) Darcy, H. *Les Fontaines Publiques de La Ville de Dijon*; Dalmont, Paris, 1856.
- (46) Camplisson, C. K.; Schilling, K. M.; Pedrotti, W. L.; Stone, H. A.; Martinez, A. W. Two-Ply Channels for Faster Wicking in Paper-Based Microfluidic Devices. *Lab Chip* **2015**.
- (47) Elizalde, E.; Urteaga, R.; Berli, C. L. a. Rational Design of Capillary-Driven Flows for Paper-Based Microfluidics. *Lab Chip* **2015**, *15*, 2173–2180.
- (48) Bird, R. B.; Stewart, W. E.; Lightfoot, E. N. *Transport Phenomena, Revised Second Edition*; John Wiley & Sons Inc., 2007.
- (49) Hong, S.; Kim, W. Dynamics of Water Imbibition through Paper Channels with Wax Boundaries. *Microfluid. Nanofluidics* **2015**, *19* (4), 845–853.
- (50) Songok, J.; Tuominen, M.; Teisala, H.; Haapanen, J.; Mäkelä, J.; Kuusipalo, J.; Toivakka, M. Paper-Based Microfluidics: Fabrication Technique and Dynamics of Capillary-Driven Surface Flow. *ACS Appl. Mater. Interfaces* **2014**, *6* (22), 20060–20066.
- (51) Böhm, A.; Carstens, F.; Trieb, C.; Schabel, S.; Biesalski, M. Engineering Microfluidic Papers: Effect of Fiber Source and Paper Sheet Properties on Capillary-Driven Fluid Flow.

- Microfluid. Nanofluidics* **2014**, *16*, 789–799.
- (52) Bazylak, A. Liquid Water Visualization in PEM Fuel Cells: A Review. *Int. J. Hydrogen Energy* **2009**, *34* (9), 3845–3857.
- (53) Carmo, M.; Fritz, D. L.; Mergel, J.; Stolten, D. A Comprehensive Review on PEM Water Electrolysis. *Int. J. Hydrogen Energy* **2013**, *38* (12), 4901–4934.
- (54) Mathias, M. F.; Roth, J.; Fleming, J.; Lehnert, W. Diffusion Media Materials and Characterisation. In *Handbook of Fuel Cells*; John Wiley & Sons Inc., 2010.
- (55) Gostick, J. T.; Fowler, M. W.; Pritzker, M. D.; Ioannidis, M. A.; Behra, L. M. In-Plane and through-Plane Gas Permeability of Carbon Fiber Electrode Backing Layers. *J. Power Sources* **2006**, *162* (1), 228–238.
- (56) Rofaiel, A.; Ellis, J. S.; Challa, P. R.; Bazylak, A. Heterogeneous through-Plane Distributions of Polytetrafluoroethylene in Polymer Electrolyte Membrane Fuel Cell Gas Diffusion Layers. *J. Power Sources* **2012**, *201*, 219–225.
- (57) Hinebaugh, J.; Lee, J.; Bazylak, A. Visualizing Liquid Water Evolution in a PEM Fuel Cell Using Synchrotron Radiography. *ECS Trans.* **2013**, *50* (2), 343–352.
- (58) Ge, N.; Chevalier, S.; Lee, J.; Yip, R.; Banerjee, R.; George, M. G.; Liu, H.; Lee, C.; Fazeli, M.; Antonacci, P.; et al. Non-Isothermal Two-Phase Transport in a Polymer Electrolyte Membrane Fuel Cell with Crack-Free Microporous Layers. *Int. J. Heat Mass Transf.* **2017**, *107*, 418–431.
- (59) Fu, E.; Lutz, B.; Kauffman, P.; Yager, P. Controlled Reagent Transport in Disposable 2D Paper Networks. *Lab Chip* **2010**, *10*, 918–920.
- (60) Lutz, B. R.; Trinh, P.; Ball, C.; Fu, E.; Yager, P. Two-Dimensional Paper Networks: Programmable Fluidic Disconnects for Multi-Step Processes in Shaped Paper. *Lab Chip* **2011**, *11* (24), 4274.
- (61) Fu, E.; Liang, T.; Houghtaling, J.; Ramachandran, S.; Ramsey, S. A.; Lutz, B.; Yager, P. Enhanced Sensitivity of Lateral Flow Tests Using a Two-Dimensional Paper Network Format. *Anal. Chem.* **2011**, *83* (20), 7941–7946.
- (62) Fridley, G. E.; Le, H.; Yager, P. Highly Sensitive Immunoassay Based on Controlled Rehydration of Patterned Reagents in a 2-Dimensional Paper Network. *Anal. Chem.* **2014**, *86* (13), 6447–6453.
- (63) Grant, B. D.; Smith, C. A.; Karvonen, K.; Richards-Kortum, R. Highly Sensitive Two-Dimensional Paper Network Incorporating Biotin–Streptavidin for the Detection of Malaria. *Anal. Chem.* **2016**, *88* (5), 2553–2557.
- (64) Kong, F.; Hu, Y. F. Biomolecule Immobilization Techniques for Bioactive Paper Fabrication. *Anal. Bioanal. Chem.* **2012**, *403*, 7–13.
- (65) Ramachandran, S.; Fu, E.; Lutz, B.; Yager, P. Long-Term Dry Storage of an Enzyme-Based Reagent System for ELISA in Point-of-Care Devices. *Analyst* **2014**, *139* (6), 1456–1462.
- (66) Holstein, C. A.; Chevalier, A.; Bennett, S.; Anderson, C. E.; Keniston, K.; Olsen, C.; Li, B.; Bales, B.; Moore, D. R.; Fu, E.; et al. Immobilizing Affinity Proteins to Nitrocellulose: A

- Toolbox for Paper-Based Assay Developers. *Anal. Bioanal. Chem.* **2016**, *408* (5), 1335–1346.
- (67) Martinez, A. W.; Phillips, S. T.; Whitesides, G. M. Three-Dimensional Microfluidic Devices Fabricated in Layered Paper and Tape. *Proc. Natl. Acad. Sci. U. S. A.* **2008**, *105* (50), 19606–19611.
- (68) Liu, H.; Crooks, R. M. Three-Dimensional Paper Microfluidic Devices Assembled Using the Principles of Origami. *J. Am. Chem. Soc.* **2011**, *133*, 17564–17566.
- (69) Li, X.; Liu, X. Fabrication of Three-Dimensional Microfluidic Channels in a Single Layer of Cellulose Paper. *Microfluid. Nanofluidics* **2014**, *1* (1), 1–9.
- (70) Renault, C.; Koehne, J.; Ricco, A. J.; Crooks, R. M. Three-Dimensional Wax Patterning of Paper Fluidic Devices. *Langmuir* **2014**, *30*, 7030–7036.
- (71) Vella, S. J.; Beattie, P.; Cademartiri, R.; Laromaine, A.; Martinez, A. W.; Phillips, S. T.; Mirica, K. a.; Whitesides, G. M. Measuring Markers of Liver Function Using a Micropatterned Paper Device Designed for Blood from a Fingertick. *Anal. Chem.* **2012**, *84*, 2883–2891.
- (72) Cunningham, J. C.; Brenes, N. J.; Crooks, R. M. Paper Electrochemical Device for Detection of DNA and Thrombin by Target-Induced Conformational Switching. *Anal. Chem.* **2014**, *86* (12), 6166–6170.
- (73) Martinez, A. W.; Phillips, S. T.; Nie, Z.; Cheng, C.-M.; Carrilho, E.; Wiley, B. J.; Whitesides, G. M. Programmable Diagnostic Devices Made from Paper and Tape. *Lab Chip* **2010**, *10*, 2499–2504.
- (74) Pollock, N. R.; Rolland, J. P.; Kumar, S.; Beattie, P. D.; Jain, S.; Noubary, F.; Wong, V. L.; Pohlmann, R. a.; Ryan, U. S.; Whitesides, G. M. A Paper-Based Multiplexed Transaminase Test for Low-Cost, Point-of-Care Liver Function Testing. *Sci. Transl. Med.* **2012**, *4* (152), 152ra129–152ra129.
- (75) Schilling, K. M.; Lepore, A. L.; Kurian, J. a.; Martinez, A. W. Fully Enclosed Microfluidic Paper-Based Analytical Devices. *Anal. Chem.* **2012**, *84*, 1579–1585.
- (76) Liu, X. Y.; Cheng, C. M.; Martinez, a. W.; Mirica, K. a.; Li, X. J.; Phillips, S. T.; Mascareñas, M.; Whitesides, G. M. A Portable Microfluidic Paper-Based Device for Elisa. *Proc. IEEE Int. Conf. Micro Electro Mech. Syst.* **2011**, 75–78.
- (77) Gerbers, R.; Foellscher, W.; Chen, H.; Anagnostopoulos, C.; Faghri, M. A New Paper-Based Platform Technology for Point-of-Care Diagnostics. *Lab Chip* **2014**, *14*, 4042–4049.
- (78) Han, K. N.; Choi, J.-S.; Kwon, J. Three-Dimensional Paper-Based Slip Device for One-Step Point-of-Care Testing. *Sci. Rep.* **2016**, *6*, 25710.
- (79) Gan, W.; Zhuang, B.; Zhang, P.; Han, J.; Li, C.; Liu, P. A Filter Paper-Based Microdevice for Low-Cost, Rapid, and Automated DNA Extraction and Amplification from Diverse Sample Types. *Lab Chip* **2014**, *14* (19).
- (80) Connelly, J. T.; Rolland, J. P.; Whitesides, G. M. “Paper Machine” for Molecular Diagnostics. *Anal. Chem.* **2015**, *87* (15), 7595–7601.

- (81) Govindarajan, A. V.; Ramachandran, S.; Vigil, G. D.; Yager, P.; Bohringer, K. F. A Low Cost Point-of-Care Viscous Sample Preparation Device for Molecular Diagnosis in the Developing World; an Example of Microfluidic Origami. *Lab Chip* **2012**, *12* (1), 174–181.
- (82) Ge, L.; Wang, S.; Song, X.; Ge, S.; Yu, J. 3D Origami-Based Multifunction-Integrated Immunodevice: Low-Cost and Multiplexed Sandwich Chemiluminescence Immunoassay on Microfluidic Paper-Based Analytical Device. *Lab Chip* **2012**, *12* (17), 3150–3158.
- (83) Liu, W.; Cassano, C. L.; Xu, X.; Fan, Z. H. Laminated Paper-Based Analytical Devices (LPAD) with Origami-Enabled Chemiluminescence Immunoassay for Cotinine Detection in Mouse Serum. *Anal. Chem.* **2013**, *85*, 10270–10276.
- (84) Sechi, D.; Greer, B.; Johnson, J.; Hashemi, N. Three-Dimensional Paper-Based Microfluidic Device for Assays of Protein and Glucose in Urine. *Anal. Chem.* **2013**, *85* (22), 10733–10737.
- (85) Scida, K.; Li, B.; Ellington, A. D.; Crooks, R. M. DNA Detection Using Origami Paper Analytical Devices. *Anal. Chem.* **2013**, *85* (20), 9713–9720.
- (86) Robinson, R.; Wong, L.; Monnat, R. J.; Fu, E. Development of a Whole Blood Paper-Based Device for Phenylalanine Detection in the Context of PKU Therapy Monitoring. *Micromachines* **2016**, *7* (2), 28.
- (87) Li, X.; Liu, X. A Microfluidic Paper-Based Origami Nanobiosensor for Label-Free, Ultrasensitive Immunoassays. *Adv. Healthc. Mater.* **2016**, *5* (11), 1326–1335.
- (88) Jeong, S.-G.; Lee, S.-H.; Choi, C.-H.; Kim, J.; Lee, C.-S. Toward Instrument-Free Digital Measurements: A Three-Dimensional Microfluidic Device Fabricated in a Single Sheet of Paper by Double-Sided Printing and Lamination. *Lab Chip* **2015**, *15* (4), 1188–1194.
- (89) Renault, C.; Li, X.; Fosdick, S. E.; Crooks, R. M. Hollow-Channel Paper Analytical Devices. **2013**.
- (90) Glavan, A. C.; Martinez, R. V.; Maxwell, E. J.; Subramaniam, A. B.; Nunes, R. M. D.; Soh, S.; Whitesides, G. M. Rapid Fabrication of Pressure-Driven Open-Channel Microfluidic Devices in Omniphobic RF Paper. *Lab Chip* **2013**, *13* (15), 2922.
- (91) Giokas, D. L.; Tsogas, G. Z.; Vlessidis, A. G. Programming Fluid Transport in Paper-Based Microfluidic Devices Using Razor-Crafted Open Channels. *Anal. Chem.* **2014**, *86* (13), 6202–6207.
- (92) Jahanshahi-Anbuhi, S.; Chavan, P.; Sicard, C. C. C.; Leung, V.; Hossain, S. M. Z.; Pelton, R.; Brennan, J. D.; Filipe, C. D. M. M. Creating Fast Flow Channels in Paper Fluidic Devices to Control Timing of Sequential Reactions. *Lab Chip* **2012**, *12* (23), 5079.
- (93) da Silva, E. T. S. G.; Santhiago, M.; de Souza, F. R.; Coltro, W. K. T.; Kubota, L. T. Triboelectric Effect as a New Strategy for Sealing and Controlling the Flow in Paper-Based Devices. *Lab Chip* **2015**, *15*, 1651–1655.
- (94) Lutz, B.; Liang, T.; Fu, E.; Ramachandran, S.; Kauffman, P.; Yager, P. Dissolvable Fluidic Time Delays for Programming Multi-Step Assays in Instrument-Free Paper Diagnostics. *Lab Chip* **2013**, *13*, 2840–2847.

- (95) Whitesides, G. M. Viewpoint on “Dissolvable Fluidic Time Delays for Programming Multi-Step Assays in Instrument-Free Paper Diagnostics.” **2013**, *13*, 4004–4005.
- (96) Houghtaling, J.; Liang, T.; Thiessen, G.; Fu, E. Dissolvable Bridges for Manipulating Fluid Volumes in Paper Networks. *Anal. Chem.* **2013**, *85*, 11201–11204.
- (97) Jahanshahi-Anbuhi, S.; Henry, A.; Leung, V.; Sicard, C.; Pennings, K.; Pelton, R.; Brennan, J. D.; Filipe, C. D. M. Paper-Based Microfluidics with an Erodible Polymeric Bridge Giving Controlled Release and Timed Flow Shutoff. *Lab Chip* **2014**, *14*, 229–236.
- (98) Noh, H.; Phillips, S. T. Metering the Capillary-Driven Flow of Fluids in Paper-Based Microfluidic Devices. *Anal. Chem.* **2010**, *82* (10), 4181–4187.
- (99) Noh, H.; Phillips, S. T. Fluidic Timers for Time-Dependent, Point-of-Care Assays on Paper. *Anal. Chem.* **2010**, *82* (19), 8071–8078.
- (100) Lewis, G. G.; Robbins, J. S.; Phillips, S. T. Point-of-Care Assay Platform for Quantifying Active Enzymes to Femtomolar Levels Using Measurements of Time as the Readout. *Anal. Chem.* **2013**, *85* (21), 10432–10439.
- (101) Weng, C.-H.; Chen, M.-Y.; Shen, C.-H.; Yang, R.-J. Colored Wax-Printed Timers for Two-Dimensional and Three-Dimensional Assays on Paper-Based Devices. *Biomicrofluidics* **2014**, *8* (6), 66502.
- (102) Jang, I.; Song, S. Facile and Precise Flow Control for a Paper-Based Microfluidic Device through Varying Paper Permeability. *Lab Chip* **2015**, *15* (16), 3405–3412.
- (103) Salentijn, G. I. J.; Hamidon, N. N.; Verpoorte, E. Solvent-Dependent On/off Valving Using Selectively Permeable Barriers in Paper Microfluidics. *Lab Chip* **2016**, *16* (6), 1013–1021.
- (104) Hoyle, C. E.; Bowman, C. N. Thiol–Ene Click Chemistry. *Angew. Chemie Int. Ed.* **2010**, *49* (9), 1540–1573.
- (105) Chen, H.; Cogswell, J.; Anagnostopoulos, C.; Faghri, M. A Fluidic Diode, Valves, and a Sequential-Loading Circuit Fabricated on Layered Paper. *Lab Chip* **2012**, *12*, 2909.
- (106) He, P. J. W.; Katis, I. N.; Eason, R. W.; Sones, C. L. Engineering Fluidic Delays in Paper-Based Devices Using Laser Direct-Writing. *Lab Chip* **2015**, *15* (20), 4054–4061.
- (107) Toley, B. J.; McKenzie, B.; Liang, T.; Buser, J. R.; Yager, P.; Fu, E. Tunable-Delay Shunts for Paper Microfluidic Devices. *Anal. Chem.* **2013**, *85*, 11545–11552.
- (108) Toley, B. J.; Wang, J. a.; Gupta, M.; Buser, J. R.; Lafleur, L. K.; Lutz, B. R.; Fu, E.; Yager, P. A Versatile Valving Toolkit for Automating Fluidic Operations in Paper Microfluidic Devices. *Lab Chip* **2015**, *15*, 1432–1444.
- (109) Shin, J. H.; Park, J.; Kim, S. H.; Park, J.-K. Programmed Sample Delivery on a Pressurized Paper. *Biomicrofluidics* **2014**, *8* (5), 54121.
- (110) Bazylak, A.; Sinton, D.; Liu, Z.-S.; Djilali, N. Effect of Compression on Liquid Water Transport and Microstructure of PEMFC Gas Diffusion Layers. *J. Power Sources* **2007**, *163* (2), 784–792.
- (111) Park, J.; Shin, J. H.; Park, J.-K. Pressed Paper-Based Dipstick for Detection of Foodborne

- Pathogens with Multistep Reactions. *Anal. Chem.* **2016**, *88* (7), 3781–3788.
- (112) Lee, K. Y.; Mooney, D. J. Hydrogels for Tissue Engineering. *Chem. Rev.* **2001**, *101* (7), 1869–1880.
- (113) Slaughter, B. V.; Khurshid, S. S.; Fisher, O. Z.; Khademhosseini, A.; Peppas, N. A. Hydrogels in Regenerative Medicine. *Adv. Mater.* **2009**, *21* (32–33), 3307–3329.
- (114) Hoare, T. R.; Kohane, D. S. Hydrogels in Drug Delivery: Progress and Challenges. *Polymer (Guildf)*. **2008**, *49* (8), 1993–2007.
- (115) Peppas, N. A.; Hilt, J. Z.; Khademhosseini, A.; Langer, R. Hydrogels in Biology and Medicine: From Molecular Principles to Bionanotechnology. *Adv. Mater.* **2006**, *18* (11), 1345–1360.
- (116) Niedl, R. R.; Beta, C. Hydrogel-Driven Paper-Based Microfluidics. *Lab Chip* **2015**, *15*, 2452–2459.
- (117) Mitchell, H.; Schultz, S.; Costanzo, P.; Martinez, A. Poly(N-Isopropylacrylamide) Hydrogels for Storage and Delivery of Reagents to Paper-Based Analytical Devices. *Chromatography* **2015**, *2* (3), 436–451.
- (118) Wei, X.; Tian, T.; Jia, S.; Zhu, Z.; Ma, Y.; Sun, J.; Lin, Z.; Yang, C. J. Target-Responsive DNA Hydrogel Mediated “Stop-Flow” Microfluidic Paper-Based Analytic Device for Rapid, Portable and Visual Detection of Multiple Targets. *Anal. Chem.* **2015**, 150402134355000.
- (119) Tian, T.; Wei, X.; Jia, S.; Zhang, R.; Li, J.; Zhu, Z.; Zhang, H.; Ma, Y.; Lin, Z.; Yang, C. J. Integration of Target Responsive Hydrogel with Cascaded Enzymatic Reactions and Microfluidic Paper-Based Analytic Devices (??PADs) for Point-of-Care Testing (POCT). *Biosens. Bioelectron.* **2016**, *77*, 537–542.
- (120) Wei, X.; Tian, T.; Jia, S.; Zhu, Z.; Ma, Y.; Sun, J.; Lin, Z.; Yang, C. J. Microfluidic Distance Readout Sweet Hydrogel Integrated Paper-Based Analytical Device (??DiSH-PAD) for Visual Quantitative Point-of-Care Testing. *Anal. Chem.* **2016**, *88* (4), 2345–2352.
- (121) Akyazi, T.; Saez, J.; Elizalde, J.; Benito-Lopez, F. Fluidic Flow Delay by Ionogel Passive Pumps in Microfluidic Paper-Based Analytical Devices. *Sensors Actuators, B Chem.* **2016**, *233*, 402–408.
- (122) Nosrati, R.; Gong, M. M.; Gabriel, M. C. S.; Pedraza, C. E.; Zini, A.; Sinton, D. Paper-Based Quantification of Male Fertility Potential. *Clin. Chem.* **2016**, *62* (3), 458–465.
- (123) Li, X.; Li, X.; Tian, J.; Tian, J.; Nguyen, T.; Nguyen, T.; Shen, W.; Shen, W. Paper-Based Microfluidic Devices by Plasma Treatment. *Lab Chip* **2008**, *80*, 9131–9134.
- (124) Liu, H.; Li, X.; Crooks, R. M. Paper-Based SlipPAD for High-Throughput Chemical Sensing. *Anal. Chem.* **2013**, *85* (9), 4263–4267.
- (125) Li, B.; Yu, L.; Qi, J.; Fu, L.; Zhang, P.; Chen, L. Controlling Capillary-Driven Fluid Transport in Paper-Based Microfluidic Devices Using Movable Valve. *Anal. Chem.* **2017**, DOI: 10.1021/acs.analchem.7b00726.
- (126) Du, W.; Li, L.; Nichols, K. P.; Ismagilov, R. F. SlipChip. *Lab Chip* **2009**, *9* (16), 2286–2292.

- (127) Li, X.; Zwanenburg, P.; Liu, X. Magnetic Timing Valves for Fluid Control in Paper-Based Microfluidics. *Lab Chip* **2013**, *13* (13), 2609.
- (128) Ngo, Y. H.; Li, D.; Simon, G. P.; Garnier, G. Paper Surfaces Functionalized by Nanoparticles. *Adv. Colloid Interface Sci.* **2011**, *163* (1), 23–38.
- (129) Fu, E.; Kauffman, P.; Lutz, B.; Yager, P. Chemical Signal Amplification in Two-Dimensional Paper Networks. *Sensors Actuators, B Chem.* **2010**, *149* (1), 325–328.
- (130) Hu, J.; Wang, L.; Li, F.; Han, Y. L.; Lin, M.; Lu, T. J.; Xu, F. Oligonucleotide-Linked Gold Nanoparticle Aggregates for Enhanced Sensitivity in Lateral Flow Assays. *Lab Chip* **2013**, *13*, 4352–4357.
- (131) Rivas, L.; Medina-Sánchez, M.; de la Escosura-Muñiz, A.; Merkoçi, A. Improving Sensitivity of Gold Nanoparticle-Based Lateral Flow Assays by Using Wax-Printed Pillars as Delay Barriers of Microfluidics. *Lab Chip* **2014**, *14* (22), 4406–4414.
- (132) Rastogi, S. K.; Gibson, C. M.; Branen, J. R.; Eric Aston, D.; Larry Branen, a.; Hrdlicka, P. J. DNA Detection on Lateral Flow Test Strips: Enhanced Signal Sensitivity Using LNA-Conjugated Gold Nanoparticles. *Chem. Commun.* **2012**, *48*, 7714.
- (133) Liu, Q.; Wang, J.; Wang, B.; Li, Z.; Huang, H.; Li, C.; Yu, X.; Chu, P. K. Paper-Based Plasmonic Platform for Sensitive, Noninvasive, and Rapid Cancer Screening. *Biosens. Bioelectron.* **2014**, *54*, 128–134.
- (134) Zhao, W.; Ali, M. M.; Aguirre, S. D.; Brook, M. a.; Li, Y. Paper-Based Bioassays Using Gold Nanoparticle Colorimetric Probes. *Anal. Chem.* **2008**, *80* (22), 8431–8437.
- (135) Badu-Tawiah, A. K.; Lathwal, S.; Kaastrup, K.; Al-Sayah, M.; Christodouleas, D. C.; Smith, B. S.; Whitesides, G. M.; Sikes, H. D. Polymerization-Based Signal Amplification for Paper-Based Immunoassays. *Lab Chip* **2014**, *15*, 655–659.
- (136) Yu, W. W.; White, I. M. Inkjet-Printed Paper-Based SERS Dipsticks and Swabs for Trace Chemical Detection. *Analyst* **2012**, *138* (4).
- (137) Chiu, R. Y. T.; Jue, E.; Yip, A. T.; Berg, A. R.; Wang, S. J.; Kivnick, A. R.; Nguyen, P. T.; Kamei, D. T. Simultaneous Concentration and Detection of Biomarkers on Paper. *Lab Chip* **2014**, *14* (16), 3021–3028.
- (138) Ho, J.; Tan, M. K.; Go, D. B.; Yeo, L. Y.; Friend, J. R.; Chang, H. C. Paper-Based Microfluidic Surface Acoustic Wave Sample Delivery and Ionization Source for Rapid and Sensitive Ambient Mass Spectrometry. *Anal. Chem.* **2011**, *83*, 3260–3266.
- (139) Rezk, A. R.; Qi, A.; Friend, J. R.; Li, W. H.; Yeo, L. Y. Uniform Mixing in Paper-Based Microfluidic Systems Using Surface Acoustic Waves. *Lab Chip* **2012**, *12* (4), 773–779.
- (140) Wong, S. Y.; Cabodi, M.; Rolland, J.; Klapperich, C. M. Evaporative Concentration on a Paper-Based Device to Concentrate Analytes in a Biological Fluid. *Anal. Chem.* **2014**, *86* (24), 11981–11985.
- (141) Smejkal, P.; Bottenus, D.; Breadmore, M. C.; Guijt, R. M.; Ivory, C. F.; Foret, F.; Macka, M. Microfluidic Isotachophoresis: A Review. *Electrophoresis* **2013**, *34*, 1493–1509.
- (142) Ma, B.; Song, Y.-Z.; Niu, J.-C.; Wu, Z.-Y. Highly Efficient Sample Stacking by Enhanced

- Field Amplification on a Simple Paper Device. *Lab Chip* **2016**, *16* (18), 3460–3465.
- (143) Ma, B.; Xie, S.-F.; Liu, L.; Fang, F.; Wu, Z.-Y. Two Orders of Magnitude Electrokinetic Stacking of Proteins in One Minute on a Simple Paper Fluidic Channel. *Anal. Methods* **2017**, *9* (18), 2703–2709.
- (144) Tia, S.; Herr, A. E. On-Chip Technologies for Multidimensional Separations. *Lab Chip* **2009**, *9* (17), 2524.
- (145) Schwartz, O.; Bercovici, M. Microfluidic Assay for Continuous Bacteria Detection Using Antimicrobial Peptides and Isotachopheresis. *Anal. Chem.* **2014**.
- (146) Lin, C. C.; Wang, J. H.; Wu, H. W.; Lee, G. Bin. Microfluidic Immunoassays. *JALA - J. Assoc. Lab. Autom.* **2010**, *15* (3), 253–274.
- (147) Moghadam, B. Y.; Connelly, K. T.; Posner, J. D. Isotachophoretic Preconcentration on Paper-Based Microfluidic Devices. *Anal. Chem.* **2014**, *86*, 5829–5837.
- (148) Moghadam, B. Y.; Connelly, K. T.; Posner, J. D. Two Orders of Magnitude Improvement in Detection Limit of Lateral Flow Assays Using Isotachopheresis. *Anal. Chem.* **2015**, *87*, 1009–1017.
- (149) Rosenfeld, T.; Bercovici, M. 1000-Fold Sample Focusing on Paper-Based Microfluidic Devices. *Lab Chip* **2014**, *14* (23), 4465–4474.
- (150) Li, X.; Luo, L.; Crooks, R. M. Low-Voltage Paper Isotachopheresis Device for DNA Focusing. *Lab Chip* **2015**.
- (151) Gong, M. M.; Zhang, P.; MacDonald, B. D.; Sinton, D. Nanoporous Membranes Enable Concentration and Transport in Fully Wet Paper-Based Assays. *Anal. Chem.* **2014**, *86*, 8090–8097.
- (152) Yang, R.-J.; Pu, H.-H.; Wang, H.-L. Ion Concentration Polarization on Paper-Based Microfluidic Devices and Its Application to Preconcentrate Dilute Sample Solutions. *Biomicrofluidics* **2015**, *9*, 14122.
- (153) Yeh, S.-H.; Chou, K.-H.; Yang, R.-J. Sample Pre-Concentration with High Enrichment Factors at a Fixed Location in Paper-Based Microfluidic Devices. *Lab Chip* **2016**, *16* (5), 925–931.
- (154) Han, S. Il; Hwang, K. S.; Kwak, R.; Lee, J. H. Microfluidic Paper-Based Biomolecule Preconcentrator Based on Ion Concentration Polarization. *Lab Chip* **2016**, *16* (12), 2219–2227.
- (155) Phan, D.-T.; Shaegh, S. A. M.; Yang, C.; Nguyen, N.-T. Sample Concentration in a Microfluidic Paper-Based Analytical Device Using Ion Concentration Polarization. *Sensors Actuators B Chem.* **2016**, *222*, 735–740.
- (156) Hölzel, A.; Tallarek, U. Ionic Conductance of Nanopores in Microscale Analysis Systems: Where Microfluidics Meets Nanofluidics. *J. Sep. Sci.* **2007**, *30* (10), 1398–1419.
- (157) Zangle, T. A.; Mani, A.; Santiago, J. G. Theory and Experiments of Concentration Polarization and Ion Focusing at Microchannel and Nanochannel Interfaces. *Chem. Soc. Rev.* **2010**, *39* (3), 1014–1035.

- (158) Kim, S. J.; Ko, S. H.; Kang, K. H.; Han, J. Direct Seawater Desalination by Ion Concentration Polarization. *Nat. Nanotechnol.* **2010**, *5* (4), 297–301.
- (159) MacDonald, B. D.; Gong, M. M.; Zhang, P.; Sinton, D. Out-of-Plane Ion Concentration Polarization for Scalable Water Desalination. *Lab Chip* **2014**, *14* (4), 681–685.
- (160) Scarff, B.; Escobedo, C.; Sinton, D. Radial Sample Preconcentration. *Lab Chip* **2011**, *11*, 1102–1109.
- (161) Ko, S. H.; Song, Y.-A.; Kim, S. J.; Kim, M.; Han, J.; Kang, K. H. Nanofluidic Preconcentration Device in a Straight Microchannel Using Ion Concentration Polarization. *Lab Chip* **2012**, *12* (21), 4472–4482.
- (162) Jeon, H.; Lee, H.; Kang, K. H.; Lim, G. Ion Concentration Polarization-Based Continuous Separation Device Using Electrical Repulsion in the Depletion Region. *Sci. Rep.* **2013**, *3*, 3483.
- (163) Song, H.; Wang, Y.; Garson, C.; Pant, K. Nafion-Film-Based Micro–nanofluidic Device for Concurrent DNA Preconcentration and Separation in Free Solution. *Microfluid. Nanofluidics* **2014**, *17* (2008), 693–699.
- (164) Wu, Z.-Y.; Ma, B.; Xie, S.-F.; Liu, K.; Fang, F. Simultaneous Electrokinetic Concentration and Separation of Proteins on a Paper-Based Analytical Device. *RSC Adv.* **2017**, *7* (7), 4011–4016.
- (165) Hong, S.; Kwak, R.; Kim, W. Paper-Based Flow Fractionation System Applicable to Preconcentration and Field-Flow Separation. *Anal. Chem.* **2016**, *88* (3), 1682–1687.
- (166) Li, X.; Luo, L.; Crooks, R. M. Faradaic Ion Concentration Polarization on a Paper Fluidic Platform. *Anal. Chem.* **2017**, *89* (7), 4294–4300.
- (167) Lee, K.; Yoo, Y. K.; Han, S. Il; Lee, J.; Lee, D.; Kim, C.; Lee, J. H. Folding-Paper-Based Preconcentrator for Low Dispersion of Preconcentration Plug. *Micro Nano Syst. Lett.* **2017**, *5* (1), 11.
- (168) Hung, L.-H.; Wang, H.-L.; Yang, R.-J. A Portable Sample Concentrator on Paper-Based Microfluidic Devices. *Microfluid. Nanofluidics* **2016**, *20* (5), 1–9.
- (169) Li, X.; Niu, Y.; Chen, Y.; Wu, D.; Yi, L.; Qiu, X. Microfluidic Paper-Based Sample Concentration Using Ion Concentration Polarization with Smartphone Detection. *Micromachines* **2016**, *7* (11), 199.
- (170) Ge, L.; Wang, S.; Ge, S.; Yu, J.; Yan, M.; Li, N.; Huang, J. Electrophoretic Separation in a Microfluidic Paper-Based Analytical Device with an on-Column Wireless Electrogenerated Chemiluminescence Detector. *Chem. Commun. (Camb)*. **2014**, *50* (4), 5699–5702.
- (171) Chen, S.-S.; Hu, C.-W.; Yu, I.-F.; Liao, Y.-C.; Yang, J.-T. Origami Paper-Based Fluidic Batteries for Portable Electrophoretic Devices. *Lab Chip* **2014**, *14* (12), 2124–2130.
- (172) Luo, L.; Li, X.; Crooks, R. M. Low-Voltage Origami-Paper-Based Electrophoretic Device for Rapid Protein Separation. *Anal. Chem.* **2014**, *86* (24), 12390–12397.
- (173) Buser, J. R.; Zhang, X.; Byrnes, S. A.; Ladd, P. D.; Heiniger, E. K.; Wheeler, M. D.; Bishop, J. D.; Englund, J. A.; Lutz, B.; Weigl, B. H.; et al. A Disposable Chemical Heater and Dry

- Enzyme Preparation for Lysis and Extraction of DNA and RNA from Microorganisms. *Anal. Methods* **2016**, 8 (14), 2880–2886.
- (174) Erickson, D.; Sinton, D.; Li, D. A Miniaturized High-Voltage Integrated Power Supply for Portable Microfluidic Applications. *Lab Chip* **2004**, 4 (2), 87–90.
- (175) Gong, M. M.; MacDonald, B. D.; Nguyen, T. V.; Van Nguyen, K.; Sinton, D. Lab-in-a-Pen: A Diagnostics Format Familiar to Patients for Low-Resource Settings. *Lab Chip* **2014**, 14, 957–963.
- (176) Li, C. G.; Joung, H.-A.; Noh, H.; Song, M.-B.; Kim, M.-G.; Jung, H. One-Touch-Activated Blood Multidiagnostic System Using a Minimally Invasive Hollow Microneedle Integrated with a Paper-Based Sensor. *Lab Chip* **2015**, 15 (16), 3286–3292.
- (177) Bariya, S. H.; Gohel, M. C.; Mehta, T. A.; Sharma, O. P. Microneedles: An Emerging Transdermal Drug Delivery System. *J. Pharm. Pharmacol.* **2012**, 64 (1), 11–29.
- (178) Kim, Y.-C.; Park, J.-H.; Prausnitz, M. R. Microneedles for Drug and Vaccine Delivery. *Adv. Drug Deliv. Rev.* **2012**, 64 (14), 1547–1568.
- (179) Ita, K. Transdermal Delivery of Drugs with Microneedles—Potential and Challenges. *Pharmaceutics* . 2015.
- (180) Romanyuk, A. V.; Zvezdin, V. N.; Samant, P.; Grenader, M. I.; Zemlyanova, M.; Prausnitz, M. R. Collection of Analytes from Microneedle Patches. *Anal. Chem.* **2014**, 86 (21), 10520–10523.
- (181) Wong, A. P.; Gupta, M.; Shevkoplyas, S. S.; Whitesides, G. M. Egg Beater as Centrifuge: Isolating Human Blood Plasma from Whole Blood in Resource-Poor Settings. *Lab Chip* **2008**, 8 (12), 2032–2037.
- (182) Brown, J.; Theis, L.; O'Connor, K.; Kerr, L.; Uthman, M.; Oden, Z. M.; Zakhidova, N.; Richards-Kortum, R. A Hand-Powered, Portable, Low-Cost Centrifuge for Diagnosing Anemia in Low-Resource Settings. *Am. J. Trop. Med. Hyg.* **2011**, 85 (2), 327–332.
- (183) Yang, S.; Undar, A.; Zahn, J. D. A Microfluidic Device for Continuous, Real Time Blood Plasma Separation. *Lab Chip* **2006**, 6, 871–880.
- (184) Kersaudy-Kerhoas, M.; Dhariwal, R.; Desmulliez, M. P. Y.; Jouvet, L. Hydrodynamic Blood Plasma Separation in Microfluidic Channels. *Microfluid. Nanofluidics* **2010**, 8, 105–114.
- (185) Mielczarek, W. S.; Obaje, E. A.; Bachmann, T. T.; Kersaudy-Kerhoas, M. Microfluidic Blood Plasma Separation for Medical Diagnostics: Is It Worth It? *Lab Chip* **2016**, 16 (18), 3441–3448.
- (186) Fung, Y. C.; Zweifach, B. W. Microcirculation: Mechanics of Blood Flow in Capillaries. *Annu. Rev. Fluid Mech.* **1971**, 3 (1), 189–210.
- (187) Doyeux, V.; Podgorski, T.; Peponas, S.; Ismail, M.; Coupier, G. Spheres in the Vicinity of a Bifurcation: Elucidating the Zweifach-Fung Effect. **2010**, 674, 25.
- (188) Amasia, M.; Madou, M. Large-Volume Centrifugal Microfluidic Device for Blood Plasma Separation. *Bioanalysis* **2010**, 2 (10), 1701–1710.

- (189) Gorkin, R.; Park, J.; Siegrist, J.; Amasia, M.; Lee, B. S.; Park, J.-M.; Kim, J.; Kim, H.; Madou, M.; Cho, Y.-K. Centrifugal Microfluidics for Biomedical Applications. *Lab Chip* **2010**, *10*, 1758–1773.
- (190) Strohmeier, O.; Keller, M.; Schwemmer, F.; Zehnle, S.; Mark, D.; von Stetten, F.; Zengerle, R.; Paust, N. Centrifugal Microfluidic Platforms: Advanced Unit Operations and Applications. *Chem. Soc. Rev.* **2015**, *44* (17), 6187–6229.
- (191) Hwang, H.; Kim, S.-H.; Kim, T.-H.; Park, J.-K.; Cho, Y.-K. Paper on a Disc: Balancing the Capillary-Driven Flow with a Centrifugal Force. *Lab Chip* **2011**, *11* (20), 3404–3406.
- (192) Godino, N.; Vereshchagina, E.; Gorkin, R.; Ducrée, J. Centrifugal Automation of a Triglyceride Bioassay on a Low-Cost Hybrid Paper-Polymer Device. *Microfluid. Nanofluidics* **2014**, *16* (5), 895–905.
- (193) Bhamla, M. S.; Benson, B.; Chai, C.; Katsikis, G.; Johri, A.; Prakash, M. Hand-Powered Ultralow-Cost Paper Centrifuge. *Nat. Biomed. Eng.* **2017**, *1* (1), 1–7.
- (194) Gong, M. M.; Macdonald, B. D.; Vu Nguyen, T.; Van Nguyen, K.; Sinton, D. Field Tested Milliliter-Scale Blood Filtration Device for Point-of-Care Applications. *Biomicrofluidics* **2013**, *7* (4), 44111.
- (195) Khan, M. S.; Thouas, G.; Shen, W.; Whyte, G.; Garnier, G. Paper Diagnostic for Instantaneous Blood Typing. *Anal. Chem.* **2010**, *82* (10), 4158–4164.
- (196) Ge, L.; Wang, S.; Song, X.; Ge, S.; Yu, J. 3D Origami-Based Multifunction-Integrated Immunodevice: Low-Cost and Multiplexed Sandwich Chemiluminescence Immunoassay on Microfluidic Paper-Based Analytical Device. *Lab Chip* **2012**, *12* (17), 3150–3158.
- (197) Yang, X.; Forouzan, O.; Brown, T. P.; Shevkoplyas, S. S. Integrated Separation of Blood Plasma from Whole Blood for Microfluidic Paper-Based Analytical Devices. *Lab Chip* **2012**, *12*, 274.
- (198) Li, H.; Han, D.; Pauletti, G. M.; Steckl, A. J. Blood Coagulation Screening Using a Paper-Based Microfluidic Lateral Flow Device. *Lab Chip* **2014**, 4035–4041.
- (199) Nilghaz, A.; Shen, W. Low-Cost Blood Plasma Separation Method Using Salt Functionalized Paper. *RSC Adv.* **2015**, *5* (66), 53172–53179.
- (200) Songjaroen, T.; Dungchai, W.; Chailapakul, O.; Henry, C. S.; Laiwattanapaisal, W. Blood Separation on Microfluidic Paper-Based Analytical Devices. *Lab Chip* **2012**, *12*, 3392.
- (201) Homsy, A.; van der Wal, P. D.; Doll, W.; Schaller, R.; Korsatko, S.; Ratzer, M.; Ellmerer, M.; Pieber, T. R.; Nicol, A.; de Rooij, N. F. Development and Validation of a Low Cost Blood Filtration Element Separating Plasma from Undiluted Whole Blood. *Biomicrofluidics* **2012**, *6*.
- (202) Liu, C.; Mauk, M.; Gross, R.; Bushman, F. D.; Edelstein, P. H.; Collman, R. G.; Bau, H. H. Membrane-Based, Sedimentation-Assisted Plasma Separator for Point-of-Care Applications. *Anal. Chem.* **2013**, *85* (21), 10463–10470.
- (203) Jobling, M. a; Gill, P. Encoded Evidence: DNA in Forensic Analysis. *Nat. Rev. Genet.* **2004**, *5* (10), 739–751.

- (204) Katsanis, S. H.; Katsanis, N. Molecular Genetic Testing and the Future of Clinical Genomics. *Nat. Rev. Genet.* **2013**, *14* (6), 415–426.
- (205) Tang, Y. W.; Procop, G. W.; Persing, D. H. Molecular Diagnostics of Infectious Diseases. *Clin. Chem.* **1997**, *43*, 2021–2038.
- (206) Byrnes, S. A.; Bishop, J. D.; Lafleur, L.; Buser, J.; Lutz, B.; Yager, P. One-Step Purification and Concentration of DNA in Porous Membranes for Point-of-Care Applications. *Lab Chip* **2015**, *15*, 2647–2659.
- (207) Craw, P.; Balachandran, W. Isothermal Nucleic Acid Amplification Technologies for Point-of-Care Diagnostics: A Critical Review. *Lab Chip* **2012**, *12*, 2469.
- (208) Allen, P. B.; Arshad, S. a.; Li, B.; Chen, X.; Ellington, A. D. DNA Circuits as Amplifiers for the Detection of Nucleic Acids on a Paperfluidic Platform. *Lab Chip* **2012**, *12*, 2951.
- (209) Rodriguez, N. M.; Wong, W. S.; Liu, L.; Dewar, R.; Klapperich, C. M. A Fully Integrated Paperfluidic Molecular Diagnostic Chip for the Extraction, Amplification, and Detection of Nucleic Acids from Clinical Samples. *Lab Chip* **2016**, *16* (4), 753–763.
- (210) Choi, J. R.; Hu, J.; Tang, R.; Gong, Y.; Feng, S.; Ren, H.; Wen, T.; Li, X.; Wan Abas, W. A. B.; Pingguan-Murphy, B.; et al. An Integrated Paper-Based Sample-to-Answer Biosensor for Nucleic Acid Testing at the Point of Care. *Lab Chip* **2016**, *16* (3), 611–621.
- (211) Linnes, J. C.; Fan, A.; Rodriguez, N. M.; Lemieux, B.; Kong, H.; Klapperich, C. M. Paper-Based Molecular Diagnostic for Chlamydia Trachomatis. *RSC Adv.* **2014**, *4* (80), 42245–42251.
- (212) Rohrman, B. a.; Richards-Kortum, R. R. A Paper and Plastic Device for Performing Recombinase Polymerase Amplification of HIV DNA. *Lab Chip* **2012**, *12*, 3082.
- (213) Liu, M.; Hui, C. Y.; Zhang, Q.; Gu, J.; Kannan, B.; Jahanshahi-Anbuhi, S.; Filipe, C. D. M.; Brennan, J. D.; Li, Y. Target-Induced and Equipment-Free DNA Amplification with a Simple Paper Device. *Angew. Chemie Int. Ed.* **2016**, *55* (8), 2709–2713.
- (214) Bercovici, M.; Han, C. M.; Liao, J. C.; Santiago, J. G. Rapid Hybridization of Nucleic Acids Using Isotachopheresis. *Proc. Natl. Acad. Sci.* **2012**, *109* (28), 11127–11132.
- (215) Bahga, S. S.; Han, C. M.; Santiago, J. G. Integration of Rapid DNA Hybridization and Capillary Zone Electrophoresis Using Bidirectional Isotachopheresis. *Analyst* **2013**, *138* (1), 87–90.
- (216) Eid, C.; Garcia-Schwarz, G.; Santiago, J. G. Isotachopheresis with Ionic Spacer and Two-Stage Separation for High Sensitivity DNA Hybridization Assay. *Analyst* **2013**, *138* (11), 3117.
- (217) Han, C. M.; Katilius, E.; Santiago, J. G. Increasing Hybridization Rate and Sensitivity of DNA Microarrays Using Isotachopheresis. *Lab Chip* **2014**, *14* (16), 2958.
- (218) Lafleur, L.; Bishop, J. D.; Heiniger, E. K.; Gallagher, R. P.; Wheeler, M. D.; Kauffman, P. C.; Zhang, X.; Kline, E.; Buser, J.; Ramachandran, S.; et al. A Rapid, Instrument-Free, Sample-to-Result Nucleic Acid Amplification Test. *Lab Chip* **2016**, *52*, 3377–3383.
- (219) Cohen, D. M.; Russo, M. E.; Jaggi, P.; Kline, J.; Gluckman, W.; Parekh, A. Multicenter

- Clinical Evaluation of the Novel Alere I Strep A Isothermal Nucleic Acid Amplification Test. *J. Clin. Microbiol.* **2015**, *53* (7), 2258–2261.
- (220) Binnicker, M. J.; Espy, M. J.; Irish, C. L.; Vetter, E. A. Direct Detection of Influenza A and B Viruses in Less Than 20 Minutes Using a Commercially Available Rapid PCR Assay. *J. Clin. Microbiol.* **2015**, *53* (7), 2353–2354.
- (221) Ritchie, A. V.; Ushiro-Lumb, I.; Edemaga, D.; Joshi, H. A.; De Ruiter, A.; Szumilin, E.; Jendrulek, I.; McGuire, M.; Goel, N.; Sharma, P. I.; et al. SAMBA HIV Semiquantitative Test, a New Point-of-Care Viral-Load-Monitoring Assay for Resource-Limited Settings. *J. Clin. Microbiol.* **2014**, *52* (9), 3377–3383.
- (222) Fang, R.; Li, X.; Hu, L.; You, Q.; Li, J.; Wu, J.; Xu, P.; Zhong, H.; Luo, Y.; Mei, J.; et al. Cross-Priming Amplification for Rapid Detection of Mycobacterium Tuberculosis in Sputum Specimens. *J. Clin. Microbiol.* **2009**, *47* (3), 845–847.
- (223) Nie, Z.; Deiss, F.; Liu, X.; Akbulut, O.; Whitesides, G. M. Integration of Paper-Based Microfluidic Devices with Commercial Electrochemical Readers. *Lab Chip* **2010**, *10* (22), 3163–3169.
- (224) Dungchai, W.; Chailapakul, O.; Henry, C. S. Electrochemical Detection for Paper-Based Microfluidics. *Anal. Chem.* **2009**, *81* (14), 5821–5826.
- (225) Lee, H. J.; Kim, J.-H.; Lim, H. K.; Cho, E. C.; Huh, N.; Ko, C.; Chan Park, J.; Choi, J.-W.; Lee, S. S. Electrochemical Cell Lysis Device for DNA extraction. *Lab Chip* **2010**, *10* (5), 626–633.
- (226) Wei, Y.-C.; Fu, L.-M.; Lin, C.-H. Electrophoresis Separation and Electrochemical Detection on a Novel Thread-Based Microfluidic Device. *Microfluid. Nanofluidics* **2013**, *14* (3–4), 583–590.
- (227) Li, X.; Scida, K.; Crooks, R. M. Detection of Hepatitis B Virus DNA with a Paper Electrochemical Sensor. *Anal. Chem.* **2015**, *87* (17), 9009–9015.
- (228) Renault, C.; Anderson, M. J.; Crooks, R. M. Electrochemistry in Hollow-Channel Paper Analytical Devices. *J. Am. Chem. Soc.* **2014**, *136* (12), 4616–4623.
- (229) Wang, Y.; Ge, L.; Wang, P.; Yan, M.; Ge, S.; Li, N.; Yu, J.; Huang, J. Photoelectrochemical Lab-on-Paper Device Equipped with a Porous Au-Paper Electrode and Fluidic Delay-Switch for Sensitive Detection of DNA Hybridization. *Lab Chip* **2013**, *13* (19), 3945.
- (230) Liu, H.; Crooks, R. M. Paper-Based Electrochemical Sensing Platform with Integral Battery and Electrochromic Read-Out. *Anal. Chem.* **2012**, *84* (5), 2528–2532.
- (231) Adkins, J.; Boehle, K.; Henry, C. Electrochemical Paper-Based Microfluidic Devices. *Electrophoresis* **2015**, *36* (16), 1811–1824.
- (232) Mettakoonpitak, J.; Boehle, K.; Nantaphol, S.; Teengam, P.; Adkins, J. A.; Srisa-Art, M.; Henry, C. S. Electrochemistry on Paper-Based Analytical Devices: A Review. *Electroanalysis* **2016**, *28* (7), 1420–1436.
- (233) Li, Z.; Li, F.; Hu, J.; Wee, W. H.; Han, Y. L.; Pingguan-Murphy, B.; Lu, T. J.; Xu, F. Direct Writing Electrodes Using a Ball Pen for Paper-Based Point-of-Care Testing. *Analyst* **2015**,

- 140 (16), 5526–5535.
- (234) Wang, C. C.; Hennek, J. W.; Ainla, A.; Kumar, A. A.; Lan, W. J.; Im, J.; Smith, B. S.; Zhao, M.; Whitesides, G. M. A Paper-Based Pop-up Electrochemical Device for Analysis of Beta-Hydroxybutyrate. *Anal. Chem.* **2016**, 88 (12), 6326–6333.
- (235) Erickson, D.; O'Dell, D.; Jiang, L.; Oncescu, V.; Gumus, A.; Lee, S.; Mancuso, M.; Mehta, S. Smartphone Technology Can Be Transformative to the Deployment of Lab-on-Chip Diagnostics. *Lab Chip* **2014**, 14 (17), 3159.
- (236) Zhu, H.; Sencan, I.; Wong, J.; Dimitrov, S.; Tseng, D.; Nagashima, K.; Ozcan, A. Cost-Effective and Rapid Blood Analysis on a Cell-Phone. *Lab Chip* **2013**, 13 (7), 1282–1288.
- (237) Lillehoj, P. B.; Huang, M.-C.; Truong, N.; Ho, C.-M. Rapid Electrochemical Detection on a Mobile Phone. *Lab Chip* **2013**, 13 (15), 2950–2955.
- (238) Laksanasopin, T.; Guo, T. W.; Nayak, S.; Sridhara, A. A.; Xie, S.; Olowookere, O. O.; Cadinu, P.; Meng, F.; Chee, N. H.; Kim, J.; et al. A Smartphone Dongle for Diagnosis of Infectious Diseases at the Point of Care. *Sci. Transl. Med.* **2015**, 7 (273), 273re1-273re1.
- (239) Guo, T.; Patnaik, R.; Kuhlmann, K.; Rai, A. J.; Sia, S. K. Smartphone Dongle for Simultaneous Measurement of Hemoglobin Concentration and Detection of HIV Antibodies. *Lab Chip* **2015**, 15 (17), 3514–3520.
- (240) Dou, J.; Chen, L.; Nayyar, R.; Aitchison, J. S. A Miniaturized Particle Detection System for HIV Monitoring. In *2013 IEEE Photonics Conference*; IEEE, 2013; Vol. 4, pp 5–7.
- (241) Martinez, A. W.; Phillips, S. T.; Carrilho, E.; Thomas, S. W.; Sindi, H.; Whitesides, G. M. Simple Telemedicine for Developing Regions: Camera Phones and Paper-Based Microfluidic Devices for Real-Time, off-Site Diagnosis. *Anal. Chem.* **2008**, 80 (10), 3699–3707.
- (242) Shen, L.; Hagen, J. a.; Papautsky, I. Point-of-Care Colorimetric Detection with a Smartphone. *Lab Chip* **2012**, 12 (21), 4240.
- (243) Mudanyali, O.; Dimitrov, S.; Sikora, U.; Padmanabhan, S.; Navruz, I.; Ozcan, A. Integrated Rapid-Diagnostic-Test Reader Platform on a Cellphone. *Lab Chip* **2012**, 12, 2678.
- (244) Oncescu, V.; O'Dell, D.; Erickson, D. Smartphone Based Health Accessory for Colorimetric Detection of Biomarkers in Sweat and Saliva. *Lab Chip* **2013**, 13 (16), 3232–3238.
- (245) Delaney, J. L.; Doeven, E. H.; Harsant, A. J.; Hogan, C. F. Use of a Mobile Phone for Potentiostatic Control with Low Cost Paper-Based Microfluidic Sensors. *Anal. Chim. Acta* **2013**, 790, 56–60.
- (246) Oncescu, V.; Mancuso, M.; Erickson, D. Cholesterol Testing on a Smartphone. *Lab Chip* **2014**, 14 (4), 759–763.
- (247) Lee, S.; Oncescu, V.; Mancuso, M.; Mehta, S.; Erickson, D. A Smartphone Platform for the Quantification of Vitamin D Levels. *Lab Chip* **2014**, 14 (8), 1437–1442.
- (248) Thom, N. K.; Lewis, G. G.; Yeung, K.; Phillips, S. T. Quantitative Fluorescence Assays Using a Self-Powered Paper-Based Microfluidic Device and a Camera-Equipped Cellular Phone. *RSC Adv.* **2014**, 4 (3), 1334–1340.

- (249) Mascarenhas, M. N.; Flaxman, S. R.; Boerma, T.; Vanderpoel, S.; Stevens, G. A. National, Regional, and Global Trends in Infertility Prevalence Since 1990: A Systematic Analysis of 277 Health Surveys. *PLoS Med.* **2012**, *9* (12), 1–12.
- (250) Schultz, R. M. The Science of ART. *Science* (80-.). **2002**, *296* (5576), 2188–2190.
- (251) Kime, D. E.; Van Look, K. J. W.; McAllister, B. G.; Huyskens, G.; Rurangwa, E.; Ollevier, F. Computer-Assisted Sperm Analysis (CASA) as a Tool for Monitoring Sperm Quality in Fish. *Comp. Biochem. Physiol. Part C Toxicol. Pharmacol.* **2001**, *130* (4), 425–433.
- (252) WHO Press. WHO Laboratory Manual for the Examination and Processing of Human Semen; Geneva (Switzerland), 2010; p 286.
- (253) Brezina, P. R.; Haberl, E.; Wallach, E. At Home Testing: Optimizing Management for the Infertility Physician. *Fertil. Steril.* **2011**, *95* (6), 1867–1878.
- (254) Maatman, T. J.; Aldrin, L.; Carothers, G. G. Patient Noncompliance after Vasectomy. *Fertil. Steril.* **1997**, *68* (3), 552–555.
- (255) Chen, C.-Y.; Chiang, T.-C.; Lin, C.-M.; Lin, S.-S.; Jong, D.-S.; Tsai, V. F.-S.; Hsieh, J.-T.; Wo, A. M. Sperm Quality Assessment via Separation and Sedimentation in a Microfluidic Device. *Analyst* **2013**, *138* (17), 4967–4974.
- (256) Segerink, L. I.; Sprenkels, A. J.; ter Braak, P. M.; Vermes, I.; van den Berg, A. On-Chip Determination of Spermatozoa Concentration Using Electrical Impedance Measurements. *Lab Chip* **2010**, *10* (8), 1018–1024.
- (257) Xie, L.; Ma, R.; Han, C.; Su, K.; Zhang, Q.; Qiu, T.; Wang, L.; Huang, G.; Qiao, J.; Wang, J.; et al. Integration of Sperm Motility and Chemotaxis Screening with a Microchannel-Based Device. *Clin. Chem.* **2010**, *56* (8), 1270 LP-1278.
- (258) Chen, Y.-A.; Chen, K.-C.; Tsai, V. F. S.; Huang, Z.-W.; Hsieh, J.-T.; Wo, A. M. Direct Characterization of Motion-Dependent Parameters of Sperm in a Microfluidic Device: Proof of Principle. *Clin. Chem.* **2013**, *59* (3), 493–501.
- (259) Coppola, M. A.; Klotz, K. L.; Kim, K. -a.; Cho, H. Y.; Kang, J.; Shetty, J.; Howards, S. S.; Flickinger, C. J.; Herr, J. C. SpermCheck® Fertility, an Immunodiagnostic Home Test That Detects Normozoospermia and Severe Oligozoospermia. *Hum. Reprod.* **2010**, *25* (4), 853–861.
- (260) Milkin, T. OTC Product: Fertell. *J. Am. Pharm. Assoc.* **2007**, *47* (5), e16–e17.
- (261) Matsuura, K.; Chen, K. H.; Tsai, C. H.; Li, W.; Asano, Y.; Naruse, K.; Cheng, C. M. Paper-Based Diagnostic Devices for Evaluating the Quality of Human Sperm. *Microfluid. Nanofluidics* **2014**, *16* (5), 857–867.
- (262) Nosrati, R.; Gong, M. M.; San Gabriel, M. C.; Zini, A.; Sinton, D. Paper-Based Sperm DNA Integrity Analysis. *Anal. Methods* **2016**, *8* (33), 6260–6264.
- (263) Zini, A.; Fischer, M. A.; Sharir, S.; Shayegan, B.; Phang, D.; Jarvi, K. Prevalence of Abnormal Sperm DNA Denaturation in Fertile and Infertile Men. *Urology* **2002**, *60* (6), 1069–1072.
- (264) Evenson, D.; Jost, L. Sperm Chromatin Structure Assay Is Useful for Fertility Assessment.

- Methods Cell Sci.* **2000**, 22 (2–3), 169–189.
- (265) Evenson, D. P. Sperm Chromatin Structure Assay (SCSA ®). In *Spermatogenesis: Methods and Protocols*; Carrell, D. T., Aston, K. I., Eds.; Methods in Molecular Biology; Humana Press: New York, 2013; Vol. 927, pp 147–164.
- (266) Feng, S.; Caire, R.; Cortazar, B.; Turan, M.; Wong, A.; Ozcan, A. Immunochromatographic Diagnostic Test Analysis Using Google Glass. *ACS Nano* **2014**, 8 (3), 3069–3079.
- (267) Pang, C.; Lee, C.; Suh, K.-Y. Recent Advances in Flexible Sensors for Wearable and Implantable Devices. *J. Appl. Polym. Sci.* **2013**, 130 (3), 1429–1441.
- (268) Son, D.; Lee, J.; Qiao, S.; Ghaffari, R.; Kim, J.; Lee, J. E.; Song, C.; Kim, S. J.; Lee, D. J.; Jun, S. W.; et al. Multifunctional Wearable Devices for Diagnosis and Therapy of Movement Disorders. *Nat Nano* **2014**, 9 (5), 397–404.
- (269) Wang, S.; Chinnasamy, T.; Lifson, M. A.; Inci, F.; Demirci, U. Flexible Substrate-Based Devices for Point-of-Care Diagnostics. *Trends Biotechnol.* **2016**, 34 (11), 909–921.
- (270) Kenry; Yeo, J. C.; Lim, C. T. Emerging Flexible and Wearable Physical Sensing Platforms for Healthcare and Biomedical Applications. *Microsystems Nanoeng.* **2016**, 2, 16043.
- (271) Mu, X.; Xin, X.; Fan, C.; Li, X.; Tian, X.; Xu, K.-F.; Zheng, Z. A Paper-Based Skin Patch for the Diagnostic Screening of Cystic Fibrosis. *Chem. Commun.* **2015**, 51 (29), 6365–6368.
- (272) Liao, X.; Zhang, Z.; Liao, Q.; Liang, Q.; Ou, Y.; Xu, M.; Li, M.; Zhang, G.; Zhang, Y. Flexible and Printable Paper-Based Strain Sensors for Wearable and Large-Area Green Electronics. *Nanoscale* **2016**, 8 (26), 13025–13032.
- (273) Khiabani, P. S.; Soeriyadi, A. H.; Reece, P. J.; Gooding, J. J. Paper-Based Sensor for Monitoring Sun Exposure. *ACS Sensors* **2016**, 1 (6), 775–780.
- (274) Nassar, J. M.; Cordero, M. D.; Kutbee, A. T.; Karimi, M. A.; Sevilla, G. A. T.; Hussain, A. M.; Shamim, A.; Hussain, M. M. Paper Skin Multisensory Platform for Simultaneous Environmental Monitoring. *Adv. Mater. Technol.* **2016**, 1 (1), 1600004--n/a.
- (275) Bandodkar, A. J.; Jia, W.; Wang, J. Tattoo-Based Wearable Electrochemical Devices: A Review. *Electroanalysis* **2015**, 27 (3), 562–572.
- (276) Guder, F.; Ainla, A.; Redston, J.; Mosadegh, B.; Glavan, A.; Martin, T. J.; Whitesides, G. M. Paper-Based Electrical Respiration Sensor. *Angew. Chemie - Int. Ed.* **2016**, 55 (19), 5727–5732.
- (277) Jiang, L.; Mancuso, M.; Lu, Z.; Akar, G.; Cesarman, E.; Erickson, D. Solar Thermal Polymerase Chain Reaction for Smartphone-Assisted Molecular Diagnostics. *Sci. Rep.* **2014**, 4, 4137.
- (278) Nguyen, T. H.; Fraiwan, A.; Choi, S. Paper-Based Batteries: A Review. *Biosens. Bioelectron.* **2014**, 54, 640–649.
- (279) Sharifi, F.; Ghobadian, S.; Cavalcanti, F. R.; Hashemi, N. Paper-Based Devices for Energy Applications. *Renew. Sustain. Energy Rev.* **2015**, 52, 1453–1472.
- (280) Lin, Y.; Gritsenko, D.; Liu, Q.; Lu, X.; Xu, J. Recent Advancements in Functionalized

- Paper-Based Electronics. *ACS Appl. Mater. Interfaces* **2016**, 8 (32), 20501–20515.
- (281) Chin, C. D.; Linder, V.; Sia, S. K. Commercialization of Microfluidic Point-of-Care Diagnostic Devices. *Lab Chip* **2012**, 12, 2118.
- (282) Volpatti, L. R.; Yetisen, A. K. Commercialization of Microfluidic Devices. *Trends Biotechnol.* **2014**, 32 (7), 347–350.
- (283) Xia, Y.; Si, J.; Li, Z. Fabrication Techniques for Microfluidic Paper-Based Analytical Devices and Their Applications for Biological Testing: A Review. *Biosens. Bioelectron.* **2016**, 77, 774–789.
- (284) Lu, Y.; Shi, W.; Qin, J.; Lin, B. Fabrication and Characterization of Paper-Based Microfluidics Prepared in Nitrocellulose Membrane by Wax Printing. *Anal. Chem.* **2010**, 82 (1), 329–335.
- (285) Mahmud, M. A.; Blondeel, E. J. M.; Kaddoura, M.; MacDonald, B. D. Creating Compact and Microscale Features in Paper-Based Devices by Laser Cutting. *Analyst* **2016**, 141 (23), 6449–6454.
- (286) U.S. Food and Drug Administration, Regulatory Controls https://www.fda.gov/MedicalDevices/DeviceRegulationandGuidance/Overview/GeneralandSpecialControls/ucm2005378.htm#class_1.
- (287) Health Canada, Medical Device Regulations <http://laws-lois.justice.gc.ca/eng/regulations/SOR-98-282/page-1.html#s-1>.
- (288) European Commission, Medical Devices: Guidance Document - Classification of medical devices http://ec.europa.eu/consumers/sectors/medical-devices/files/meddev/2_4_1_rev_9_classification_en.pdf.

TABLE OF CONTENTS GRAPHIC

